ABSTRACT

DYRRDAL, ANITA VERPE. A Statistical Analysis of Snow Depth Variability in Norway and Evaluation of Norwegian Snow Maps. (Under the direction of Dr. Frederick H.M. Semazzi).

This study examines snow depth variability in Norway by applying a number of statistical tools. A time series analysis of snow depth and length of snow season is carried out at eleven meteorological stations situated in three different parts of the country, named Region 1, Region 2, and Region 3. In addition, empirical orthogonal function (EOF) analysis and simple correlation analysis is performed in order to determine the spatial patterns and dominant modes of snow depth variability in Norway. The snow map service introduced by the Norwegian Meteorological Institute and Norwegian Water Resources and Energy Directorate in 2004 is evaluated at the same stations mentioned above. The focus is on the start and end of the snow season and the total number of snow days per hydrological year (Sep 1st – Aug 31st).

A decreasing trend in snow depth is evident at nine of eleven stations. Stations in Region 1 and Region 2 reveal a later start of snow season, while stations in Region 3 reveal a slightly earlier start of snow season. An earlier end of snow season and a decrease in number of snow days is seen at all eleven stations. Region 3 shows the strongest decrease in the number of snow days and daily snow depth, probably due to low elevation and proximity to the coast, leaving this region more sensitive to global warming.

Two leading eigenmodes (EOF1 and EOF2) accounting for 41.4% and 18.6% of the variability in snow depth, respectively, are identified and attempted defined. Existing Northern Hemisphere teleconnection indices are mainly established to explain variability in temperature and precipitation. Snow accumulation is dependent on both previous mentioned

variables, and so the EOFs cannot be defined by one single teleconnection index. EOF1 appears to be related to East Atlantic/Western Russia (EA/WR) pattern, Arctic Oscillation (AO) and possibly to enhanced onshore flow, where the prevailing wind perpendicular to the southern coast of Norway helps push precipitation inland. The time series reveal a decadal variability which might be attributable to the Gulf Stream or to other unknown internal oceanic processes. EOF2 has an inter-annual variability and an obvious increasing trend. This leads us to believe that it is connected to climate change, and previous studies have shown that the North Atlantic Oscillation (NAO) exhibits the same increasing trend. The correlation analysis, however, shows strong correlations to the East Atlantic pattern (EA) and the Scandinavia pattern (SCAND).

In evaluating the snow maps, simulations by a precipitation / degree-day snow model were compared to observations. The approach of calculating snow depth used in the model tends to compact the snow too much, resulting in underestimation of snow depth at most stations. In Region 1 the snow model simulates a shorter snow season than what is observed. In Region 2 the results are ambiguous and correlations between simulations and observations are low. In Region 3, on the other hand, the model performs really well, and there are no significant differences between simulated and observed snow season.

A Statistical Analysis of Snow Depth Variability in Norway and Evaluation of Norwegian Snow Maps

by
Anita Verpe Dyrrdal

A thesis submitted to the Graduate Faculty of
North Carolina State University
In partial fulfillment of the
Requirements for the degree of
Master of Science

Marine, Earth and Atmospheric Sciences

Raleigh, North Carolina

2008

APPROVED BY:

_____	_____
Dr. Frederick H.M. Semazzi Committee Chair	Dr. Gary M. Lackmann
_____	
Dr. John F. Monahan	

BIOGRAPHY

Anita Verpe Dyrrdal was born on March 26th 1982 in Bø, Norway. She attended Bø Vidaregåeande Skule (Bø High School) where her elective subjects were Mathematics, Physics, and Chemistry. Before graduating from High school, Anita spent a year as an exchange student in the Dominican Republic, attending a Dominican High school and learning Spanish in a Dominican host family. After High school she started her bachelor degree in Meteorology and Oceanography at the University of Bergen, Norway. She obtained parts of her bachelor degree at the University of Costa Rica, San Jose, and at the University Centre in Svalbard, Arctic Norway. She graduated from the University of Bergen in 2005. In the spring of 2007, Anita started her master degree in Atmospheric Science at North Carolina State University under the advisory of Dr. Frederick H.M. Semazzi.

ACKNOWLEGMENTS

First I want to extend my gratitude to my advisor Frederick H.M. Semazzi, and my committee members, John F. Monahan and Gary M. Lackmann for their support and advice. My gratitude also goes out to Eirik Førland, Inger Hanssen-Bauer, and Dagrun Vikhamar-Schuler at the Norwegian Meteorological Institute, and Thomas Skaug at the Norwegian Water Resources and Energy Directorate, for the opportunity to write this thesis, and for supplying information and feedback throughout the process. I would like to give thanks to my lab partners for their help and suggestions. My highest gratitude goes to my Mom and Dad back in Norway, who, despite my absence, always support me in everything. I could not have asked for better parents. Also, a great thanks to my sister Kari-Helga, my brother Harald, and my friends around the world for making my life easier with their positivity and friendship. Last, but not least, I want to thank my amazing boyfriend Bradley (mk), who has been a great motivation during my thesis writing. Thank you for your energy and enthusiasm and for all the great moments we share.

TABLE OF CONTENTS

LIST OF TABLES

.

LIST OF FIGURES

1. Introduction

1.1 Purpose and Objectives

Norway stretches from 58˚N to 71˚N, and is one of Europe's most mountainous countries. Due to complex topography, proximity to the sea, and the fact that the country covers 13˚ latitude, snow accumulation in Norway varies significantly. Greatest snow accumulation is found in high altitudes where more precipitation falls as snow, and in mountains close to the coast where it precipitates more frequently. In these areas snow accumulation can reach 290 cm, while in the least snow rich areas maximum snow depth is only 45 cm (Vikhamar-Schuler et al., 2008).

Change in snow accumulation can influence our society in several ways. Most important is the aspect of potential danger associated with extreme flood events and avalanches. The economy will suffer in the case of decreased energy resources from hydroelectric power production and complications within agriculture due to decreased water supply through rivers. Climate and weather is also greatly affected by snow conditions, as is national wildlife. There is a social part to it as well, as Norway is known for good skiing conditions and winter sports in general, and snow activities are an important recreational element to the Norwegian population. Another reason why it's important to study snow is its vulnerability to global warming, and the great uncertainties associated with future snow projections.

Both observations and climate models show strongest warming at high latitudes in the Northern Hemisphere (Figures 1.1 and 1.2), and so an amplified climate change signal can be expected in Norway. According to the Norwegian Meteorological Institute, known as met.no, snow storage will decrease in the entire country, except in areas higher than 800 meters above sea level. In the study of Vikhamar-Schuler et al. (2006) on current (1961-1990) and future (2071-2100) snow conditions, the three following data sets of temperature and precipitation were used as input in a gridded water balance (GWB) model described in Sælthun (1996) and Beldring et al. (2002,2003): observations from met.no (1961-1990) and climate model estimations from HadAm3 and ECHAM4/OPYC3. Future projections from this study show a later start and an earlier end of the snow season almost everywhere in Norway, and a lower number of days with snow at several drainage basins in the country. The start of the snow accumulation season is projected to occur approximately 3-4 weeks later. The snow melt season will start earlier, resulting in an earlier end of the snow season. In the twelve studied drainage basins that were investigated the ending date will be 1-7 weeks earlier than in the present climate. The date of maximum snow water equivalent is in many cases projected to occur 0-4 weeks earlier. Generally, the decrease in the length of the snow season will become smaller with increasing altitude and distance from the sea.

The purpose of our study is to evaluate the snow maps described in section 1.3.1 by comparing them to observations at eleven different meteorological stations in three regions in Norway. In addition, we will analyze the historical time series at these same eleven stations, concentrating on long time variation in snow season and snow depth. Evaluation of the snow

maps is important since the maps are made available to the public and several different organizations are using them as a source for carrying out their activities. One of the main users is the national flood forecasting service. The snow map system makes it possible to track the development of floods and the contributions from snow and precipitation prior and during the flood (Engeset et.al, 2004). The maps are also used in preparing for avalanches, in power production, wildlife management, agriculture, tourism, transportation, construction, extreme weather forecasting, consumer analysis, military activities, wind power construction, among others. In addition, climate researchers use the snow maps to investigate changes and variability in snow season, energy balance, and in determining if climate models of different types provide reasonable results (Skaugen, personal communication). Due to the small number of meteorological stations with snow observations in Norway, interpolation is not an option. Simulation of snow maps is therefore a better way to present past snow conditions. It is essential to have a consistent set of maps showing snow conditions in the entire country, and at all times. It is also important to study climate change in the past, and to evaluate if climate models can describe the historical snow variations in all parts of the country. Evaluation of these simulations of the past will be used to improve the snow model, and hopefully in that way also improve the forecast.

1.2 Background

This thesis work is part of a larger project called NorClim, where the primary focus is the climate of Norway and the Arctic in the 21st century. The project is sponsored by the

Research Council of Norway under their national large scale research program NORKLIMA (2004-2013) – Climate change and impacts in Norway. NorClim is a follow up on NORKLIMA´s *RegClim* and *NOClim* research projects that ended in 2006. The coordinator for the NorClim project is Helge Drange from Nansen Environmental and Remote Sensing Center (NERSC) in Bergen, Norway, and the lead administrator is Eystein Jansen from the Bjerknes Centre for Climate Research (BCCR) in Bergen, Norway. In addition, a number of investigators associated with several research institutions are involved in the project. The motivation for this project is the observed increase in air and sea temperatures, ocean salinity, and precipitation, decreasing sea ice, and numerous severe weather events during the last couple of decades. One of the main objectives of the NorClim project is to find ways to improve the global climate models for Norway, which, due to the country's complex topography, do not present an accurate characterization of Norwegian climate variability (Drange et al., 2007). The component of NorClim that we focus on in this thesis work is called "WP6.3: Improvement of historical climate time series and –fields", led out by Eirik J. Førland at the Norwegian Meteorological Institute (hereafter, met.no).

1.3 Snow Maps

1.3.1 Norwegian Snow Maps

In 2004, a new snow map service was introduced by met.no and the Norwegian Water Resources and Energy Directorate (hereafter, NVE), and made available to the public at www.senorge.no (Figures 1.3 and 1.4). Maps for present day and next day are forecasts,

while maps from earlier dates back to 1971 are based on observations. These new snow maps account for snow accumulation, snow melt, refreezing and winter rain, and they substituted traditional snow accumulation maps. Data are also available for monthly and annual values, as well as for climate periods and scenarios. The snow maps are in the form of images in the portable networks graphics (PNG) format, and they show snow water equivalent (SWE), snowmelt, total runoff, snow state, fresh snow, snow age, and snow depth. Although snow maps only go back to 1971, we have simulated snow data back to 1961, which will be our starting year of comparison with observations.

1.3.2 Snow Model creating Norwegian Snow Maps

This section gives some background information on the Norwegian snow model (hereafter, NSM) which was used to create the Norwegian snow maps (hereafter SM). Snow variables are simulated daily using interpolated fields for precipitation and air temperature with 1 km x 1 km grid spacing as input in a precipitation/degree-day type model. The temperature grids are created using observations from around 150 stations along with residual interpolation. The interpolation is based on the kriging method (Journel and Huijbregts, 1978), which is one of the preferred methods for establishing climatological maps. The main assumption in residual kriging is that a physical process can be divided into deterministic and stochastic components (Tveito & Førland, 1999). The deterministic component represents the influence of local and regional physiographical conditions, like distance to the sea and altitude (Jansson et.al, 2007). This deterministic value is subtracted from the observed value, and ordinary kriging is performed on the residuals, creating the

stochastic component. The estimated temperature is found by adding the deterministic trend to the interpolated field. Temperature is interpolated to all meteorological stations, since many of them only measure precipitation. Precipitation is more complicated, due to discontinuous distribution, the strong influence of terrain and distance to the sea, and the complex topography in Norway. The precipitation grids are created using observations from around 630 stations, and triangulation with terrain adjustment, where triangles are created between three and three points (Tveito&Førland, 1999, Tveito et al., 2000). A surface describing the elevation between the precipitation stations is established because the model simulates a 10% increase in precipitation for every 100 meter increase in altitude (5% for altitudes above 1000 meters a.s.l.) (Jansson et al, 2007). This is based on several studies showing 8–10% increase for every 100 meter in altitude up to 1000 meters a.s.l, and half the rate above that (Førland, 1979, 1984). Observed precipitation is corrected for systematic wind losses according to Førland et.al. (1996), and observed or estimated temperature at the station is used to determine the state of the precipitation (Engeset et.al., 2004). The correction due to under catchment is believed to better adjust simulated snow to the actual snow on the ground (Førland, personal communication). The downside to using triangulations is that it only covers areas between stations, and extrapolation is not allowed for. The snow model makes use of a straightforward inverse distance weighting technique (Tveito & Schöner 2002), with a snow routine similar to the one applied in the HBV model (Engeset et al., 2004). Temperature dependent thresholds are used to separate snow from rain, and to recognize snow melt and refreezing. Snow depth, which is what we are concentrating on in

this analysis, is estimated from the three following factors: Decrease in snow depth due to melting, increase in snow depth due to snowfall and decrease in snow depth due to the weight of the fresh snow, decrease in snow depth due to ageing (Alfnes, 2008). The snow depth algorithm is based on the Variable Infiltration Capacity (VIC) hydrologic model (Liang et al., 1994; Cherkauer and Lettenmaier, 1999). Constants are obtained from the snow and soil model SNTHERM (SNow THERmal Model) (Jordan, 1991). The simulated parameters were tuned against observations at snow pillows, which measure the snow's water equivalent, or in other words, the weight of the snow pack.

1.3.3 Snow Maps in Other Countries

Maps showing snow cover and other snow variables, such as snow water equivalent (SWE), are produced in some other countries. The Finnish Environment Institute (SYKE) and Regional Environment Centres publish daily snow maps with SWE and snow melt at *http://www.ymparisto.fi/*. Swedish Meteorological and Hydrological Institute (SMHI) publish monthly snow maps of simulated SWE at *http://www.smhi.se/*. National Operational Hydrologic Remote Sensing Center at the National Weather Service, USA, publish a larger set of snow variables, including SWE, snow depth, snow pack temperature, snow precipitation, snow melt and blowing snow sublimation. The maps, which are available at *http://www.nohrsc.nws.gov/*, are supported by a web-based navigation facility, a system that does not exist in Nordic snow map services. Meteorological Service of Canada publish SWE maps at *http://www.msc-smc.ec.gc.ca/* (Engeset et al., 2004).

1.4 Previous Related Research

An evaluation of the snow maps such as in this thesis work has to the author's knowledge not been done before. Several variables have been validated against observations, but we believe we are the first to study the length of the snow season. In addition, other stations have been used in earlier studies of the snow model. Engeset et al (2004) evaluated the performance of the precipitation triangulation method by leaving out ten stations for 1962-69. They found that the elevation gradient is too large, resulting in over estimation of precipitation at higher altitudes, and slight under estimation of precipitation at lower altitudes. In the same study, observations of snow water equivalent (SWE) at two snow pillows and simulations by Sweden's Meteorological and Hydrological Institute's HBV model (Bergstrøm, 1992) of snow reservoir in two catchments are compared to snow model simulations at yearly snow maxima. Some hydropower production companies collect snow depth and snow density data from their catchment areas during the winter, which are used in estimating SWE. At these locations, the snow model was evaluated comparing simulations to the estimated SWE. It was concluded that the snow model shows good agreement with SWE observations, in terms of deviation from the normal. The geographical patterns are well reproduced in the entire country, including years of extremes, but there is some over estimation in a few locations in the south. This problem was also related to the interpolation of precipitation, and the elevation gradient being too large.

An evaluation of the VIC approach of calculating snow depth due to compaction was

carried out by NVE and the results were described in an internal report (Alfnes, 2008). The model was compared to the ECOMAG model (Motovilov, 1993), the other approach considered for the Norwegian snow map application, and also validated against observations at snow pillows, meteorological weather stations, density samples at glaciers, and a snow course. The algorithm used in the VIC model seems to compact the snow too much and thus the simulated amounts of snow density were too high, which resulting in under estimation of snow depth. In many locations, however, the simulated SWE was too high compared to observations, which combined with higher simulated density results in simulated snow depth being similar to observed snow depth.

All the previous studies have only examined data for a few years. This thesis work takes a more comprehensive approach by analyzing data for all the available years for our evaluation. Analysis of long time variations at about 40 stations is currently being carried out by met.no, but they are using different stations and methods. The indicators studied are maximum snow depth, mean snow depth, snow season duration, number of days with snow on the ground, number of skiing days, and maximum increase in daily snow depth (Vikhamar-Schuler, 2008). We believe their study will be complimentary to ours.

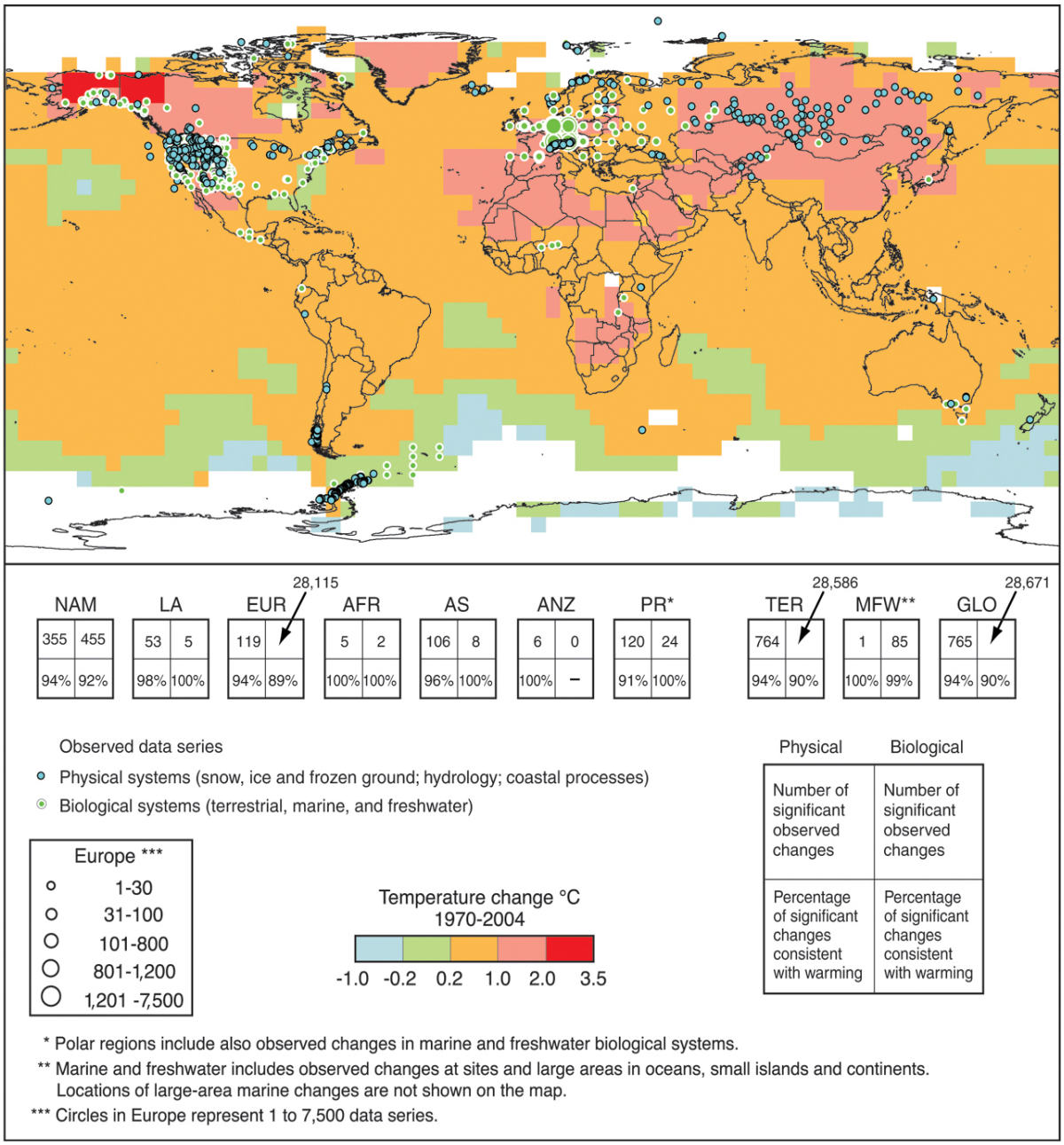

Figure 1.1: Locations of significant changes in data series of physical systems (snow, ice and frozen ground; hydrology; and coastal processes) and biological systems (terrestrial, marine, and freshwater biological systems), are shown together with surface air temperature changes over the period 1970-2004 (Adapted from IPCC climate change synthesis report 2007).

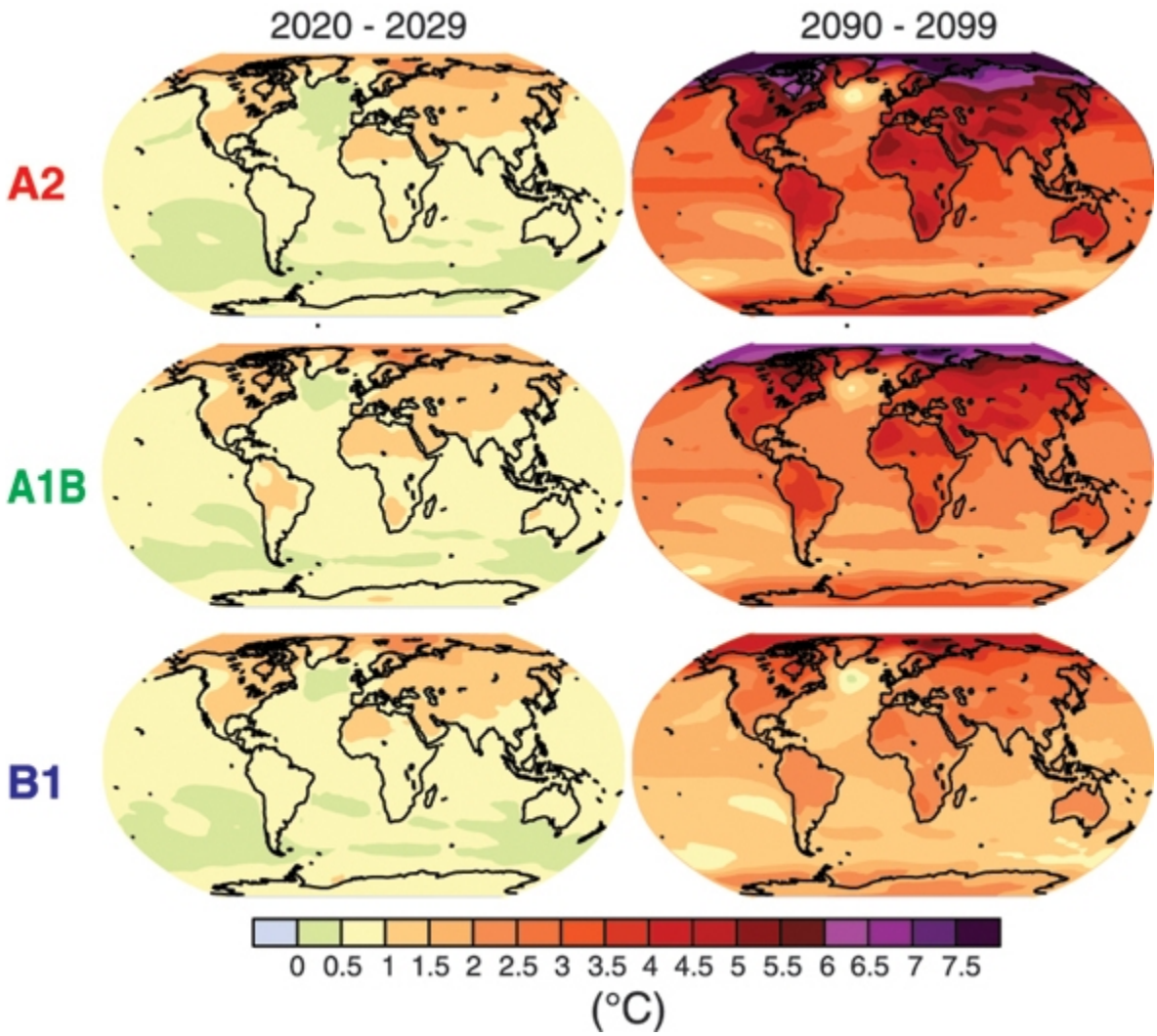

Figure 1.2: Projected surface temperature changes for the early and late 21st century relative to the period 1980-1999. The panels show the multi-AOGCM average projections for the A2 (top), A1B (middle) and B1 (bottom) SRES scenarios averaged over decades 2020-2029 (left) and 2090-2099 (right) (Adapted from IPCC climate change synthesis report 2007).

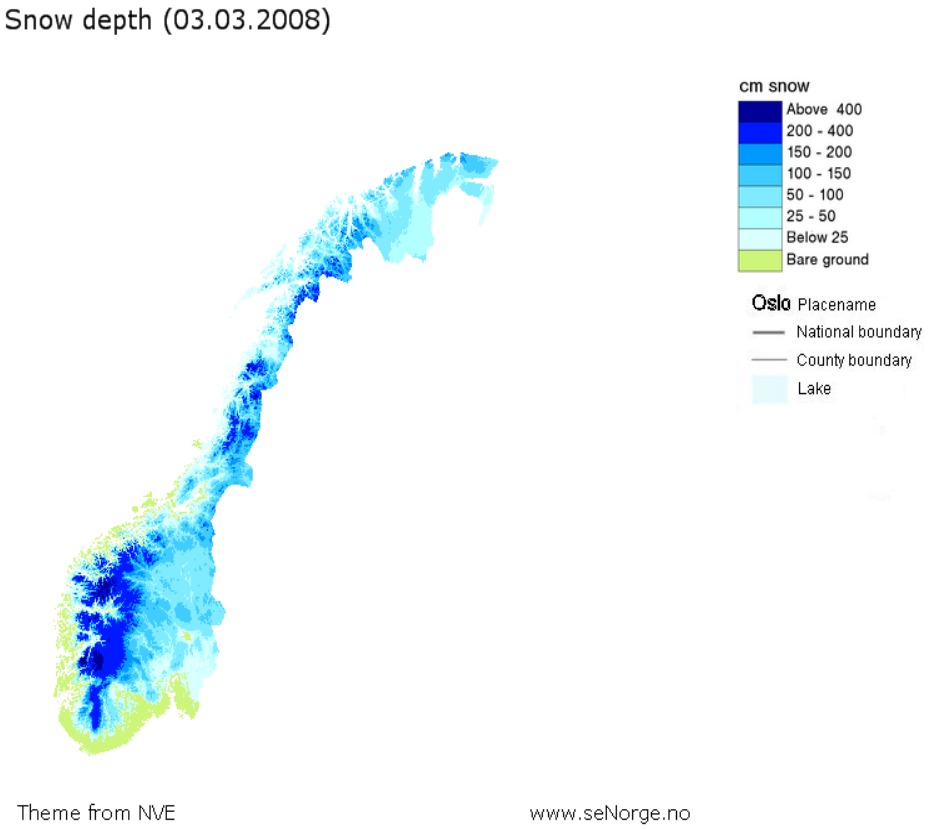

Figure 1.3: Snow map from senorge.no, showing snow depth on March 3rd, 2008.

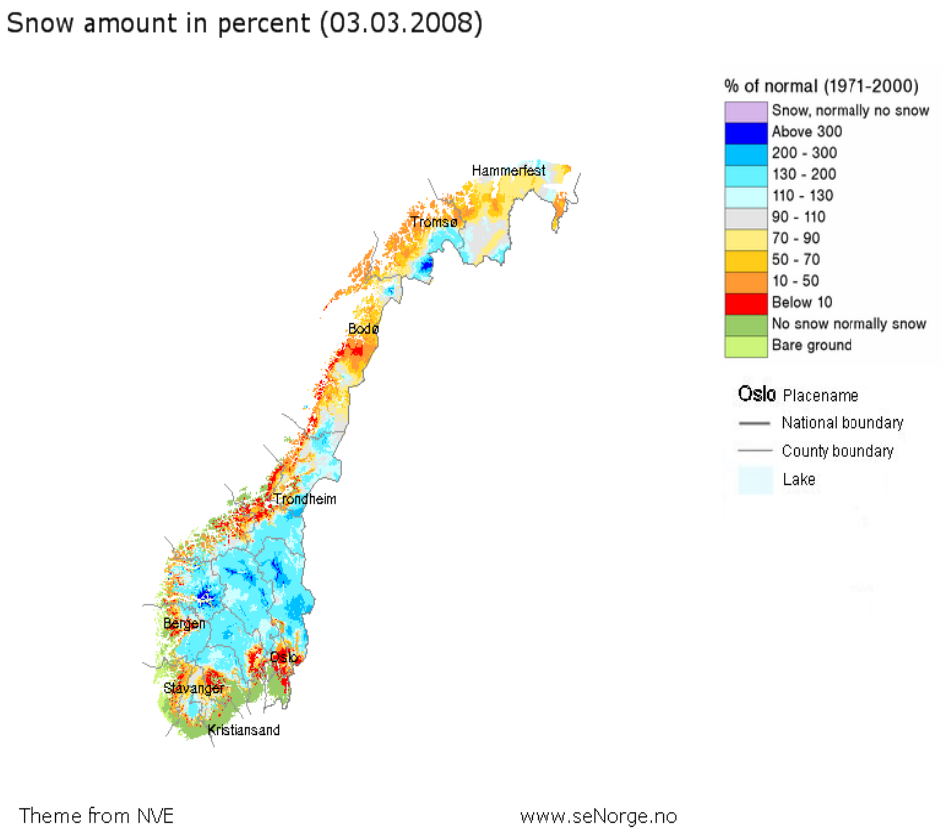

Figure 1.4: Snow map from senorge.no showing snow amount in percent of normal (1971-2000) on March 3rd, 2008.

2. Data and Methods

2.1 Stations

We analyzed snow accumulation data at eleven stations in three different regions of Norway. We had three main requirements for the stations:

1. Smooth topography.
2. Terrain model height comparable with real station height.
3. Observations should be of good quality and time series should start before 1970.

The first two requirements were partly evaluated by examining the terrain model used in simulations of the snow maps, and partly by knowledge from researchers at met.no, Oslo. Observational data (see section 2.2) have been quality controlled, and in addition we made sure the observations are continuous and do not contain large periods of missing values. Table 2.1 shows the names of the regions and stations, along with a short description and whether or not temperature is measured at the station. The description is taken from pictures and reports in the met.no archive, provided by Gabriel Kielland. Figure 2.1 shows where the different stations are located. Our main reason for selecting these three regions for analysis was the flat topography, the quality of the observations, and latitudinal representativeness. When deciding on which regions to analyze we were mainly concerned about the second part of the analysis where we evaluate the Norwegian Snow Model. We realize that a fourth region on the west coast would be a valued supplement to our analysis, especially for understanding how climate change affect snow accumulation in Norway.

2.2 Observations

In January 2008 Norway had a number of 224 operating weather stations that report several times a day, and 396 operating precipitation stations that only measure precipitation and snow depth/cover, and report once a day (Førland, private communication). These observational data from the Norwegian Meteorological Institute are made available at no charge at www.eklima.no and can be obtained by registered users. The eklima portal also provides meteorological and climatological data from other station owners. The observed values are processed in several steps, by both automatic and manual routines. Nevertheless, the quality of the data varies from station to station. Some stations were disregarded for analysis in this study due to the excessive amount of missing data. Some stations still have a few missing observations. In the process of the statistical analysis, we left out the simulated values on the days with missing observations. Snow depth in centimeters is measured once a day at most precipitation- and weather stations. The precipitation stations also report snow cover, from 0 to 4. 0 being no snow observed in approximately 1 km radius around the station, and 4 being 100% snow cover (eklima.no, 2008).

2.3 Simulations

Snow simulations were carried out using the snow model described in chapter 1, and data were provided to us by Dagrun Vikhamar Schuler from met.no. In order to compare the snow maps with observations at the eleven selected stations, we obtained simulated daily

values from a 1 km x 1 km pixel that contains the same coordinates as the station in question. This means that the height above sea level used in the snow model can be different from the real elevation of the station. The difference between real station elevation and elevation used in the snow model is shown in Table 2.2.

2.4 Analysis of Historical Time Series

2.4.1 Long Time Variations in Snow Depth

An important part of the NorClim project is to examine the long time variations of historical time series for temperature, precipitation and snow variables. In this part of our study we analyze variations in snow depth at the eleven selected stations, using various analysis methods. The lengths of the time series vary from approximately 40 to 100 years. Direct plots of snow depth for the months November through May were created, in addition to plots of the entire time series of daily snow depth. Some of the stations in the southern part of the country showed very little snow in May, and this month is therefore left out at the particular stations. We searched for trends in the start and end of snow season, and the number of snow days (see section 2.5.1 for further description on these variables). All trend lines were tested for statistical significance at the 0.1, 0.05, and 0.01 alpha levels. For a closer examination of the variation, we made box plots for each winter month.

2.4.2 Nonlinear Data Fitting

The start and end of snow season are complicated variables and sometimes hard to detect, which is why we applied a second method of evaluation. In addition, the date of

maximum snow depth is tricky to determine manually, since peaks can occur at several times during the winter season. Information on the date of maximum snow depth is important to production planners and stakeholders in the energy market. Around this date, which usually occurs during April or May, electricity demands are high and reservoir contents are at a minimum due to high production and reduced precipitation (Engeset et al., 2004). A two piece nonlinear model was fitted to the daily snow depth data for every year at the eleven stations. The data is plotted from July 1st to June 30th. The 'nlin' procedure in SAS was used to solve the least squares problem of the following function

$$max (0, min (m*(t-a)/(b-a), m*(c-t)/(c-b)))$$

where m = maximum snow depth, t = date, a = start of snow season, b = date of maximum snow depth, and c = end of snow season (see Figure 2.2). The code, which was provided by Dr. John Monahan at the Department of Statistics, NCSU, first searches the data set to find years with too many missing values, and delete these. Then values for m, a, b, and c are found for each of the remaining years. A year is flagged if the conversion criterion is not met, or if there seems to be a problem with the model, and these years are deleted before the final output is created. A multivariate regression on all four variables is performed as a last step, and any trend is evaluated for significance and reported with a p value. This procedure was adopted for the entire observational time series at all eleven stations.

2.4.3 Spectral Analysis

In order to identify possible periodicities in the time series, we performed a spectral analysis on snow depth data, averaged over the winter season. Spectral analysis is also known as frequency domain analysis, and it applies the concept of fast Fourier transform to represent the original signal as a combination of sinusoidal functions of different frequencies. The power spectral density PSD, representing the power content of each frequency, is calculated, and presented in a periodogram. The dominant frequencies correspond to the coefficients with the highest magnitude and appear as peaks in the periodogram (Vlachos et al., 2004). In other words, significant periodicities in time series are recognized by their periods showing large contributions to the total variability (Wilks, 2006). The SSA-MTM toolkit distributed by the Department of Atmospheric Sciences at University of California was applied in this analysis. Six out of the eleven stations originally contained some missing values, and a singular spectrum analysis (SSA) gap-filling technique from the same software was applied to create continuous time series. The SSA gap filling procedure utilizes temporal correlations in the data to iteratively estimate and fill in the missing points (Kondrashov and Ghil, 2006). Further, the multitaper method (MTM) was chosen to perform the actual spectral analysis on out data sets. MTM is a nonparametric method that attempts to reduce the variance of spectral estimates by using a small set of tapers (three in our case) (Thomson, 1982; Percival and Walden, 1993). The tapers are the discrete set of eigenfunctions that minimizes leakage outside of a frequency band (Ghil et al, 2002). An estimated red noise background is chosen as the null hypothesis to isolate the frequency peaks corresponding to

significant periodicities. We are mainly interested in narrowband signals (not harmonic), thus the raw MTM spectrum is plotted with the 50%, 90%, 95%, and 99% significance levels relative to the estimated red noise background.

2.4.4 Empirical Orthogonal Function (EOF) Analysis

An Empirical Orthogonal Function (EOF) approach was employed to gain insight in the dominant spatial patterns in snow depth for the winter months December through March. By implementing this method, we expect to better understand the climatic differences seen in different parts for the country, particularly our three regions of interest. We also hope to identify the leading modes of snow depth variability in the entire country and for our three regions. EOF analysis, also referred to as principal component analysis (PCA), is a multivariate statistical technique and is widely used in atmospheric sciences. The EOF analysis was performed using the function ‘prcomp’ in Fortran, which reduces a large data set to a smaller data set containing linear combinations of the original data set. These linear combinations, called principal component loadings or eigenvectors, represent the maximum possible fraction of the variability contained in the original data (Wilks, 2006). In order to avoid influence from other correlated modes, and to obtain better sampling properties, all leading eigenvectors are rotated. Each eigenvector has an eigenvalue, which represents the percentage of the total variability in the feature studied that is accounted for by that mode. Hence, the most important modes are features of the climatic system that generate most of the climate variability in a certain location. One example is the ENSO variability, which

represents one of the leading global eigenmodes. Since EOF analysis is a statistical tool, there is no guaranty that the results are physically meaningful. EOF time series, representing how the specific mode oscillates in time, is also computed and plotted. The EOF time series value at a certain time weighted by its variance and multiplied by the loading at a certain place and at the same time, gives us the actual value of the climate variable in question, at that specific time and place. This way we can go back and forth between the EOF time series and the snow depth value. We applied the separation criteria described in North et al. (1982), known as the North et al. rule of thumb, to determine significant eigenvalues. This method implies that if the standard deviation of an EOF is larger or comparable to the spacing between the EOF and its neighboring EOF, the sampling error of the first EOF will be comparable to the size of the second EOF. A set of monthly averaged snow depth data from 233 meteorological stations throughout the country was used in the EOF analysis. One concern which needs to be addressed is that due to the geography of the country, the majority of the stations are located in the south, and thus too much weight is put on this region. Adding stations from Sweden would possibly improve the results, and is recommended in future research. A simple interpolation technique, using climatological averages, was applied to fill in any missing values. The data went from 1960 until 2000 (41 years), and only the winter months December through March were included to create seasonal averages. This 233×41 seasonal average matrix was the basis for the EOF analysis. The loadings are presented as color images over the map of Norway using ArcMap from GIS software, and an inverse distance weighted (IDW) interpolation is applied. These images show us how snow

depth in different parts of the country is affected by the governing modes of variability.

2.4.5 Correlation Analysis

Atmospheric circulation greatly affects the spatial variations in snow accumulation over Northern Europe, including Norway. Due to the latitudinal extent of the country different parts experience different modes of climate variability. The EOF analysis described in the previous section along with a linear correlation analysis is expected to help us determine significant climatic features affecting snow depth in Norway, and particularly at our locations of interest. We adopted 5 standardized Northern Hemisphere teleconnection indices described by the Climate Prediction Center where the data was obtained. In addition we included the Arctic Oscillation as a sixth teleconnection index.

1. North Atlantic Oscillation (NAO)
2. East Atlantic Pattern (EA)
3. West Pacific Pattern (WP)
4. East Atlantic/Western Russia Pattern (EA/WR)
5. Scandinavia Pattern (SCAND)
6. Arctic Oscillation (AO)

We used cluster averages at our three regions, in order to smooth out spatial fluctuations in snow depth, and correlated these to the seasonal means (December through March) of the 6 indices by computing the correlation coefficient R and testing it for significance at the 0.1, 0.05, and 0.01 alpha levels. We also correlated the time series of the dominant EOFs to each index. Some climatic indices influence the future state of the atmosphere, and so lag

correlations were computed, with lags of 1 month, 2 months, and 3 months. The years used in the correlation analysis varied between the time series. For Region 1 data from 1966/67 to 2000/01 was correlated, for Region 2 data from 1957/58 to 2000/01 was correlated, and for Region 3 data from 1965/66 to 2000/01 was correlated. For the EOF time series data from 1960/61 to 2000/01 was correlated.

We performed a spectral analysis described in section 2.4.3 on December through March averages of the indices identified above, to see if any periodicities found in the snow depth data were repeated in any of the indices. As a final step, we correlated the significant EOF time series with global sea surface temperature (SST) and sea level pressure (SLP), again averaged over the winter months. We used NOAA Extended Reconstructed SSTs, and SLP from NCAR/NCEP surface reanalysis, both obtained at NOAA Earth System Research Laboratory websites. The correlations were computed and plotted in GrADS using a script provided by Michael Diaz from the Department of Marine, Earth, and Atmospheric Sciences, NCSU. One concern when trying to correlate such great amount of numbers is that something will always be correlated, and it is problematic to determine whether or not the correlation is relevant or if it is nearly a coincidence.

2.4.6 Northern Hemisphere Teleconnection Indices

Teleconnection patterns refer to repeating large-scale pressure and circulation anomalies (Climate Prediction Center, 2008), and are associated with variability in temperature, precipitation, jet stream location and intensity, and storm tracks which are

particularly important in Norwegian climate. We should be careful about addressing climate variability in a region to a single teleconnection pattern, since some patterns are structurally similar and project on one another.

2.4.6.1 North Atlantic Oscillation (NAO)

NAO has long been known as the primary driver of winter precipitation and temperature variability in Europe. The NAO index is defined as the difference in normalized pressure between the Azores High and the Icelandic Low during the winter months December through March (Rogers, 1984; Hurrell, 1995). A positive index (Figure 2.3) is related to a deeper than normal Icelandic Low, and a stronger than normal Azores High, and is associated with warmer and wetter climate in Scandinavia, due to enhanced westerlies in the North Atlantic. Uvo (2003) found that winter precipitation in Southwestern Norway is greatly influenced by NAO. Westerly winds associated with NAO together with orographic lifting directly affects the Norwegian coast in particular. The NAO manifests itself in terms of numerous oscillations. Spectral analysis of the NAO index has revealed periodicities of 2-3 years. In addition, the NAO also exhibits a long–term trend. From 1900 until about 1930, the NAO showed a positive trend. From the early 1940s to early 1970s, however, we see a negative trend, while during the past 25 years we observe strong positive NAO values (Hurrell, 1995, 1996). Consistent with this, winters in the past 25 years have been relatively mild and wet over Scandinavia and northern Europe (Hurrell and van Loon, 1997; Kushnir, 1999). Since NAO is positively correlated to both temperature and precipitation, the

relationship between NAO and snow depth is hard to determine, especially in locations where the temperature is close to 0˚C. Mysterud et.al. (2000) states that snow depth is negatively correlated to the NAO at low altitudes (below approximately 400 m a.s.l.), and positively correlated above this altitude.

2.4.6.2 East Atlantic Pattern (EA)

The East Atlantic pattern is the second prominent teleconnection pattern affecting low-frequency variability over North Atlantic, and it appears in all months. EA pattern (Figure 2.4) is similar to that of NAO, but the center dipole is shifted southeastward. A positive EA phase is associated with above-average surface temperatures in Europe throughout the year, and above-average precipitation over northern Europe and Scandinavia. The EA pattern shows strong multi-decadal variability. A negative phase governed from 1950 to 1976, while a positive phase has been dominant since then (Climate Prediction Center, 2008).

2.4.6.3 West Pacific Pattern (WP)

West Pacific pattern is the leading mode of low-frequency variability over the North Pacific throughout the year. During the winter months, a north-south dipole is centered over the Kamchatka Peninsula and another center of opposite sign is centered over southeastern Asia and the western subtropical North Pacific (Figure 2.5) (Climate Prediction Center, 2008). The West Pacific Pattern is, to the authors understanding, not known to affect Scandinavia directly.

2.4.6.4 East Atlantic/Western Russia Pattern (EA/WR)

The East Atlantic/Western Russia pattern (also known as Eurasia-2 pattern) is one of three prominent teleconnection pattern affecting Eurasia in all months. The positive phase is characterized by above normal pressure over Europe and Northern China and below normal pressure over central North Atlantic and north of the Caspian Sea (Figure 2.6) (Climate Prediction Center, 2008). The effects of the EA/WR on Scandinavia has to the authors knowledge not been discussed.

2.4.6.5 Scandinavia Pattern (SCAND)

The SCAND index (previously known as Eurasia-1) is identified by a main circulation center over Scandinavia, and weaker centers of opposite sign over Western Europe and eastern Russia/ western Mongolia (Figure 2.7). Positive SCAND phases are associated with below-average temperatures over central Russia Western Europe and below-average precipitation across Scandinavia (Climate Prediction Center, 2008). Popova (2007) evaluates the influence of Northern Hemispheric circulation modes on snow depth variation in Northern Eurasia using multiple stepwise backward regression (MSBR). The results from the MSBR show that SCAND was the most important mode associated with snow depth variability in 1951–1974. After 1975, SCAND has passed over the leading role to NAO. We tested this by correlating NAO and SCAND time series with our dominant EOF time series for the years 1960-1974 and 1975-2000.

2.4.6.6 Arctic Oscillation (AO)

The Arctic Oscillation is the prevailing pattern of non-seasonal sea level pressure variations on high latitudes in the Northern Hemisphere. AO is identified by pressure anomalies over the Arctic and pressure anomalies of opposite sign further south at about 37-45ºN (Figure 2.8). AO positive phase is associated with warmer and wetter conditions over northern Europe, while a negative phase gives drier and colder conditions (Climate Prediction Center, 2008).

2.5 Evaluation of the Norwegian Snow Model (NSM)

2.5.1 Snow Season Indices

Our main focus in this part of the thesis work is to compare simulated snow season to observations. The snow season does not have an absolute definition, thus it is up to the individual person or research group to define reasonable indices that fit their data, and follow these consistently. Start of snow season is here defined as the first day of permanent snow cover, and the end of snow season is the last day of permanent snow cover. The indices used in this study are as follows:

Start of snow season (START): Ten or more consecutive days with snow cover of ` 50% or more.

End of snow season (END): Last day of 50% or more snow cover, followed by at least ten consecutive days of less than 50% snow cover, and no snow events of five days or more of 50% or more snow cover after that.

Number of snow days (DAYS): Number of days with snow cover of 50% or more per hydrologic year (September 1st through August 31st).

The comparison of these three variables was carried out for the years 1961 to 2003.

Since snow cover is of greater interest and higher accuracy over a larger area, this was the variable in focus when evaluating the observed snow season. Unfortunately, snow cover is not simulated by the snow model, and we therefore had to convert snow depth using 1 cm or more as an indicator of 50% or more snow cover (Førland, private communication). This conversion seems to be quite accurate, with only smaller fluctuations of 1-2 days. From 1961 to 1970 only snow water equivalent is simulated. We converted SWE to snow depth by using 2 mm SWE equals 1 cm snow depth. This conversion was defined by searching through years with both SWE and snow depth simulations. Again, there are only small fluctuations of 1-2 days, which should not affect the results significantly.

2.5.2 Comparison between Simulations and Observations

We plotted the yearly observed and simulated start and end of the snow season and the number of snow days, along with their trend lines. In these plots we examined how well the snow model captures the pattern, as well as maxima and minima. The trend lines were tested using GraphPad Prism version 5 for Windows which calculates a P value from an F test with a 0.05 alpha level, in order to determine whether the inclinations and intercepts are significantly different between simulations and observations. We also created scatter plots with observations on the x-axis and simulations on the y-axis. These plots are helpful in

determining biases in the simulated data by comparing the plotted line with the 45 degree line. If the correlation is perfect between observations and simulations, the points should follow the 45 degree line perfectly. The scatter plots also give a general picture of the overall performance of the model at a particular station.

There is great uncertainty associated with the indices for snow season. Consequently, we chose to also examine some more stable features, in order to determine if the model shows any systematic biases when it comes to simulating snow depth. We considered total seasonal snow depth and the snow depth on certain dates for the years 1971 to 2003. The total seasonal snow depth is obviously a meaningless number, only computed for easier comparison. We focused on the following dates: December 15th, January 15th, February 15th, and March 15th. All plots are created in Matlab. Statistical values for all features were calculated, including means and standard deviations, linear correlations between observations and simulations, and root mean squared errors.

One explanation for possible biases in the snow depth simulations might be inaccurate interpolation of precipitation and temperature in the grid point containing the station coordinates, given that model elevation might be different from real elevation. Consequently we examined scatter plots of observed and simulated values for the two before mentioned variables. Observed temperature is only available at five of the eleven stations (see Table 2.1)

Table 2.1: Names of regions and stations with short description of area around the station and whether or not temperature is measured at the station.

Region	**Station**	**Description**	**Temperature**
1.Finnmarksvidda	1. 93500 Jotkajavre	Flat, water and hill close	No
	2. 97350 Cuovddatmohkki	River valley	Yes
	3. 97250 Karasjok	Shallow valley, river and close	Yes
	4. 93900 Sihcajavri	Flat, water close	Yes
2.Røros	5. 10400 Røros	Flat	Yes
	6. 10600 Aursund	Trees and small hills around	No
	7. 10100 Os i Østerdal	On a steep hill, water close	No
	8. 10900 Vauldalen	Trees and small hills around	No
3.Romerike	9. 4780 Gardermoen	Flat	Yes
	10. 4740 Ukkestad	Flat	No
	11. 11120 Eidsvoll-verk	Trees and other obstacles around, river close	No

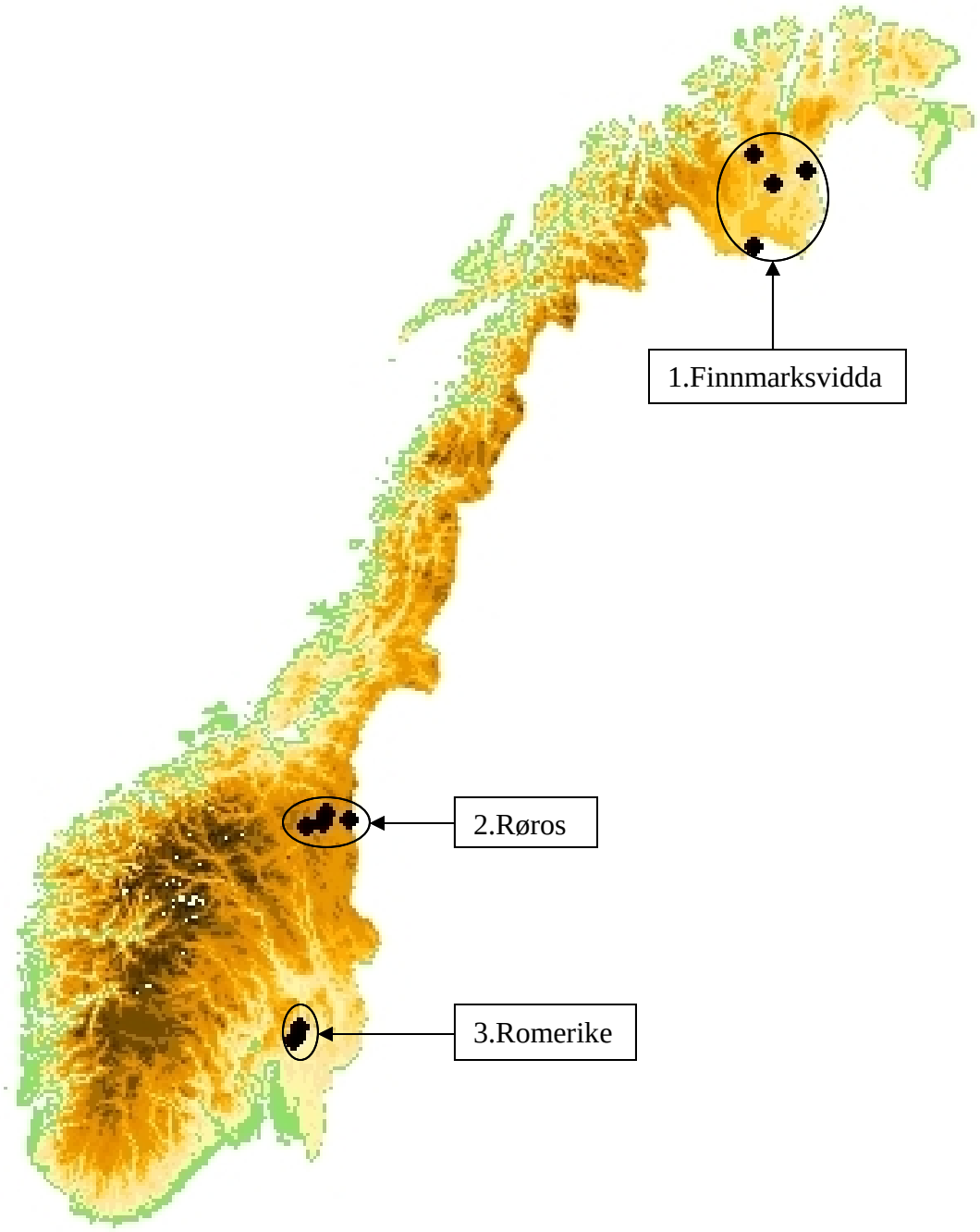

Figure 2.1: Map of Norway indicating the eleven stations in the three regions studied.

Table 2.2: Station elevation used in snow model versus real station elevation.

Station	Real elevation [m]	Elevation used in snow model [m]	Difference (Real – Model) [m]
1.Jotkajavre	389	400	-11
2.Cuovddatmohkki	286	300	-14
3.Karasjok	130	146	-16
4.Sihcajavri	382	378	-4
5.Røros	628	650	-22
6.Aursund	685	690	-5
7.Os i Østerdal	788	700	88
8.Vauldalen	830	880	-50
9.Gardermoen	202	208	-6
10.Ukkestad	187	160	27
11.Eidsvoll-verk	181	180	1

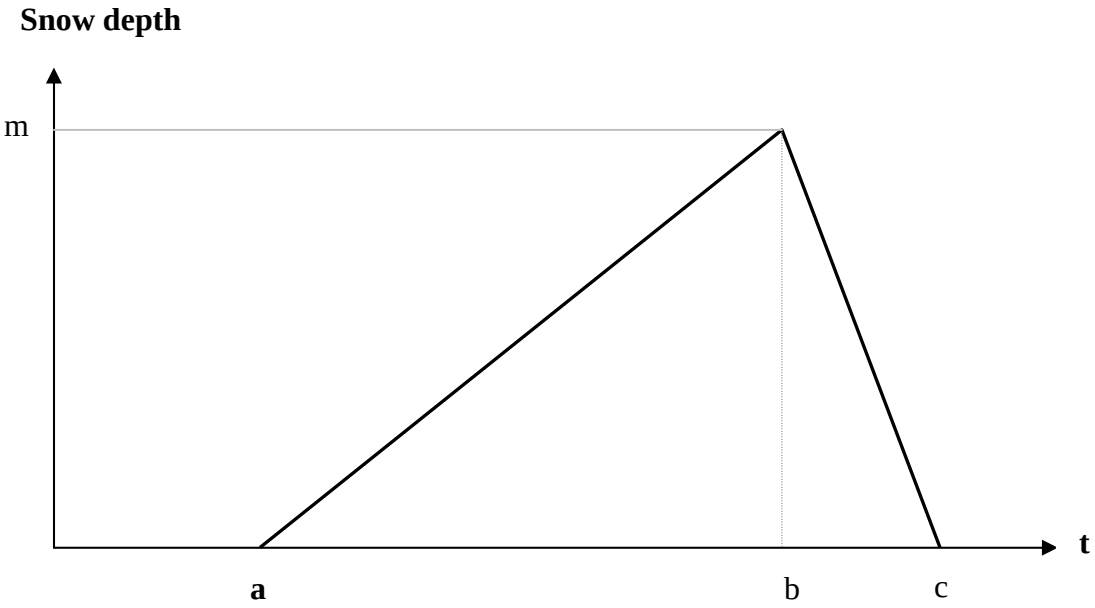

Figure 2.2: Example of two piece nonlinear model plot.

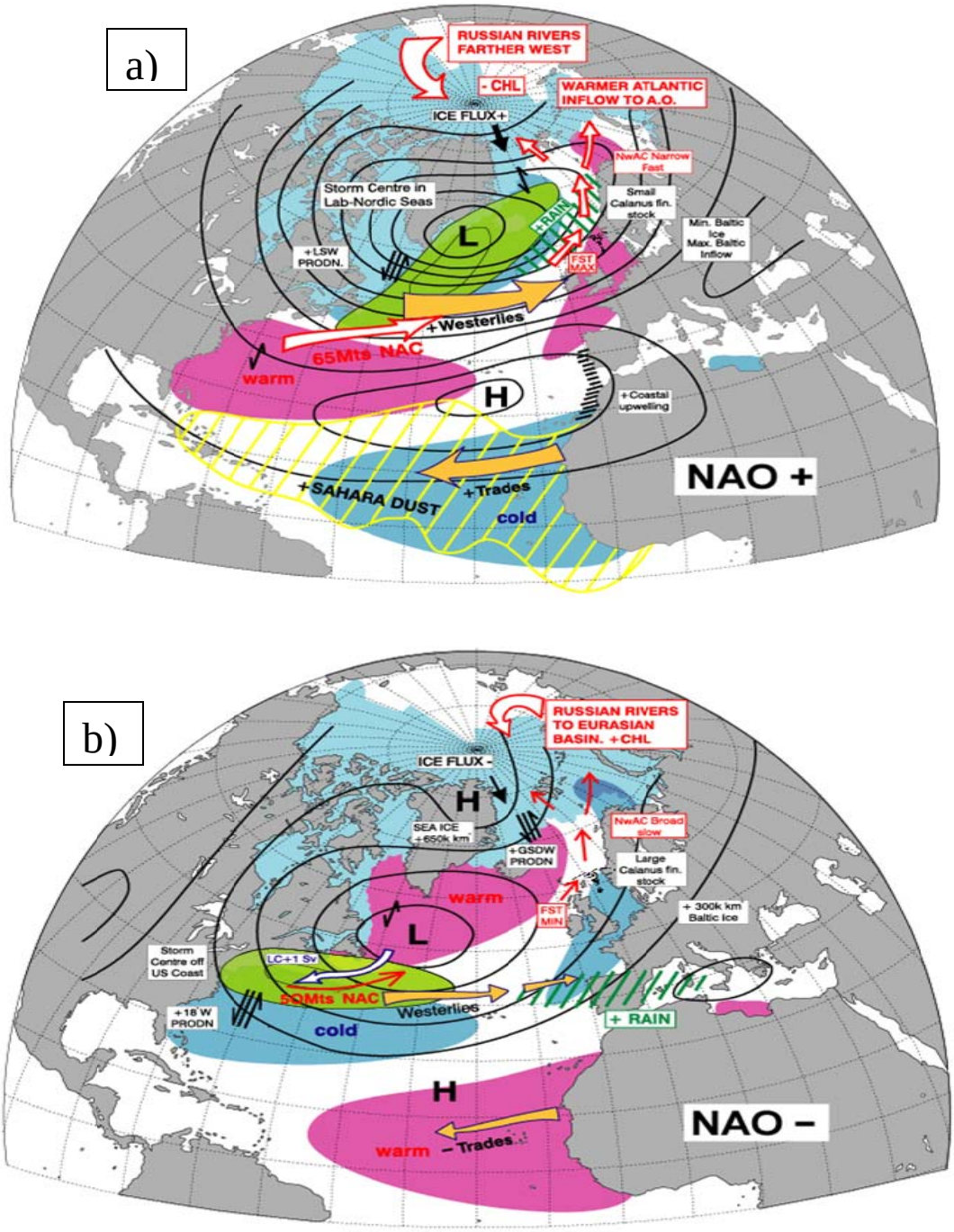

Figure 2.3: Conditions during North Atlantic Oscillation
a) high phase and b) low phase (adapted from CEFAS, UK).

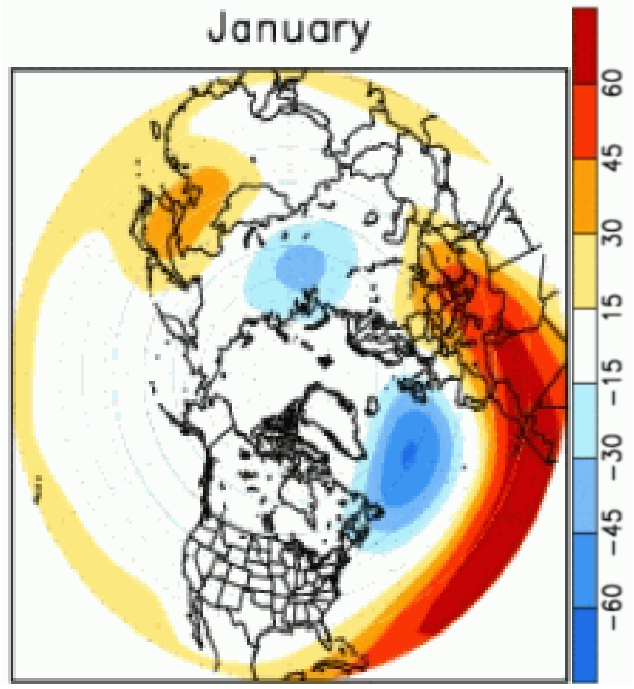

Figure 2.4: Temporal correlation between the monthly standardized height anomalies and the East Atlantic Pattern for January (adapted from Climate Prediction Center).

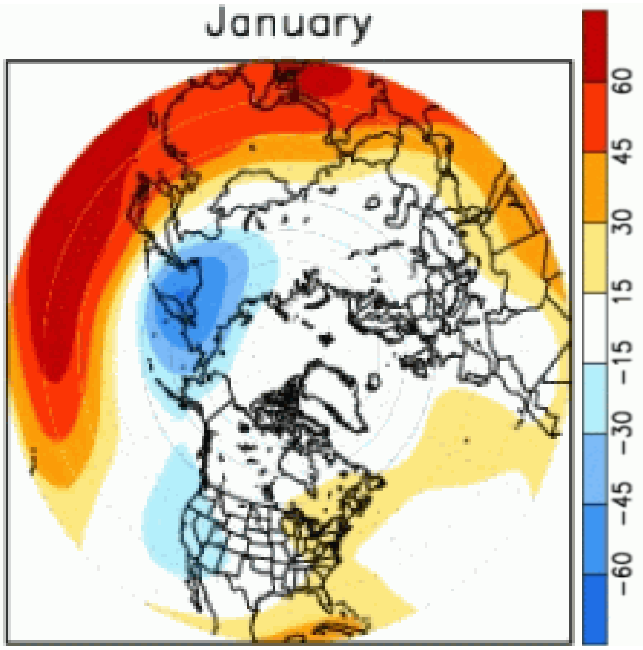

Figure 2.5: Temporal correlation between the monthly standardized height anomalies and the West Pacific Pattern for January (adapted from Climate Prediction Center).

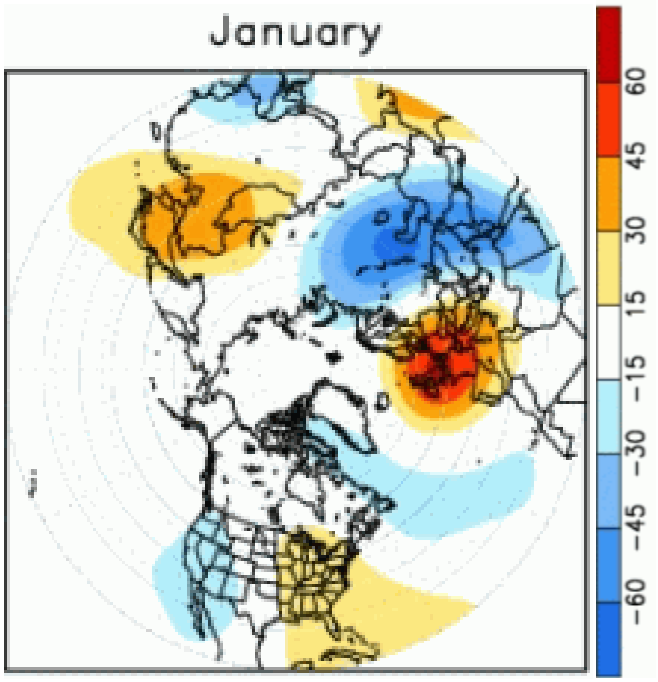

Figure 2.6: Temporal correlation between the monthly standardized height anomalies and the East Atlantic/Western Russia pattern for January (adapted from Climate Prediction Center).

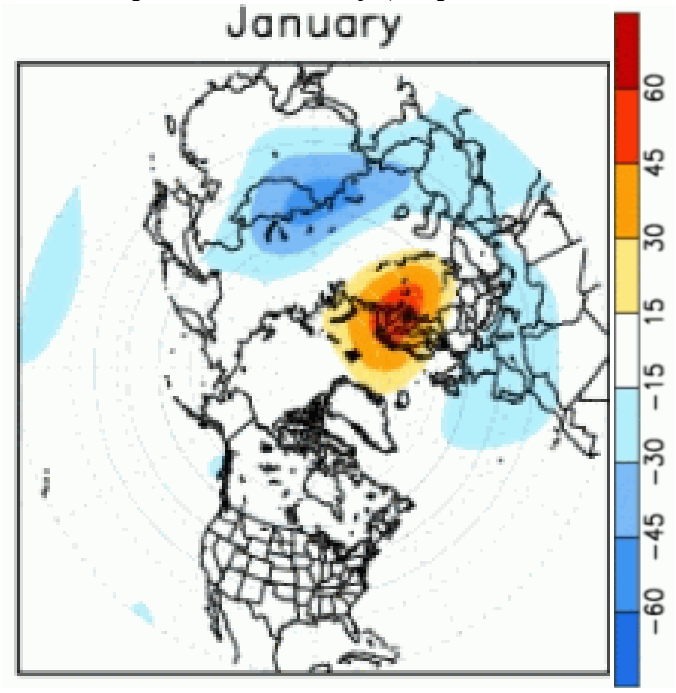

Figure 2.7: Temporal correlation between the monthly standardized height anomalies and the Scandinavia pattern for January (adapted from Climate Prediction Center).

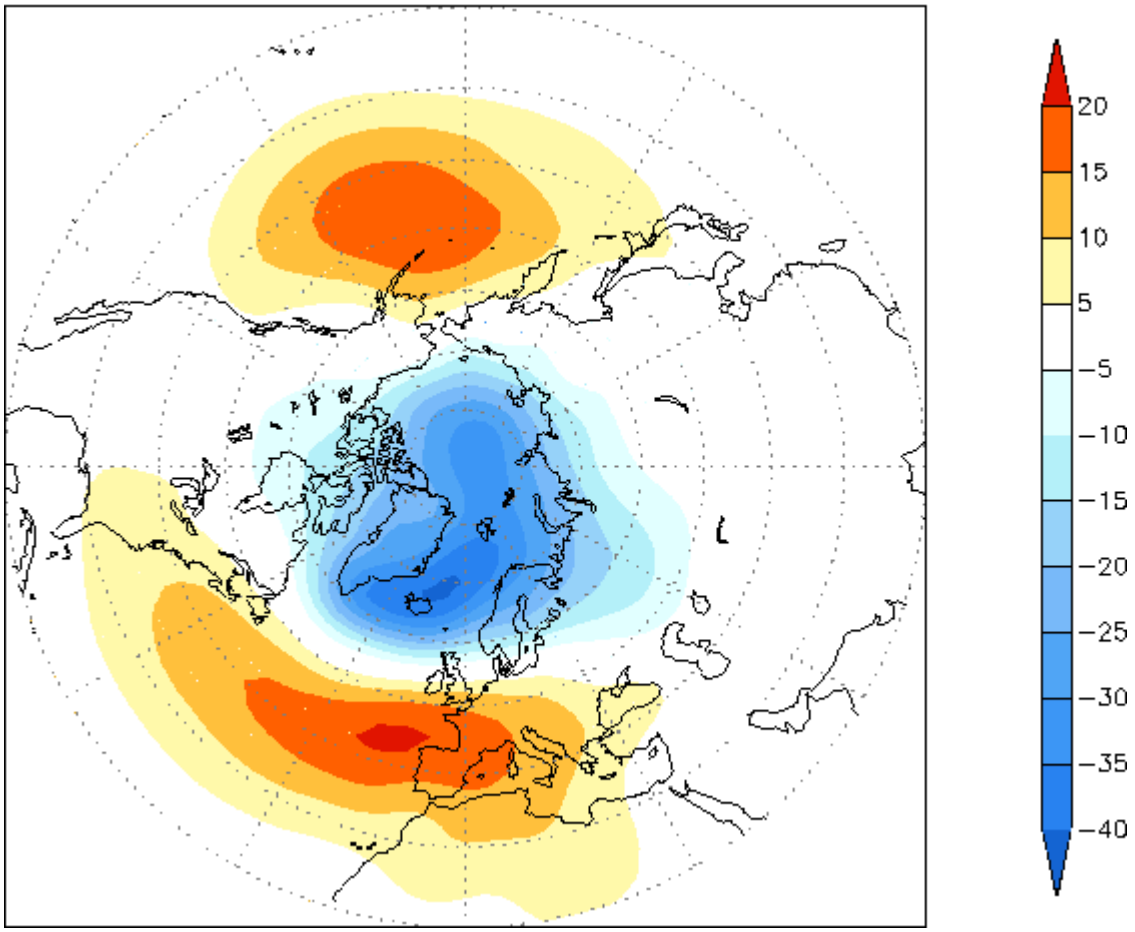

Figure 2.8: The loading pattern of the Arctic Oscillation, which is defined as the leading mode of Empirical Orthogonal Function (EOF) analysis of monthly mean 1000mb height during 1979-2000 period (adapted from Climate Prediction Center).

3. Results and Discussion

3.1 Analysis of Long Time Variations in Snow Depth

3.1.1 EOF Analysis and Correlation Analysis of Snow Depth

Based on the North et al. rule of thumb described in section 2.4.4 we found that only the first eigenvalue (EOF1) was clearly separated from the neighboring eigenvalue (Figure 3.1). However, the overlapping of the second and the third eigenvalue is minimal, thus we decided to include the second eigenvalue (EOF2) in our analysis as well. EOF1 and EOF2 (Figures 3.2 and 3.3) account for 41.4% and 18.6% of snow depth variability, respectively. We need to keep in mind that the pattern outside of the country borders is only an artifact of the interpolation, and do not represent any results. EOF1 patterns illustrate positive loadings across Southern and Central Norway, including Region 3. Loadings are close to zero in the north except for a small area which experiences slight negative loadings. Strongest positive loadings resemble a horse shoe pattern following the Southern coast. EOF2 patterns show strong positive loadings in North and Central Norway, including Regions 1 and 2, and across the western coast. Negative loadings are found in the southeastern part of the country, including Region 3. The boundary between positive and negative loadings in the south follows the mountain range, implying that both geographical and atmospheric features come play a role in the EOF analysis. Both EOF patterns show a transition from positive loadings to negative loadings right around our Region 2. EOF1 shows high values in the south, and low values in the north, while EOF2 shows the opposite pattern. It is obvious that the north

and south is governed by different climatic regimes. Since snow depth is directly influenced by both temperature and precipitation, along with other factors, it is not straightforward to define the EOFs. We cannot expect to identify the EOFs by only one of the pre defined atmospheric indices, because they were not established to explain accumulative precipitation. Both EOFs are somewhat correlated to at least a couple teleconnection indices, and together with the SLP and SST patterns they give an ambiguous picture of the leading modes. Most of the teleconnection patterns that are known to affect Norway are associated with warmer and wetter winter conditions. This means that the effects can actually work against each other, as and wetter weather leads to more precipitation, while warmer weather leads to more precipitation falling as rain instead of snow. Another complication is the fact that the teleconnection patterns are more dominant in certain periods over the years, and the leading role can switch back and forth between the different patterns. We also have to keep in mind that influences of the different teleconnections are affected by local topography and regional circulation; consequently their effects vary spatially within a region (Uvo, 2003). We are a little surprised to see the weak correlation to NAO, which we know to be the dominant mode of atmospheric variability in Northern Europe. This is however consistent with previous findings of Scherrer and Appenzeller (2006) where the third EOF of snow pack variability in the Swiss Alps was related to NAO.

EOF1 varies on a decadal scale and is negatively correlated to East Atlantic/Western Russia pattern using no lag and 1 month lag. It is also weakly negatively correlated to the Arctic Oscillation, and when comparing Figure 2.8 and Figure 3.4 a) we find that the patterns

are somewhat similar. Another hypothesis based on the plotted correlations between EOF1 time series and global SSTs (Figure 3.4 b)) suggest a connection to enhanced synoptic onshore flow, as we see very negative correlations around the entire south coast. Figure 3.4 a) shows a very strong pressure gradient across Norway, in the Northwest-Southeast direction. This might be the mechanism creating prevailing winds from the Southwest, and pushing precipitation inland. These winds might also be the reason for colder SSTs by overturning and bringing cold deep water to the surface. Another possible trigger for SST variability south of Norway is the heat transported by the North Atlantic Current (Figure 3.7). The variability of this heat transport is however not well known to this day. An ocean only experiment by Wu et al. (2004) indicates that SST variability in high latitudes of the North Atlantic Ocean, especially in the Gulf Stream extension area, is mainly caused by processes internal to the ocean, and thus complicated to identify.

The EOF2 time series shows inter-annual variation and is most likely related to climate change, as it demonstrates an increasing trend. At first glance, this second EOF is related to NAO due to its 2-3 year variability and the positive trend in NAO over the four last decades of the past century (Hurrell 1995). Figure 3.5 a) shows an area of very positive correlation with SLP right west of Great Britain. This might be one of the poles identifying the NAO pattern, but it resembles the EA pattern as well. It has been shown that winter precipitation along the Norwegian Southwestern coast line is greatly affected by the NAO produced moist westerly winds, together with orographic lift (Uvo, 2003). We also recognize the tripole SST anomaly pattern which accompanies the NAO (Figure 3.5 b)) described by

Seager et al. (2000). However, Table 3.1 shows relatively high negative correlations to EA and SCAND. We divided the 41 years period in two: 1960-1974 and 1975-2000, as done in Popova (2007) (section 2.4.6). We found that EOF2 is negatively correlated to SCAND in both periods, and positively correlated to NAO in the last period. Correlations were significant at 0.01, 0.05 and 0.1 alpha level, respectively. The first period was governed by a negative EA phase and correlation with EOF2 is significant at the 0.1 alpha level. The last period was governed by a positive EA phase, and in this period the correlation with EOF2 is significant at the 0.01 alpha level. This implies that EOF2 is strongly related to EA and SCAND throughout the entire period, and weakly related to NAO at least in the last couple of decades of the past century. The nature of the teleconnection influences differ. The signs of the correlations imply that mostly NAO and SCAND induced precipitation variability, and EA induces temperature variability dominate snow depth variability explained by EOF2. It is worth mentioning that we see some relation between EOF2 and El Niño Southern Oscillation (ENSO) as well. Merkel and Latif (2002) suggest an El Niño-related weakening of the NAO over Europe. Figure 3.5 b) shows some indication of a relationship between EOF2 and the ENSO SST patterns in the South Pacific, and the sea surface pressure pattern in Figure 3.5 a) resembles January-February anomalies of mean sea level pressure during strong El Niño years presented in Toniazzo and Scaife (2006) (Figure 3.6). For future research a combined precipitation and temperature EOF analysis is recommended, to facilitate the study of snow accumulation variability, and further investigation is needed in the significance of the previous mentioned correlations.

3.1.2 Spectral Analysis

Significant periodicities between 2 and 5 years were repeated at all eleven stations. These are likely to be associated with NAO, and possibly SCAND which shows a 2.5 years cycle. A 51 and 51.5 years cycle was identified at station 3 Karasjok and station 7 Os, respectively. These stations had the longest time series, making it possible to identify periodicities of smaller frequencies. We also found a 17.5 years cycle at stations 2 Cuovddatmohkki, and a 24 years cycle at station 4 Sihcajavri, but these are only significant at the 0.01 alpha level. The 24 years cycle might be the same as the 25.5 years cycle seen in the NAO time series mentioned in section 2.4.6.1.

3.1.3 Results of Time Series Analysis at Each Station

Our two piece nonlinear model (section 2.4.2) did a decent job fitting the date of maximum snow depth, and the end of snow season, but had some trouble with the start of snow season for certain years. As this was merely a supplementary approach, and a technique to detect any shift in the date of maximum snow depth, we only comment on the significant results. The results are summarized in Table 3.2.

3.1.3.1 Station 1: Jotkajavre (1926-2003)

Jotkajavre (Figure 3.8) shows a later start and an earlier end of snow season compared to the beginning of the analyzed period. We also see a slight decrease in the total number of snow days, but none of the three trends are statistically significant. Our nonlinear model shows an earlier date of maximum snow depth of about 10 days. This result has a p

value of 0.0334. Decrease in daily snow depth over the whole period is statistically significant at the 0.01 alpha level. All months except November show a decreasing trend in snow depth, but only trend lines for April and May are significant at the 0.05 alpha level. Cycles with periods of 2.68 and 2.83 years were found significant at the 0.01 alpha level, and cycles with periods of 3.07 and 3.35 years were found significant at the 0.05 alpha level.

3.1.3.2 Station 2: Cuovddatmohkki (1967-2003)

There are several observations missing at this station, and the time series are additionally quite short, which complicates the analysis. Cuovddatmohkki (Figure 3.9) shows a later start of the snow season. We also found that the snow season ends about 2 weeks earlier, and the number of snow days has decreased by 28 days. The two latter are shown as statistically significant at the 0.01 alpha level. Results from the nonlinear model imply that the snow season ends over a month earlier ($p = 0.0004$). Daily snow depth shows a significant decreasing trend using the 0.01 alpha level. We found a decreasing trend in snow depth for most months, except November and March. The only significant trend at the 0.05 alpha level is found in May. No cycles were significant at 0.01 or 0.05 alpha levels, but cycles with periods of 17.5, 2.57, and 2.27 years were found significant at the 0.01 alpha level.

3.1.3.3 Station 3: Karasjok (1901-2003)

Karasjok (Figure 3.10) shows a later start and an earlier end of snow season, and a decrease in the number of snow days, but none of the changes are statistically significant.

Daily values of snow depth only go back to 1957, showing a slight increase. However, we have monthly data from 1901 that reveal a decrease in snow depth in the first half of the century, and an increase in the last half of the century. The overall trend is slightly positive. The month of May was not plotted due to very low snow depth values. January, February, and March all show significant trends at the 0.01 alpha level, and the trend in April is significant at the 0.05 alpha level. At this station we found a cycle with a period of 51.0 years that is significant at the 0.01 alpha level. This cycle is evident in the monthly snow depth data, as mentioned above. Three cycles with periods of 4.11, 3.1, and 2.55 years were found significant at the 0.05 alpha level.

3.1.3.4 Station 4: Sihcajavri (1954-2003)

Sihcajavri (Figure 3.11) shows only minor changes to the start and end of snow season. We do see a 12 days decrease in the number of snow days, but the trend is not statistically significant. Our nonlinear model however, indicates that the snow season ends about 10 days earlier compared to the beginning of the period, with a p value of 0.0685.

Daily snow depth shows a significant decreasing trend at the 0.01 alpha level. All months show a decreasing trend as well. For January, February, and March, the trends are significant at the 0.01 alpha level, while for December and April, the trends are significant at the 0.05 alpha level. One 2.0 years cycle was found significant at the 0.01 alpha level, and two cycles with period of 24.0, and 4.83 years were found significant at the 0.1 alpha level.

3.1.3.5 Station 5: Røros (1954-2001)

Røros (Figure 3.12) shows about a week later start, and only a slightly earlier end of snow season. There is a decrease in the number of snow days of about 10 days, but none of these three trends are shown as statistically significant. Daily snow depth reveals a decreasing trend that is significant at the 0.01 alpha level. Also at this station we see a decreasing trend in snow depth for all months (May was not plotted here due to low values). The trend lines for December and January are significant at the 0.05 alpha level. Only one cycle stood out at this station, showing a period of 2.95 years. The cycle is significant at the 0.05 alpha level.

3.1.3.6 Station 6: Aursund (1957-2003)

We do not see any significant trends in the start and end of snow season or the number of snow days when analyzing the data series manually (Figure 3.13). However, our nonlinear model estimates a 10 days earlier date of maximum snow depth ($p = 0.0681$). We see a slightly decreasing trend in the daily snow depth data, but it is not statistically significant. There is no repeated trend in the monthly data, as some months show decreasing snow depth with time, while other months show increasing snow depth. In addition, none of the trend lines are significant. A cycle with a 2.49 years period was found significant at the 0.05 alpha level, and two cycles with periods of 2.93 and 2.7 years were found significant at the 0.1 alpha level.

3.1.3.7 Station 7: Os i Østerdal (1900-2003)

The snow season at Os (Figure 3.14) is found to start over a week later, and to end a few days earlier. The number of snow days has decreased by about 15 days. Both the start of snow season and number of snow days show statistically significant trends. Our nonlinear model shows a very significant trend in the end of snow season as well, estimating it to occur 2-3 weeks earlier compared to the beginning of the period. The p value is less than 0.0001. The first half of the century up to about 1958 is governed by a negative trend in snow depth. After that we see a positive trend, while the overall trend is significantly negative at the 0.01 alpha level. All months also reveal a decreasing trend. Trends for all months, except November, are significant at the 0.01 alpha level. A 51.5 years cycle was found significant at the 0.01 alpha level, and three cycles of 5.04, 3.01, and 2.61 years were found significant at the 0.05 alpha level.

3.1.3.8 Station 8: Vauldalen (1957-2003)

We don’t see a major change in the start and end of snow season at Vauldalen (Figure 3.15). However, the total number of snow days is reduced by about eleven days, and this reduction is statistically significant. The nonlinear model, on the other hand, estimates the snow season to end more than 10 days earlier ($p = 0.0218$). Daily snow depth shows a decreasing trend that is significant at the 0.01 alpha level. The same trend is found for all months, but only the trend for May is significant at the 0.05 alpha level. One 2.95 years cycle was found significant at the 0.05 alpha level at this station.

3.1.3.9 Station 9: Gardermoen (1957-2003)

The snow season at Gardermoen (Figure 3.16) starts a few days earlier at the end of the analyzed period, and it ends about 10 days earlier, but the changes are not statistically significant. The trend for the number of snow days, however, is statistically significant, with a decrease of about 25 days. We found a significant decreasing trend in daily snow depth at the 0.01 alpha level. All months show a decreasing trend in snow depth as well, but only the trend in February is significant at the 0.05 alpha level. Due to low values, we did not plot snow depth for May. A 2.93 years cycle was found significant at the 0.1 alpha level.

3.1.3.10 Station 10: Ukkestad (1966-2003)

Ukkestad (Figure 3.17) shows a slightly earlier start of snow season, and an earlier end of snow season of almost two weeks. The number of snow days has decreased by as much as 45 days. The trends for the end of snow season and the number of snow days are shown to be statistically significant. Also at this station the observations show a decrease in snow depth with time for daily values and for all months. The decreasing trend in February is significant at the 0.01 alpha level, so is the trend in the daily values. For January, March, and April, the trends are significant at the 0.05 alpha level. May is not plotted due to low values. One cycle with a period of 2.93 years was found significant at the 0.1 alpha level.

3.1.3.11 Station 11: Eidsvoll-verk (1957-2003)

We don’t see a change in the start of snow season at Eidsvoll-verk (Figure 3.18), but it ends over two weeks earlier than at the beginning of the analyzed period. In addition, the

number of snow days decreased by around 23 days. Also here, the end of snow season and the number of snow days show statistically significant trends. The trend in snow depth is decreasing for daily data and for all months at this station. The trend in daily values is significant at the 0.01 alpha level, and the trend for February is significant at the 0.05 alpha level. One cycle with a period of 2.94 years was found significant at the 0.1 alpha level.

3.1.3.12 Summary and Regional Differences

Region 1 and Region 2 are positively affected by EOF2, while the effect of EOF1 is minimal. Region 3 is affected positively by EOF1 and negatively by EOF2. This might be one of the reasons why the variability is greater in this region as shown in Figure 3.19. Region 2 is situated close to the transition area from positive to negative EOF1 and EOF2 loadings, which might explain the inconsistent results between the four stations. The spectral analysis also indicates that all regions are influenced by EOF2. We see a later start of snow season at all stations in Region 1 and Region 2, but a slightly earlier start of snow season at the stations in Region 3. All eleven stations reveal an earlier end of snow season and a decrease in number of snow days, but the largest decrease is found in Region 3. This region also experiences the strongest decrease in snow depth. This is most likely connected to the low altitude and proximity to the ocean, which leaves Region 3 more sensitive to global warming. Region 3 is located in an area with negative EOF2 loadings, and this builds further evidence for our argument, since we already related EOF2 to climate change. Karasjok is the only station that illustrates an overall increase in snow depth. It must be mentioned that direct

comparison between stations is not accurate, since the time series are of different lengths.

3.2 Evaluation of the Norwegian Snow Model (NSM)

3.2.1 Underestimation of Snow Depth

The statistical results shown in Table 3.3, Table 3.4, and Table 3.5 imply a systematic negative bias in the snow model, resulting in underestimation of snow depth. At all stations except station 8 Vauldalen we found that the model simulates less total seasonal snow. Vauldalen is located at 830 meters above sea level, the highest elevation of the eleven stations. As we know, the algorithm for increased precipitation with elevation is a little exaggerated, resulting in overestimation of snow depth in high mountain areas. Least underestimation was found at the three stations in Region 3, particularly at station 10 Ukkestad, which did not show much difference from observations. The model also underestimates snow depth on the four selected dates. The exceptions are at station 1 Jotkajavre on December 15th, and again at station 8 Vauldalen on the same date. However, snow depth simulations on the other dates at the last mentioned station showed very good resemblance to the observations. Least underestimation was also here found in Region 3. Region 2 did better in this first part of the analysis than Region 1. In an analysis of the snow depth algorithms used in the snow model, carried out by NVE, it is concluded that the VIC approach for calculating snow depth due to compaction tends to compact the snow slightly too much, resulting in too high snow density (Alfnes, 2008). This might be one of the reasons for the negative bias in the model. The same study shows that simulated snow water

equivalent is in many places higher than that observed, compensating for the high snow density. However, this might not be the case everywhere. Another possible explanation for under prediction of snow depth can be the precipitation and temperature data used as input in the snow model. It is obvious that the snow model misses some peak snow depth values. This is most likely a consequence of simulating less precipitation during extreme snow events, which is a common problem among climate models. In the validation of the interpolated temperature and precipitation values used in the snow model, described in Jansson et al., 2007, it is found that interpolated values of temperature are generally colder than observations, and the interpolated precipitation is higher for small precipitation amounts, and lower for large precipitation amounts compared to observations. For our analysis regions, we found that temperature, at the stations where measurements are available, shows very high resemblance between observations and simulations. However, simulated precipitation values are higher than observed values at most stations, except at station 10 Ukkestad. This is probably due to the correction for wind attributable under catchment of precipitation. The greatest overestimations were found at stations 5 Røros, 6 Aursund, and 8 Vauldalen, although Røros also showed underestimation many places. The snow depth simulations at these three stations were however relatively good. This leads us to believe that the VIC approach is the actual reason for the model's underestimation of snow depth, as discussed above. It is possible that the strong over prediction of snow fall at stations 5 Røros, 6 Aursund, and 8 Vauldalen compensates for the exaggerated snow compaction, resulting in simulated snow depth closer to the observed value, or higher than the observed value in the case of station 8 Vauldalen.

3.2.2 Real Elevation versus Model Elevation

The difference in station height (Table 2.2) does at first glance seem to have some influence on the results. As mentioned in the introduction, the snow model uses the assumption that precipitation increases with increasing elevation (Engeset et al., 2004). This means that a higher elevation used in the snow model could potentially result in a longer snow season, and/or a higher number of snow days. If we take a look at the two stations with the biggest differences, Os i Østerdal, and Vauldalen, we notice this exact pattern. Os simulations use an elevation that is 88 meters lower than the real station height, and at this station we find that the simulated snow season is shorter, and the number of snow days is considerably less. The simulated mean total snow depth for the snow season is almost 42% less than the observed value, and at all four dates studied there is considerably lower snow depth in the simulations. At Vauldalen, the elevation used in the snow model is 50 meters higher than the real station height, and at this station we see a longer simulated snow season, and the number of snow days is higher. This is also the only station that simulates greater snow depth at some of the dates studied, and a higher mean total snow depth for the snow season. This pattern can be seen at a few other stations, but not all.

Engeset el.al., 2004 found in their validation report, that the elevation gradient for precipitation is too large, resulting in overestimation at stations located higher than the surrounding stations, and slight underestimation at stations located at lower levels. On the other hand, the majority of our stations show over prediction of precipitation or snow fall during the winter months, regardless of the elevation difference. This leads us to believe that

the elevation difference does influence some stations, while at other locations there might be additional factors influencing the simulated snow depth.

3.2.3 Examination of the Snow Season at Each Station

Statistical results from the manual comparison of snow season indicators are presented in Table 3.6 and Table 3.7.

3.2.3.1 Station 1: Jotkajavre

Figures 3.20 and 3.21 reveal underestimation of snow accumulation at Jotkajavre, which is also true for March 15th (Figure 3.22 d)). Figure 3.22 a), however, demonstrates overestimation of snow accumulation on December 15th. Figure 3.23 a) shows that the simulated start of snow season follows the observed trend pretty well, and the trend line is similar with a slightly positive inclination. There is more variability in the simulations, and we see a slightly later start of the season (Figure 3.23 b)). The simulated end of snow season shows some trouble in the 1970's, with earlier dates than the observations. The trend line is similar with a decreasing trend, but the intercepts are extremely significantly different (Figure 3.24 a)). Also here, the simulations vary more, and the season ends a few days earlier on average (Figure 3.24 b)). The simulated number of snow days per hydrologic year is lower than the observations, especially in the 1970's, and the intercepts are very significantly different (Figure 3.25 a)). The trend line, however, is similar, with a negative inclination. There is a little more variability in the simulations here as well, and in general we see fewer snow days in the simulations (Figure 3.25 b)).

3.2.3.2 Station 2: Cuovddatmohkki

Also at this station there is underestimation of snow accumulation by the snow model (Figures 3.26 and 3.27). Figure 3.28 support this statement, showing lower simulated values on all four selected dates. Figures 3.29 a), 3.30 a), and 3.31 a) reveal that the observed and simulated trends are not significantly different but the patterns are not well conserved for any of the three parameters. The variability is higher for the simulated start of snow season, and the data shows a later start date (Figure 3.29 b)). The simulated end of snow season is slightly earlier than the observed end of snow season (Figure 3.30 b)), and the simulations show less variability. The number of snow days shows a decreasing trend, but this is much more pronounced for the observations. The simulations show a little more variability, and the number of snow days is lower on average (Figure 3.31 b)).

3.2.3.3 Station 3: Karasjok

This station is strongly affected by inversion, and the model has shown to fail significantly at temperatures below -10°C (Tveito et al., 2005). We see severe underestimation of total seasonal snow depth (Figure 3.32), mean daily snow depth (Figure 3.33) and snow depth on the four selected dates (Figure 3.34). The simulated start of snow season shows a slightly later date (Figure 3.35 b)), but the trend line is similar with an increasing trend (Figure 3.35 a)), and there is no significant difference in the variability. Figure 3.36 b) reveal that the simulated snow season ends slightly earlier, and the intercepts are significantly different. The trend lines are similar with a decreasing trend, and the

variability is the same here as well (Figure 3.36a)). The simulated number of snow days shows lower values in Figure 3.37 b) but the trend is conserved (Figure 3.37 a)). The same figure shows similar trend lines, with a negative inclination, and the same amount of variability is seen.

3.2.3.4 Station 4: Sihcajavri

Figures 3.38-40 demonstrate that snow accumulation is severely underestimated also at this station. As seen in Figure 3.41 a) the simulated start of snow season follows observations very well, and the trend line, which is decreasing, is similar. We see some higher variability. The simulated end of snow season shows an earlier date (Figure 3.42 b)), and the intercept is very significantly different. The trend lines are not significantly different, but the simulations show a decreasing trend while the observations show an increasing trend (Figure 3.42 a)). The variability is lower for the simulations. The simulated number of snow days follows the pattern, but has some trouble from1986 to 1996 as seen in Figure 3.43 a). The trend line is almost the same, although it slightly decreases for the simulations, and slightly increases for the observations (Figure 3.43 b)). The variability is slightly less.

3.2.3.5 Station 5: Røros

Figures 3.44 and 3.45 do not reveal great differenced in total seasonal snow depth and average daily snow depth for this stations. We do see slight underestimation of snow depth on the four selected dates (Figure 3.46), but the difference is minimal here as well. The simulated start of snow season follows the observed pattern pretty well, with an exception in

1968 (Figure 3.47 a)). The trend line increases less for simulations than for observations, but the slopes are not significantly different. In Figure 3.47 b) we see an earlier start date, and there is a little more variability in the simulated data. The simulated end of snow season conserves the pattern well, which we see in Figure 3.48 a) but Figure 3.48 b) shows a somewhat later date. The intercepts are extremely significantly different. The trend lines are not significantly different, but we see a decreasing trend for the simulations and a slight increase for the observations. The simulated data demonstrate more variability. The simulated number of snow days shows a good pattern but higher values than the observations and the intercepts are very significantly different (Figure 3.49). There is more variability in the simulations.

3.2.3.6 Station 6: Aursund

In Figures 3.50-51 we see that snow accumulation is underestimated at this station. This is also seen on the four dates in Figure 3.52. The simulations show a later start of snow season (Figure 3.53), and there is more variability than in the observations. The trend line is similar, but simulations show slight decrease, while observations show slight increase. The simulated end of snow season shows a slightly earlier date (Figure 3.54), and the trend line decreases more for simulations than for observations. There is less variability. In Figure 3.55 we see that the simulated number of snow days shows slight undershooting and less variability, but the trend line is almost the same with a decreasing trend.

3.2.3.7 Station 7: Os i Østerdal

Figures 3.56-57 demonstrate strong underestimation of total seasonal snow accumulation, and average daily snow depth. The same is seen for snow depth on the four dates analyzed in Figure 3.58. The simulated data shows a later start date in Figure 3.59, and more variability. The trend lines show the same positive inclination, but the intercepts are significantly different. The simulated end of snow season is much earlier than the observed (Figure 3.60), and there is a little more variability. The trend line is also different, with the simulations showing lower values and a decreasing trend, while the observations show a slightly increasing trend. The intercepts are extremely significantly different. Figure 3.61 reveals that the simulated number of snow days also shows strong undershooting, and less variability. The simulated trend line has lower values and a negative inclination, while the observed trend line increases. Also for this variable, the intercepts are extremely significantly different. Os is the stations with the lowest correlation between simulations and observations (Table 3.6). One possible explanation to the bad results found at this station might be the huge difference in elevation discussed in section 3.2.2. The fact that the station is situated on a steep hill might create difficulties for the snow model, and the interpolated temperatures might be inaccurate.

3.2.3.8 Station 8: Vauldalen

Total seasonal snow depth (Figure 3.62), average daily snow depth (Figure 3.63) and snow depth on the four selected dates (Figure 3.64) all show very high resemblance between

observations and simulations. In Figure 3.65 the simulated start of snow season shows a slightly earlier date, and the intercept is significantly different. The simulated trend line decreases, while the observed trend line increases, but the slopes are not found significantly different. There is not much difference in the variability. The simulated end of snow season shows a later date, the intercept is significantly different, and there is a little more variability in the data (Figure 3.66). The trend lines both decrease, but the simulated trend line decreases less. In Figure 3.67 we see that the simulated number of snow days shows higher values, and the intercept is extremely significantly different. The simulated trend line decreases more than the observed trend line, but the slopes are not significantly different, and the variability is the same.

3.2.3.9 Station 9: Gardermoen

We see slight underestimation of total seasonal snow depth (Figure 3.68) and average daily snow depth (Figure 3.69) at this station. Figure 3.70 demonstrates slight overestimation of snow depth on the four dates in the beginning of the analyzed period, and slight underestimation of snow depth in the end of the analyzed period. The simulated start of snow season shows some trouble from 1995 to 2000, but conserves the trend well overall (Figure 3.71). The same figure reveals that the snow season starts only a few days earlier. The trend lines are not significantly different, but the simulations show increase, while the observations show no trend at all. Also there is less variability in the simulated data. The simulated end of snow season is very close to observations as seen in Figure 3.72, and there is little difference

in variability. The trend is similar, with an exception in 1996 and slight overshooting between 1966 and 1972. The trend lines both decrease, but the simulations decrease more. There is no considerable difference in the variability. The simulated number of snow days also shows good results (Figure 3.73), with the same variability and similarly decreasing trend lines.

3.2.3.10 Station 10: Ukkestad

Figure 3.74 demonstrates slight underestimation of total seasonal snow depth in the last part of the analyzed period. The same is seen on the four dates in Figure 3.76. Slight underestimation of average daily snow depth is also evident in Figure 3.75. All three simulated parameters show very good results as seen in Figures 3.77-79, except for missing a few peaks. No trend lines are found significantly different, but the trend line for the simulated start of snow season shows a positive inclination, while the observed trend line is slightly negative. For the end of snow season the trend lines both decrease, but the simulated decreases more. There is more variability in the simulations. The trend lines for number of snow days show the same decreasing trend, but the simulations show less variability.

3.2.3.11 Station 11: Eidsvoll-verk

Also here slight underestimation of total seasonal snow depth (Figure 3.80) and snow depth on the four selected dates (Figure 3.82) is seen in the end of the analyzed period. Figure 3.81 demonstrates underestimation of average daily snow depth as well. This station shows very good results overall when it comes to the snow season, and the highest

correlation between simulations and observations (Table 3.6). The dates for start and end of snow season are nearly identical (Figures 3.83-84), as is the number of snow days (Figure 3.85), and the variability differs minimally. The trend lines for start of snow season are similar, and show positive inclination. For the end of snow season, the simulated trend line decreases more, but does not differ significantly, and for the number of snow days the trend lines show almost the same decreasing trend.

3.2.3.12 Summary and Regional Differences

Region 1 shows reasonable results, with average coefficients of determination (R^2) of 0.53, 0.50, and 0.65 for start and end of the snow season and the number of snow days, respectively (Table 3.7). Here the snow model simulates a shorter snow season for all four stations, ending 3-7 days earlier than the observed snow season. This is consistent with the findings in the first part of the analysis, where the model shows significant under prediction of snow depth at all four stations. There is no statistical evidence that the trend lines or intercepts are different at any of the three stations. From the EOF analysis we find that snow depth variability at Region 1 is mainly influenced by the second EOF mode, which we believe is related to EA, SCAND and NAO.

Although the snow model does not underestimate snow to the same extent in Region 2 compared to Region 1, the worst results in the comparison of the snow season are found here. The average coefficients of determination for start and end of the snow season and the number of snow days were 0.50, 0.33, and 0.58, respectively. In this region the difference in

number of snow days go up to 20 days at the most. There is also no consistency between the differences, as two stations reveal a longer simulated snow season than the observations, while the other two stations reveal a simulated shorter snow season. The simulated start of snow season shows higher variability than observations. Being located in a transition area between climate regimes might explain the poor performance of the snow model in Region 2, and the inconsistent results we find at the four stations. Another possibility might be the fact that three of the four stations do not have observations of temperature, meaning temperature is interpolated at these stations.

Region 3 shows the best result overall with the highest average coefficients of determination of 0.61, 0.48, and 0.83 for start and end of the snow season and the number of snow days, respectively. This is the only region where all three variables show significant correlation coefficients at the 0.05 alpha level. There is only a 1-6 days difference between observed and simulated average number of snow days. We also see less variability in the simulated start of snow season.

Logically one would think that the great variability in snow depth and snow season features seen in Region 3 makes it harder for the model to perform well, but this does not seem to be the case. The fact that the model does good at all three stations in this region is not all that surprising, since the stations are located close to each other. In Region 1, the distance between stations is much larger, while in region 2 the variance in station elevation is much greater, which might explain the varying performance of the snow model. Hence, by examining the spread between the stations at the three regions, we find that the two first

regions situated furthest north show a much greater spread than the third region. This supports our earlier statement of the model performing well in the regions with less spread between the stations.

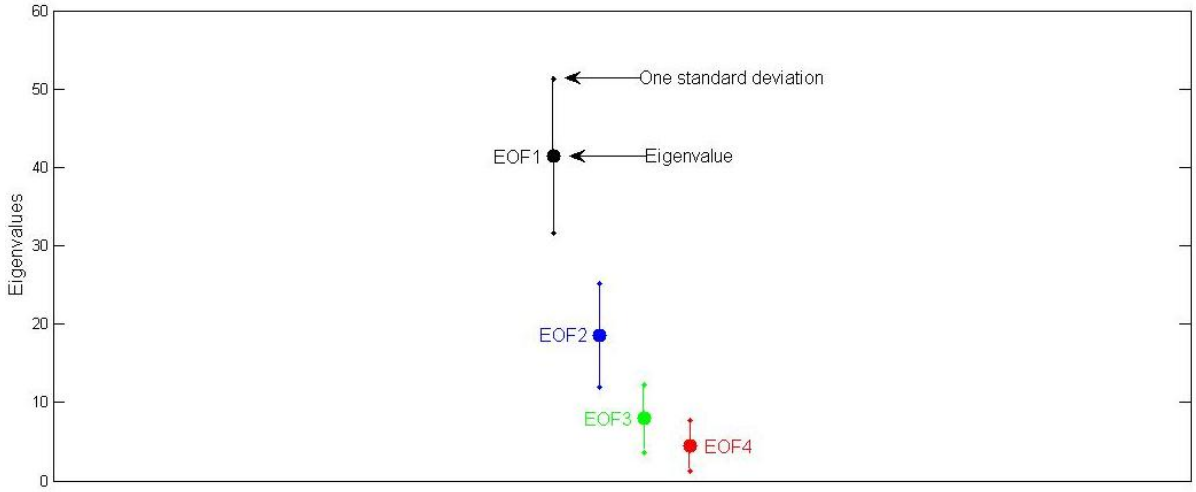

Figure 3.1: North et al. Rule of Thumb for testing separation between eigenvalues.

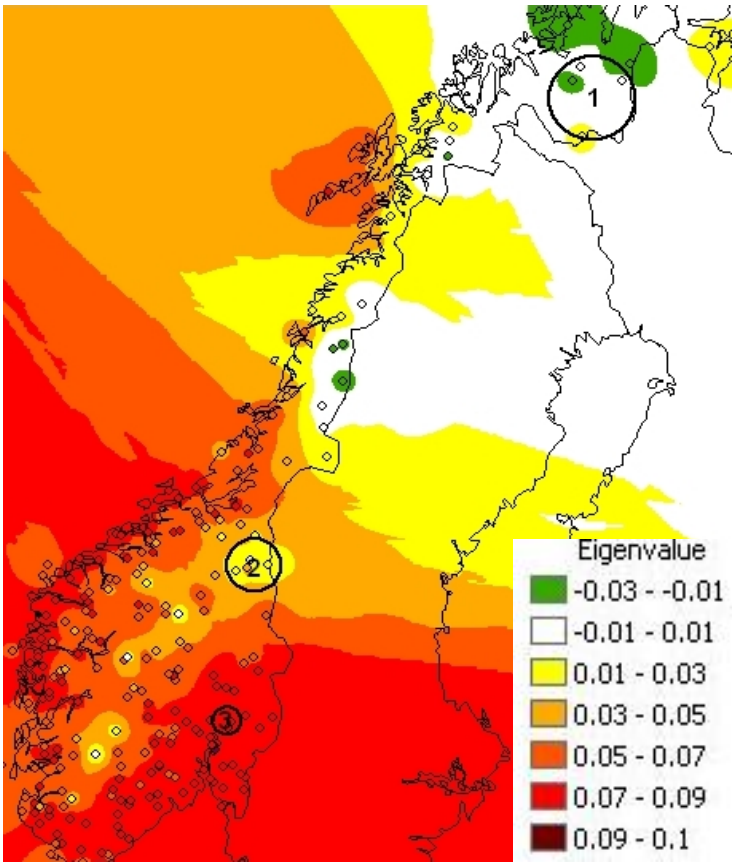

Figure 3.2: EOF1 loadings with Inverse distance weighted (IDW) interpolation. Our three regions are circled.

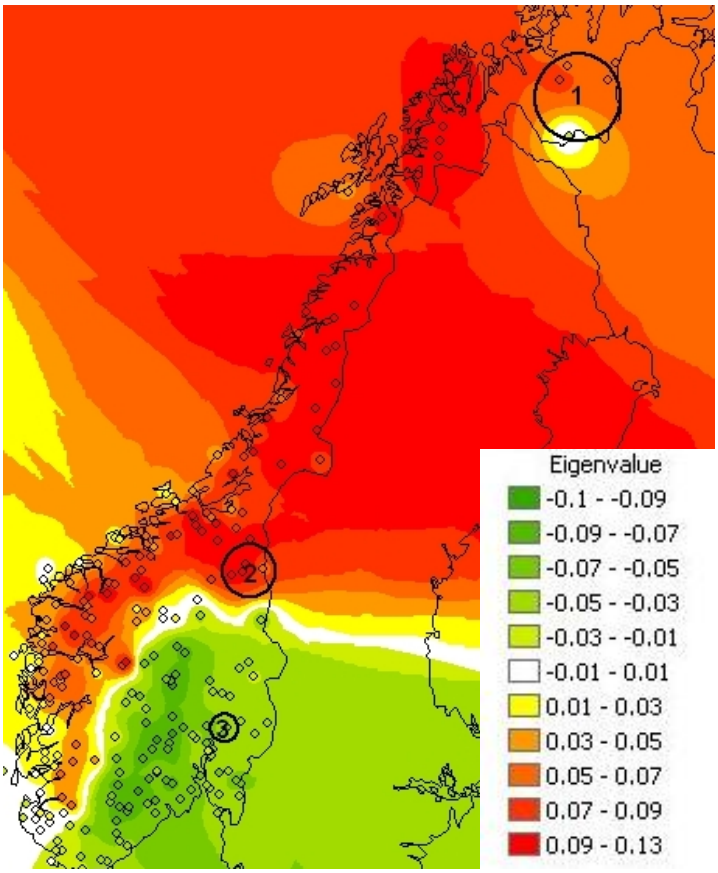

Figure 3.3: EOF2 loadings with Inverse distance weighted (IDW) interpolation. Our three regions are circled.

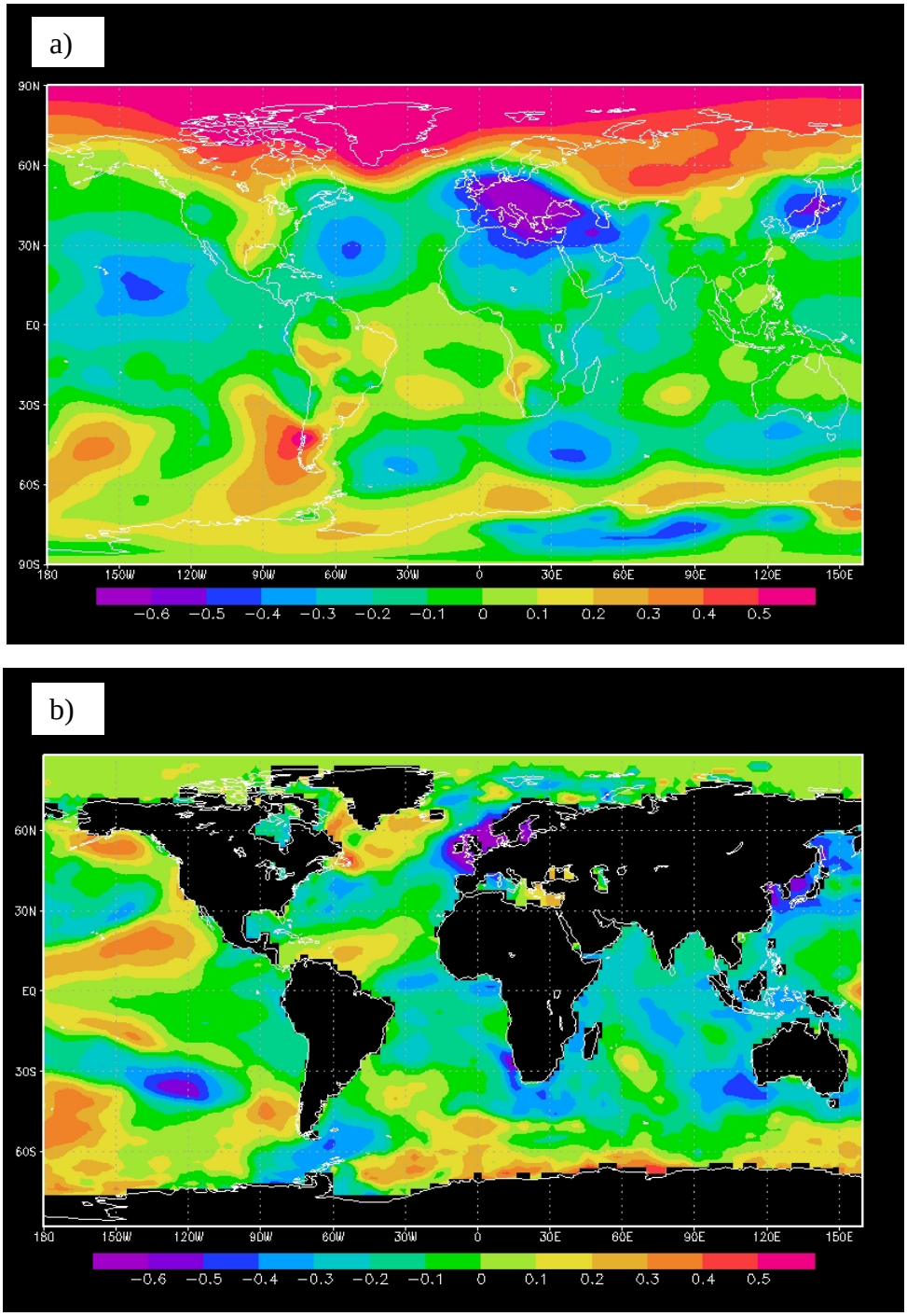

Figure 3.4: EOF1 time series correlated with a) global sea level pressure (SLP) b) global sea surface temperature (SST), for the winter season December through March.

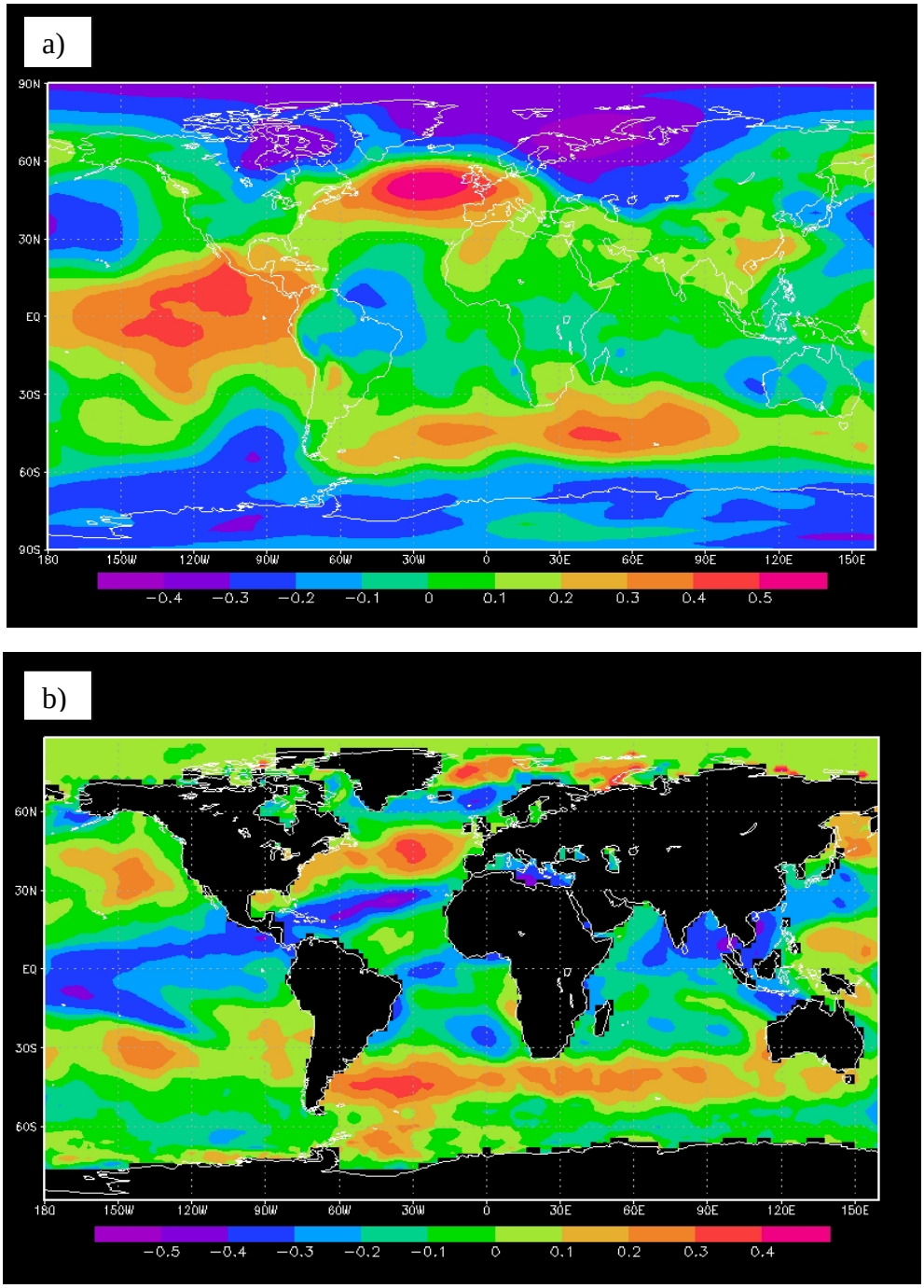

Figure 3.5: EOF2 time series correlated with a) global sea level pressure (SLP) b) global sea surface temperature (SST), for the winter season December through March.

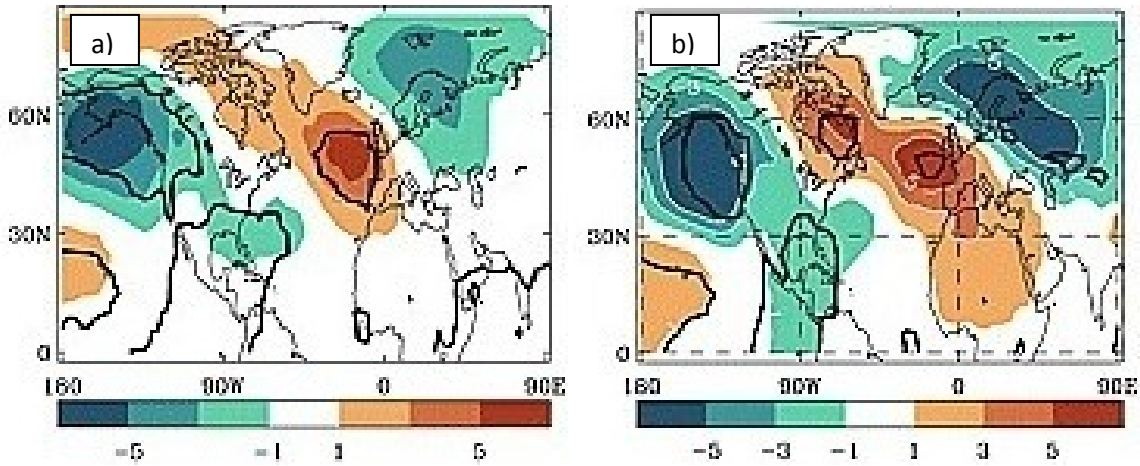

Figure 3.6: January-February anomalies of pressure at mean sea-level during strong El Niño years derived from a) HadSLP2 data from 1850 and from b) NCEP data for the period 1950–2000. The black contour marks the 2.5 and 97.5 percentiles (adapted from Toniazzo, 2006).

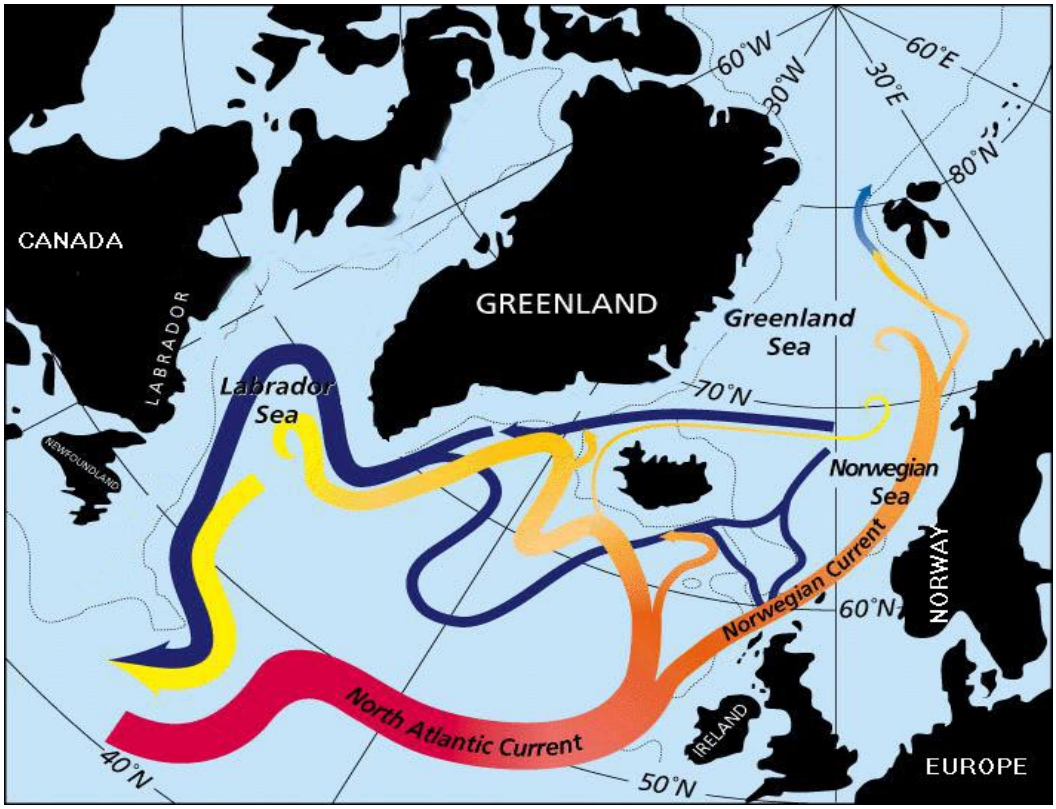

Figure 3.7: Subpolar currents in the North Atlantic (credit to Jack Cook, Woods Hole Oceanographic Institute).

Table 3.1: Linear correlation (R) between NH teleconnections and: 1. EOF1 and EOF2 and 2. Mean snow depth in our three regions, for the winter season December through March. Dark colored cell and bold number: Significant at the 99% confidence level. Dark colored cell: Significant at the 95% confidence level. Light colored cell: Significant at the 90% confidence level.

Index	EOF1	EOF2	Region 1	Region 2	Region 3
1.NAO	-0.29	0.23	0.31	0.11	-0.34
1 month lag	-0.22	0.29	0.23	0.12	0.29
2 months lag	0.01	0.22	0.05	0.02	-0.04
3 months lag	0.13	0.26	-0.12	0.01	0.01
2.EA	-0.18	**-0.45**	-0.11	**-0.47**	-0.04
1 month lag	-0.17	**-0.47**	-0.20	**-0.50**	-0.02
2 months lag	-0.13	-0.38	-0.26	**-0.42**	-0.05
3 months lag	-0.01	-0.05	0.02	-0.10	0.01
3.WP	-0.18	-0.38	-0.26	-0.25	-0.04
1 month lag	-0.16	-0.31	-0.18	-0.20	-0.06
2 months lag	-0.09	-0.35	-0.23	-0.18	0.11
3 months lag	0.01	-0.36	-0.32	-0.16	0.14
4.EA/WR	-0.38	0.12	-0.19	-0.01	-0.32
1 month lag	**-0.52**	0.28	-0.05	0.12	**-0.50**
2 months lag	0.32	0.23	0.13	-0.05	-0.31
3 months lag	-0.01	0.10	0.23	-0.11	0.01
5.SCAND	0.14	**-0.54**	-0.37	**-0.46**	0.35
1 month lag	0.22	**-0.68**	**-0.44**	**-0.56**	0.39
2 months lag	0.13	**-0.65**	**-0.44**	**-0.54**	0.24
3 months lag	0.15	**-0.43**	**-0.43**	-0.34	0.15
6.AO	-0.24	0.19	-0.02	-0.01	-0.30
1 month lag	-0.28	0.16	0.00	-0.06	-0.33
2 months lag	-0.24	0.04	0.01	-0.11	-0.20
3 months lag	-0.23	-0.15	0.04	-0.25	-0.07

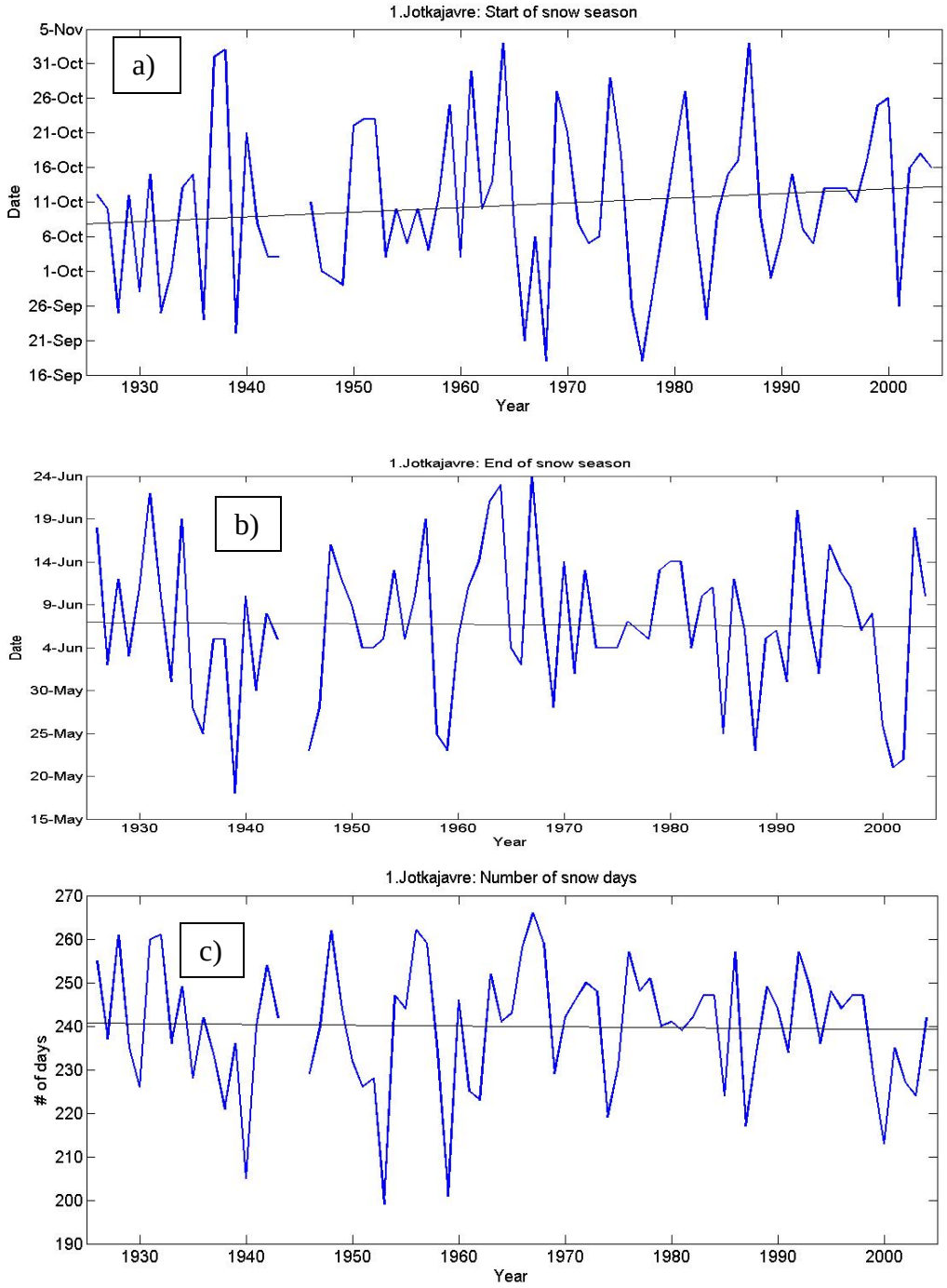

Figure 3.8: Station 1 Jotkajavre: a) Start of snow season b) End of snow season c) Number of snow days per hydrological year.

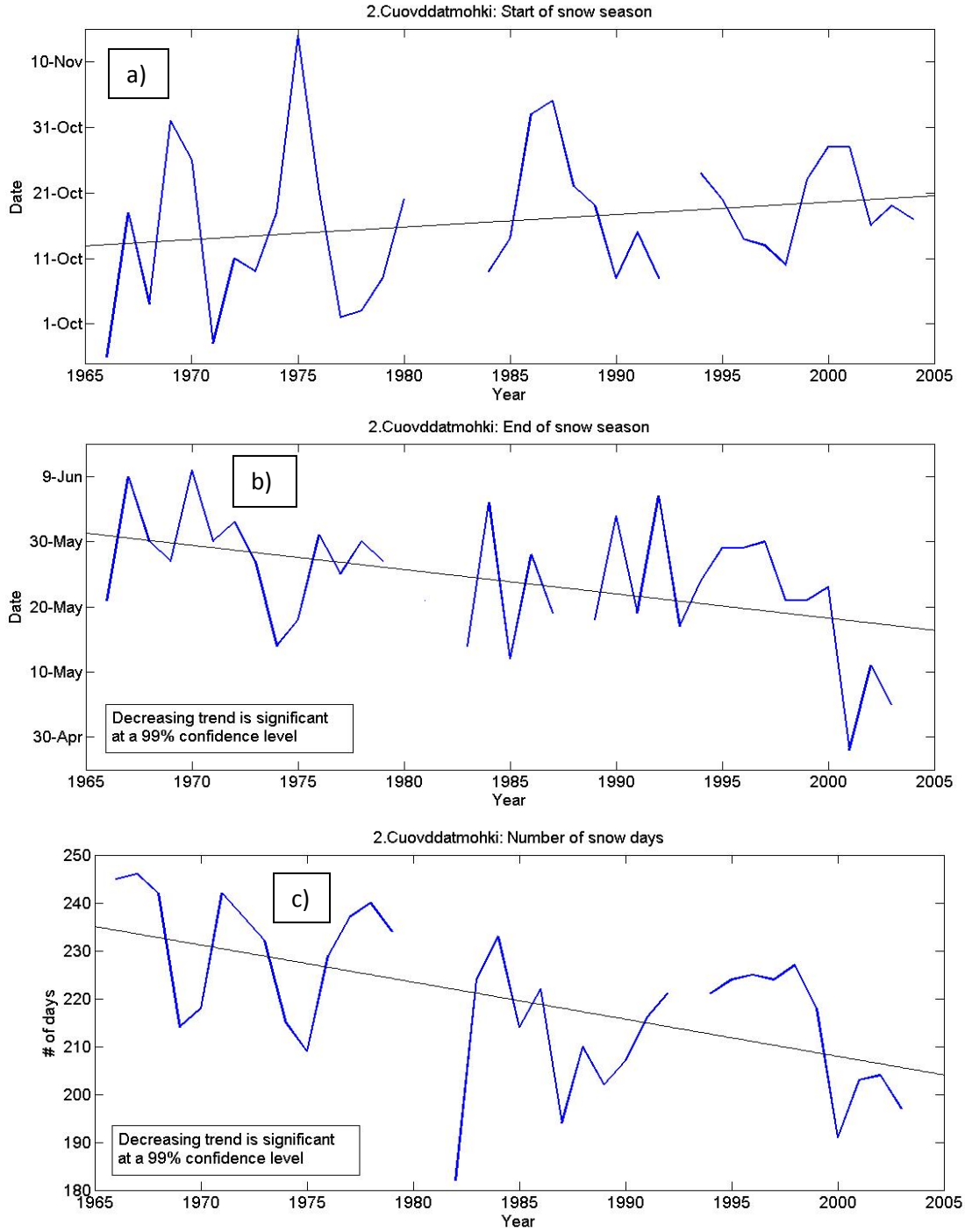

Figure 3.9: Station 2 Cuovddatmohkki: a) Start of snow season b) End of snow season c) Number of snow days per hydrological year.

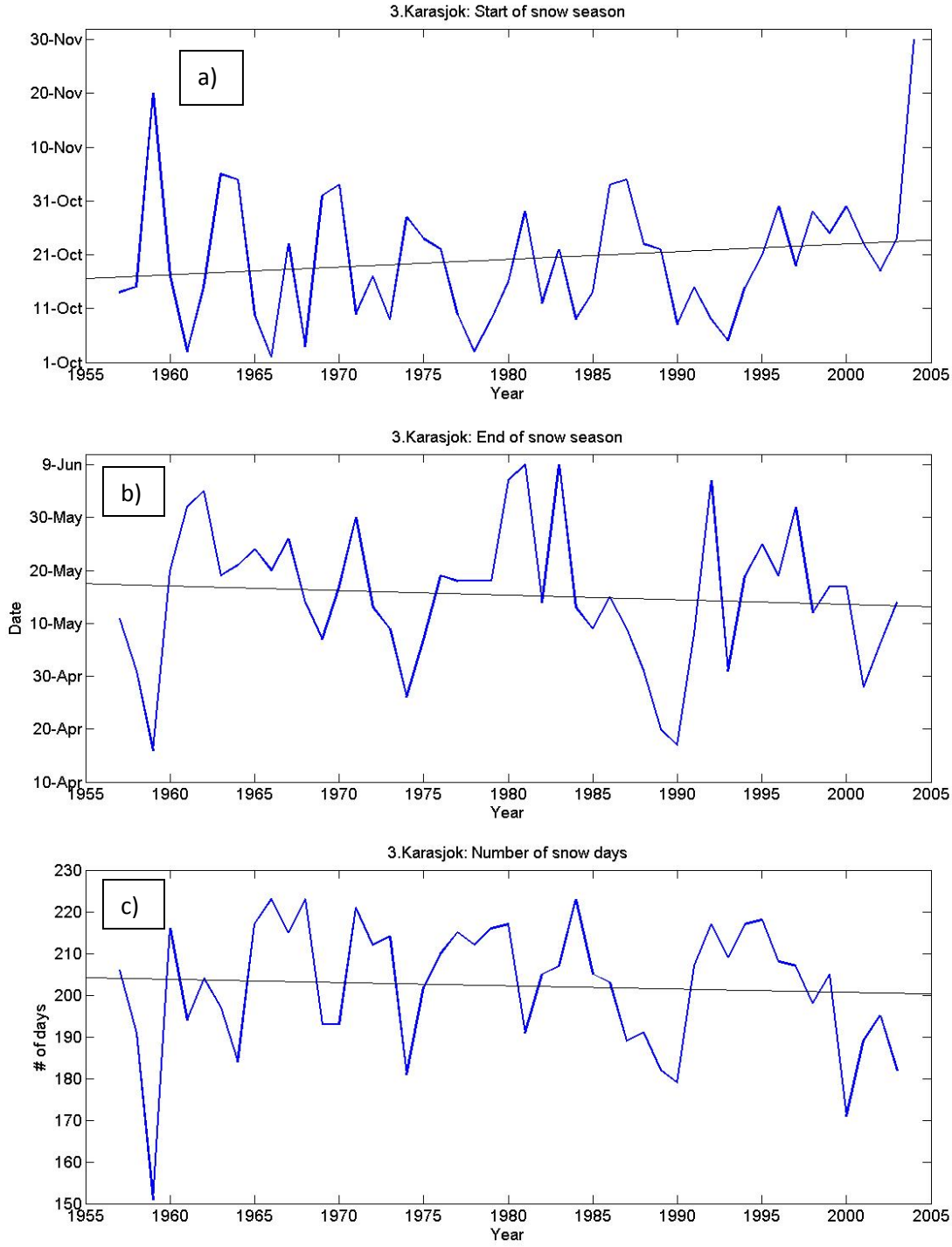

Figure 3.10: Station 3 Karasjok: a) Start of snow season b) End of snow season c) Number of snow days per hydrological year.

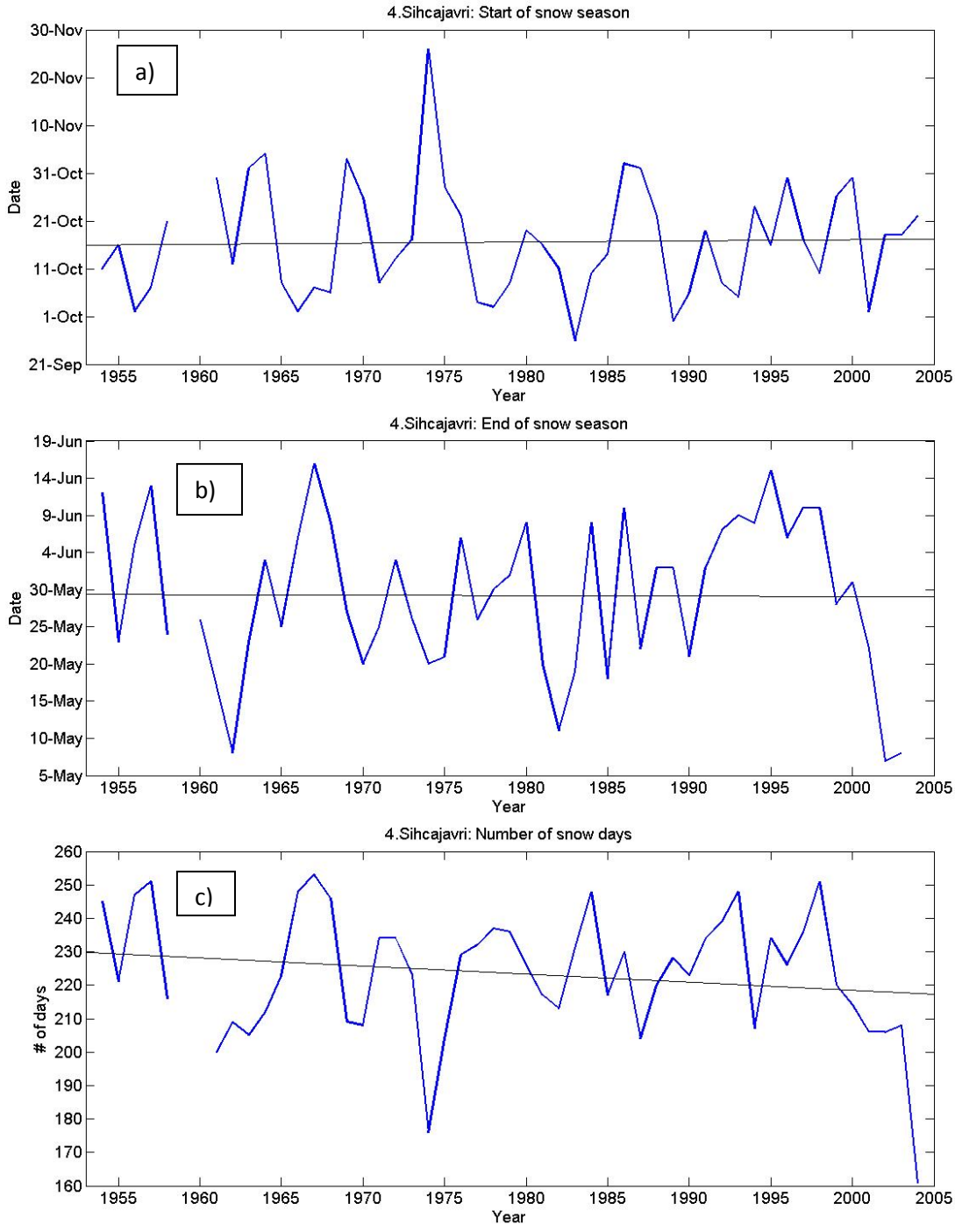

Figure 3.11: Station 4 Sihcajavri: a) Start of snow season b) End of snow season c) Number of snow days per hydrological year.

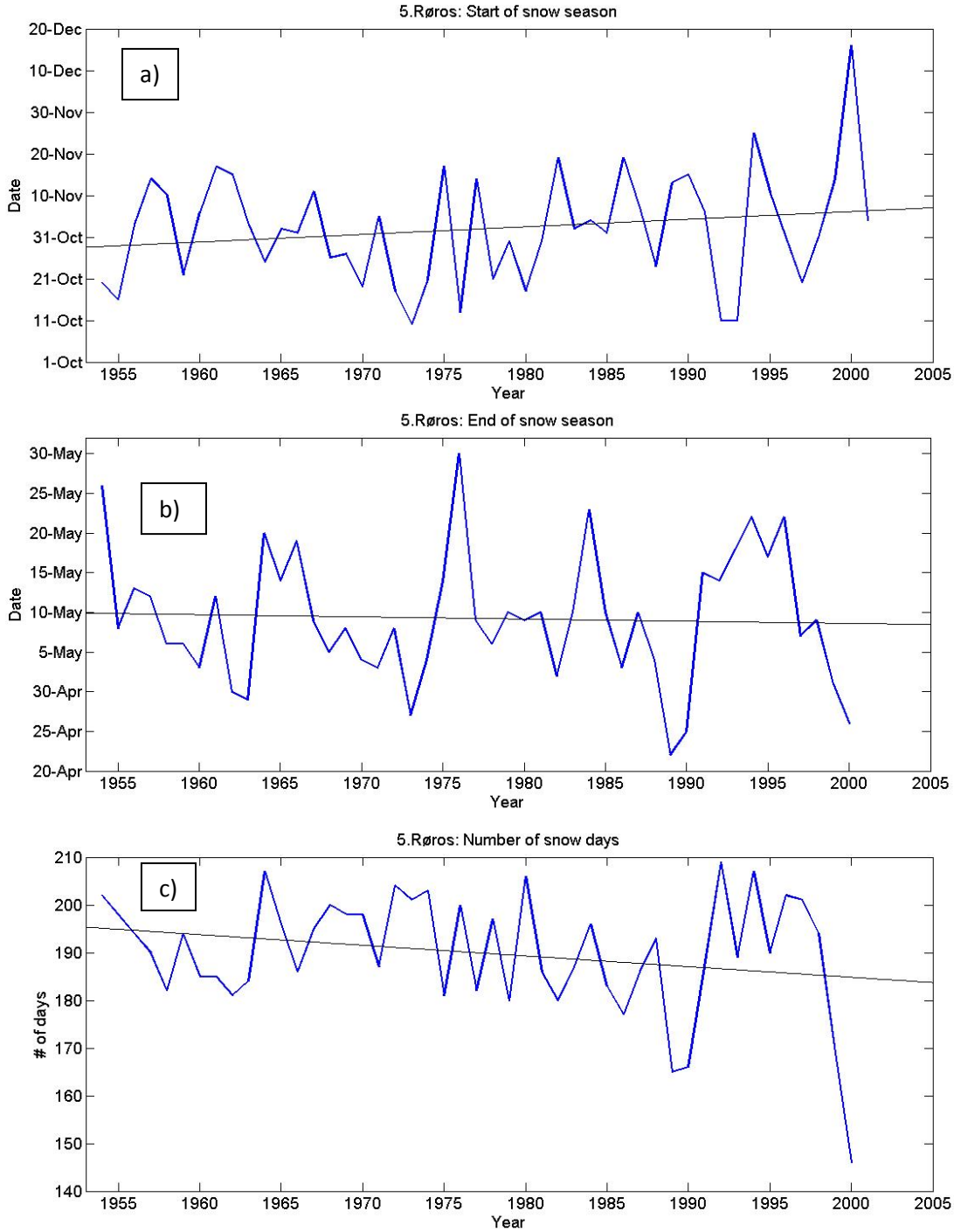

Figure 3.12: Station 5 Røros: a) Start of snow season b) End of snow season c) Number of snow days per hydrological year.

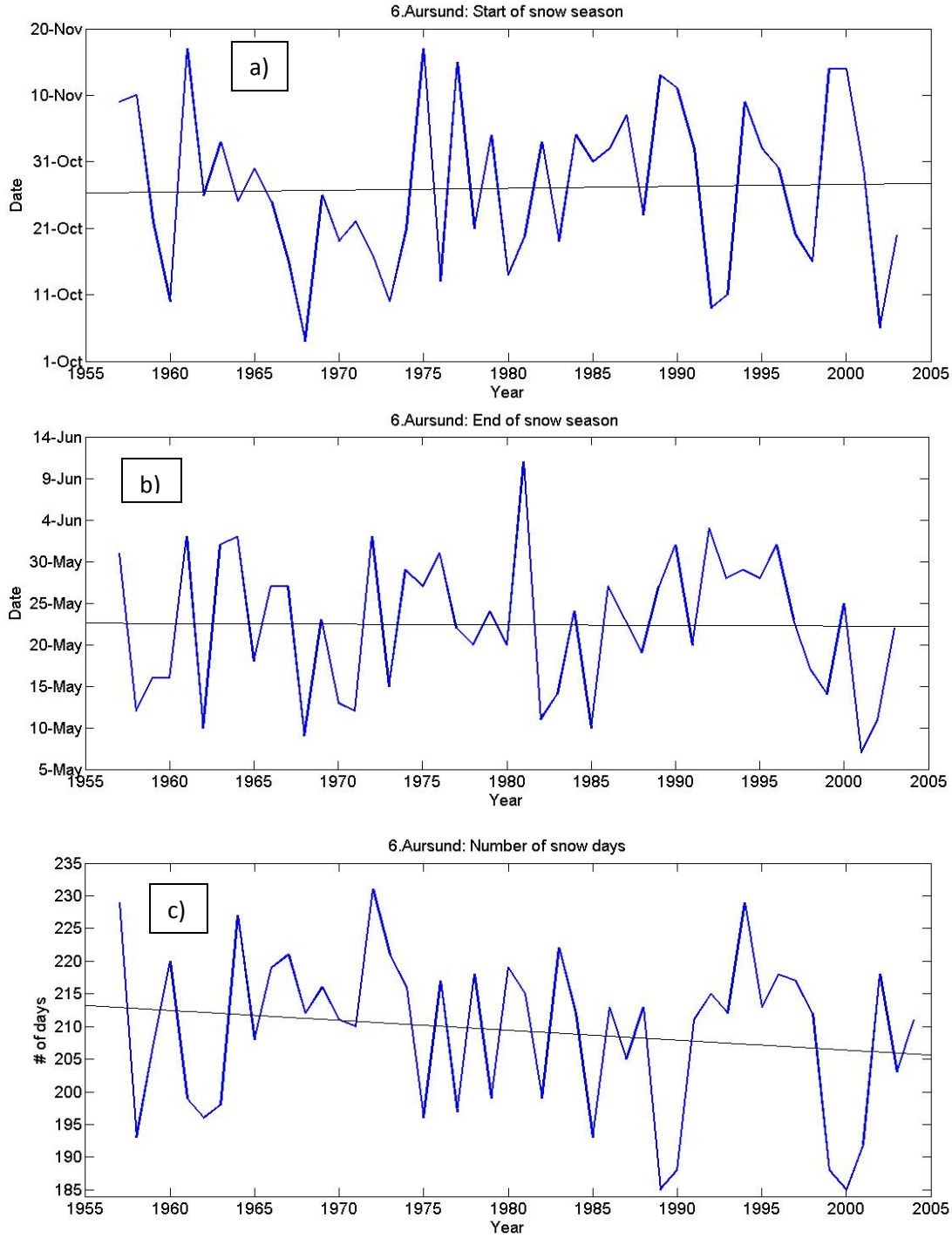

Figure 3.13: Station 6 Aursund: a) Start of snow season b) End of snow season c) Number of snow days per hydrological year.

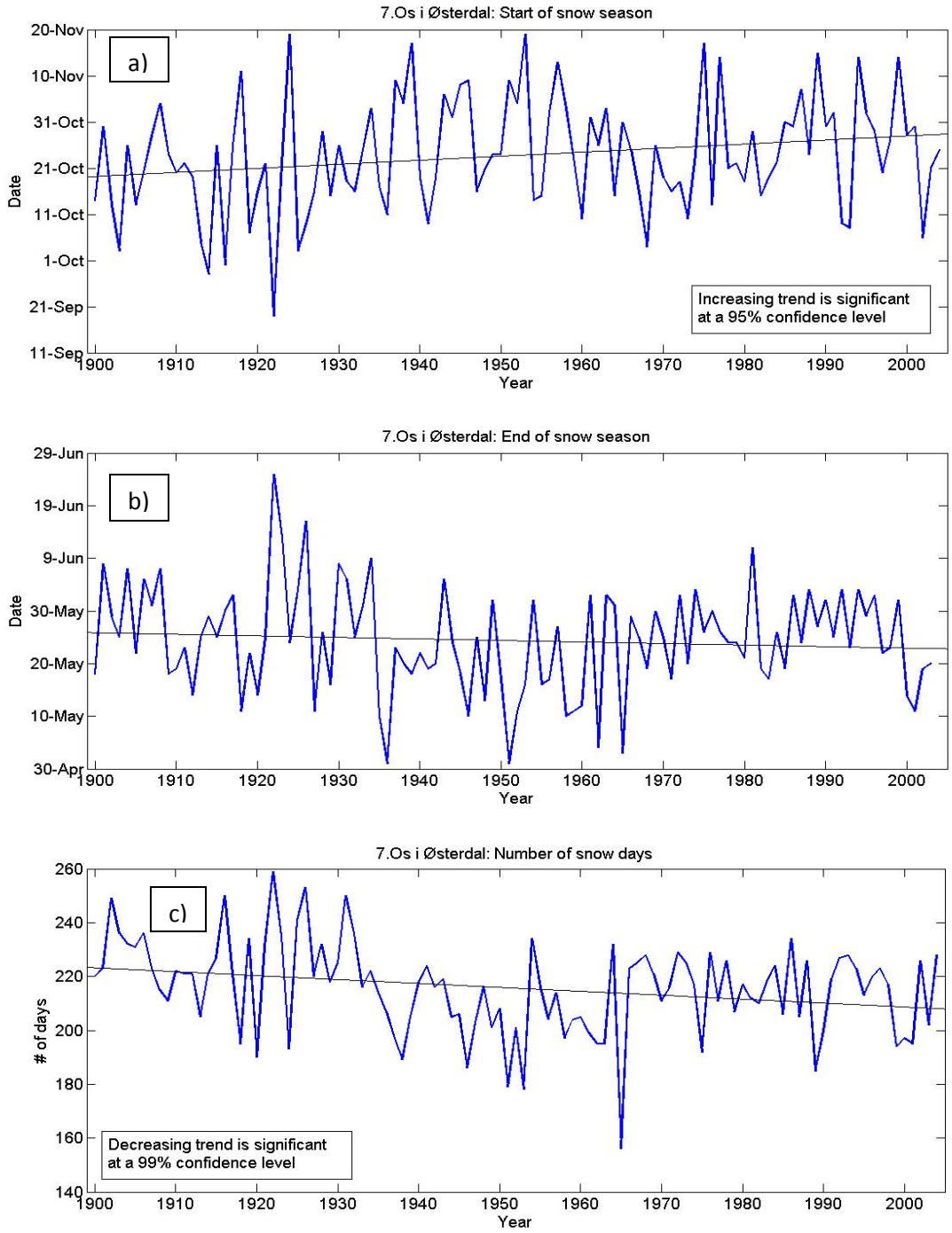

Figure 3.14: Station 7 Os i Østerdal: a) Start of snow season b) End of snow season c) Number of snow days per hydrological year.

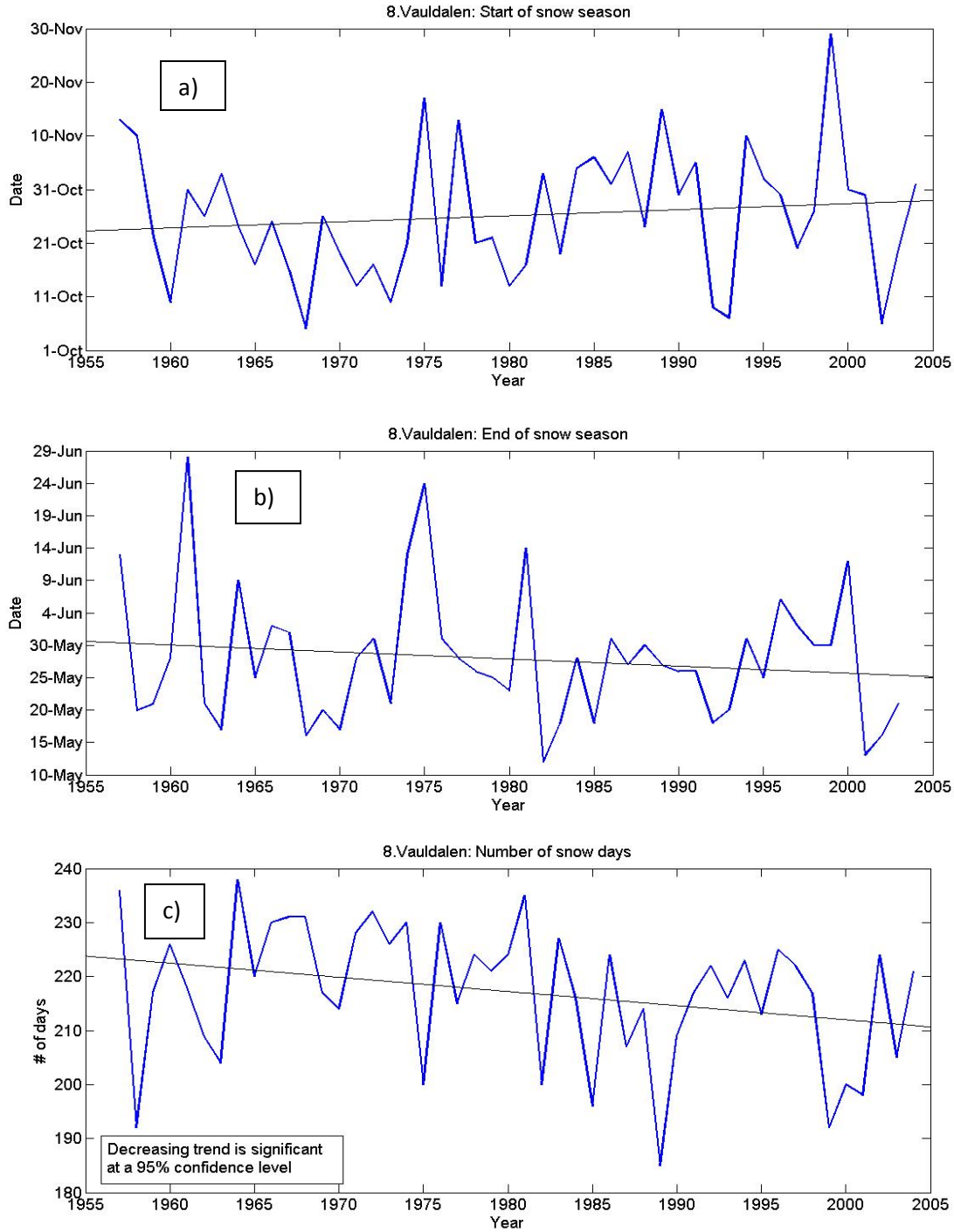

Figure 3.15: Station 8 Vauldalen: a) Start of snow season b) End of snow season c) Number of snow days per hydrological year.

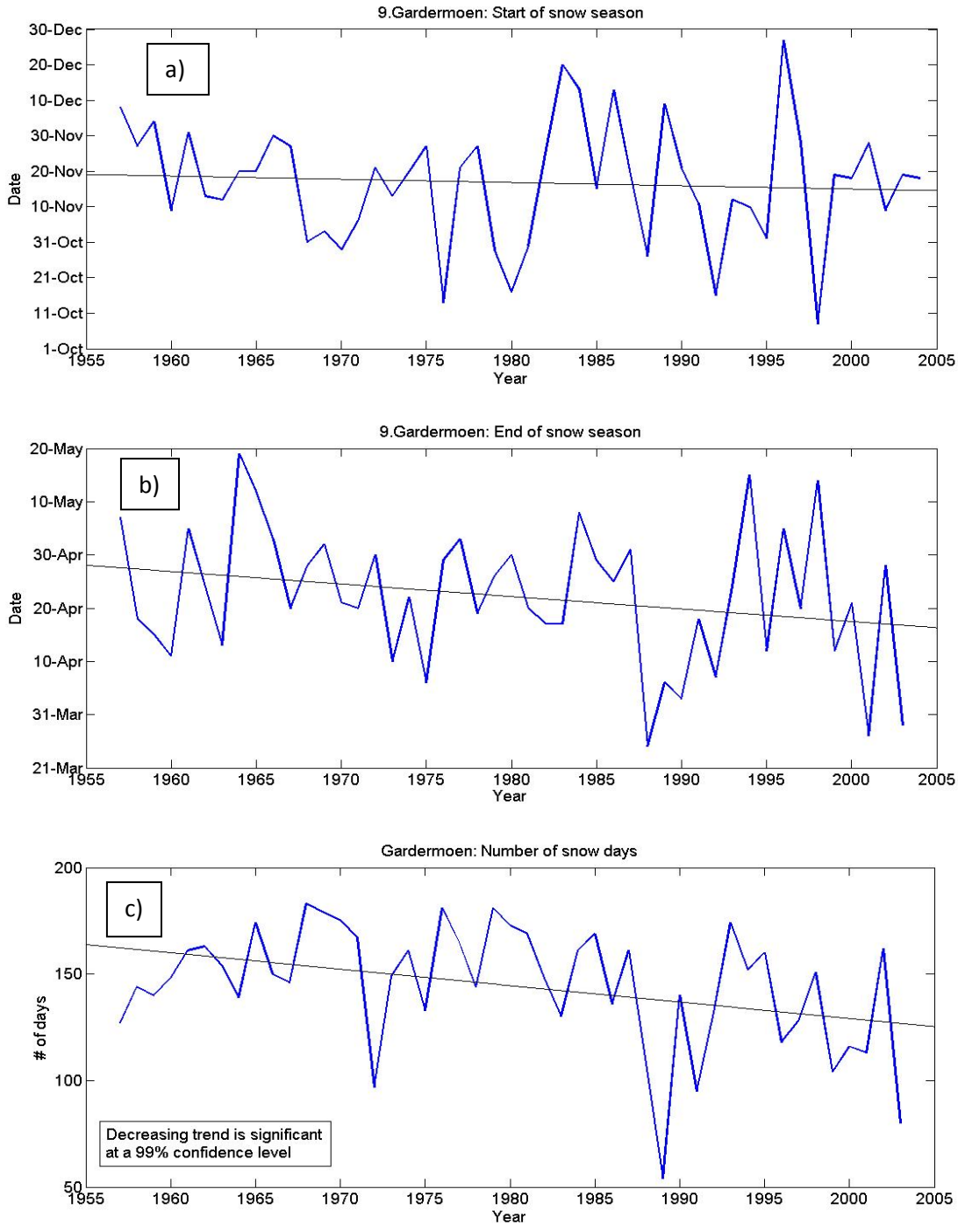

Figure 3.16: Station 9 Gardermoen: a) Start of snow season b) End of snow season c) Number of snow days per hydrological year.

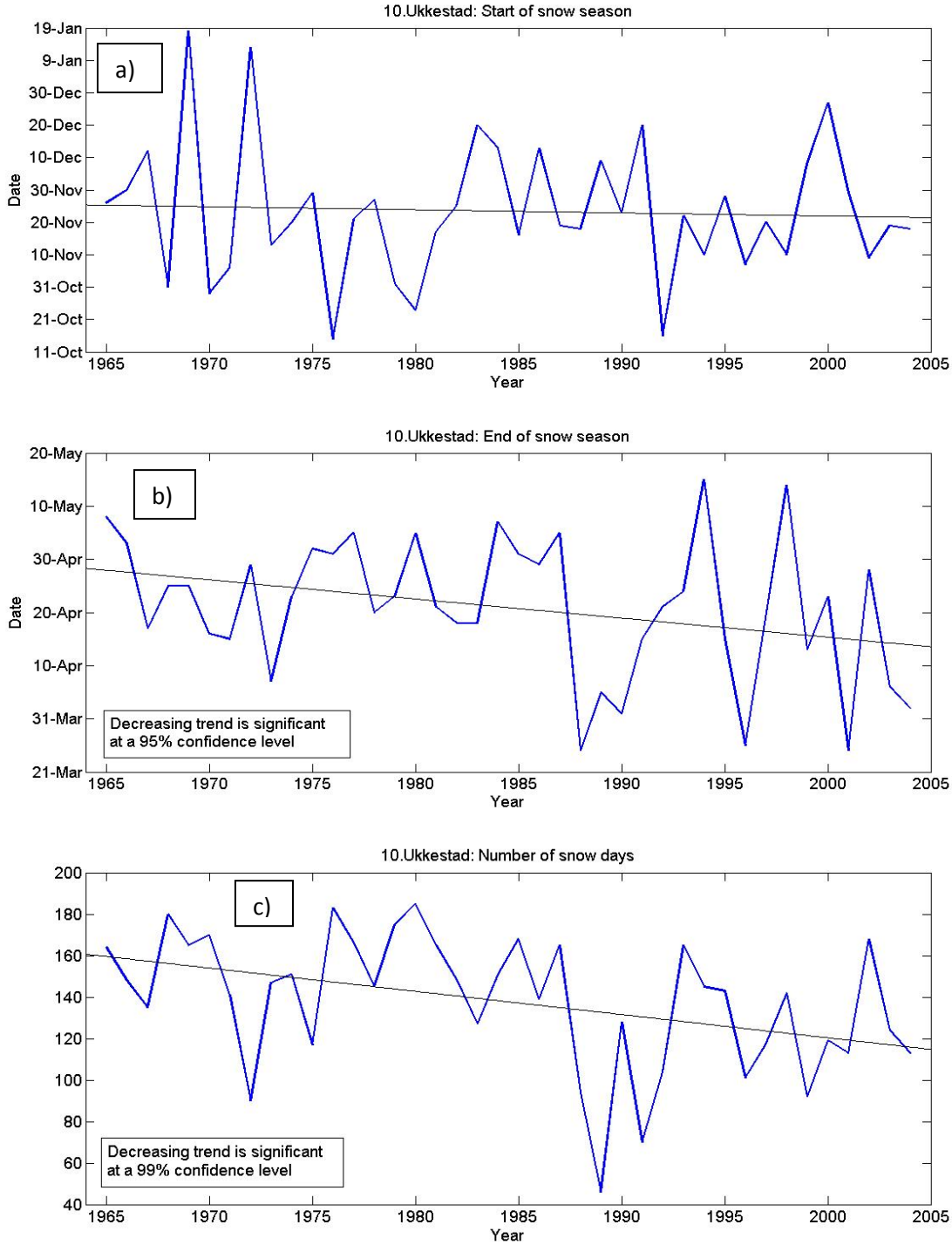

Figure 3.17: Station 10 Ukkestad: a) Start of snow season b) End of snow season c) Number of snow days per hydrological year.

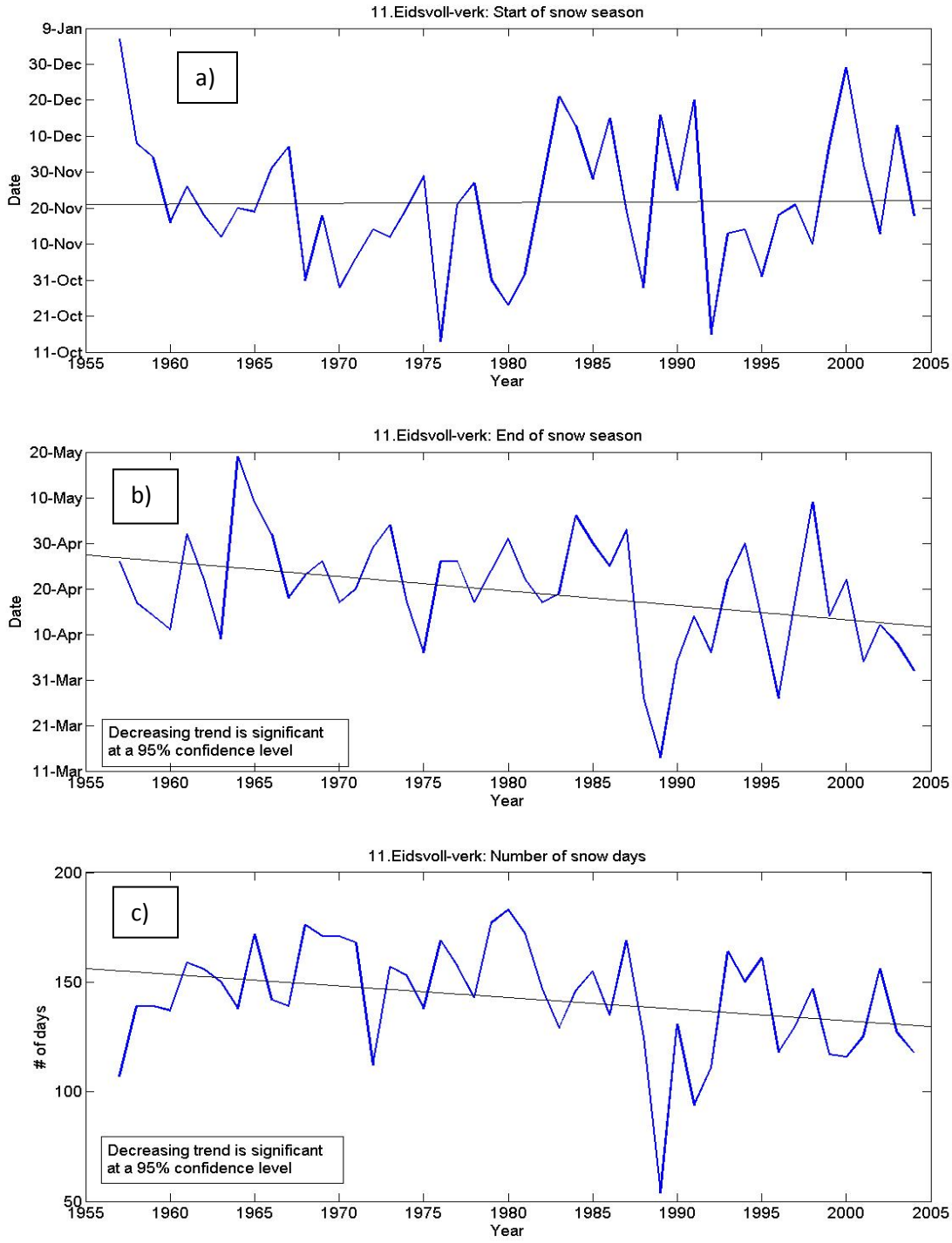

Figure 3.18: Station 11 Eidsvoll-verk: a) Start of snow season b) End of snow season c) Number of snow days per hydrological year.

Table 3.2: Results from fitting the nonlinear model to time series at each station. Bolded results are significant at the 0.1 alpha level.

Station	Max snow depth (m)	Start of snow season (a)	Date of max snow depth (b)	End of snow season (c)	# of deleted years
1.Jotkajavre	15 cm less	1 week earlier	**2 weeks earlier**	3 days earlier	2
2.Cuovddatmohkki	5 cm less	2 days earlier	5 days earlier	**3 weeks earlier**	2
3.Karasjok	15 cm more	2 days later	2 weeks later	2 days earlier	1
4.Sihcajavri	**15 cm less**	10 days earlier	2 days later	**10 days earlier**	0
5.Røros	**40 cm less**	2 days later	4 days later	5 days later	2
6.Aursund	10 cm more	1 week later	**10 days earlier**	1 week earlier	0
7.Os i Østerdal	**45 cm less**	NO TREND	NO TREND	**3 weeks earlier**	2
8.Vauldalen	20 cm less	1 week later	10 days earlier	**2 weeks earlier**	0
9.Gardermoen	20 cm less	2 weeks later	1 week later	1 week earlier	9
10.Ukkestad	25 cm less	10 days later	2 weeks earlier	10 days earlier	10
11.Eidsvoll-verk	**30 cm less**	3 weeks earlier	2 days earlier	18 days earlier	5

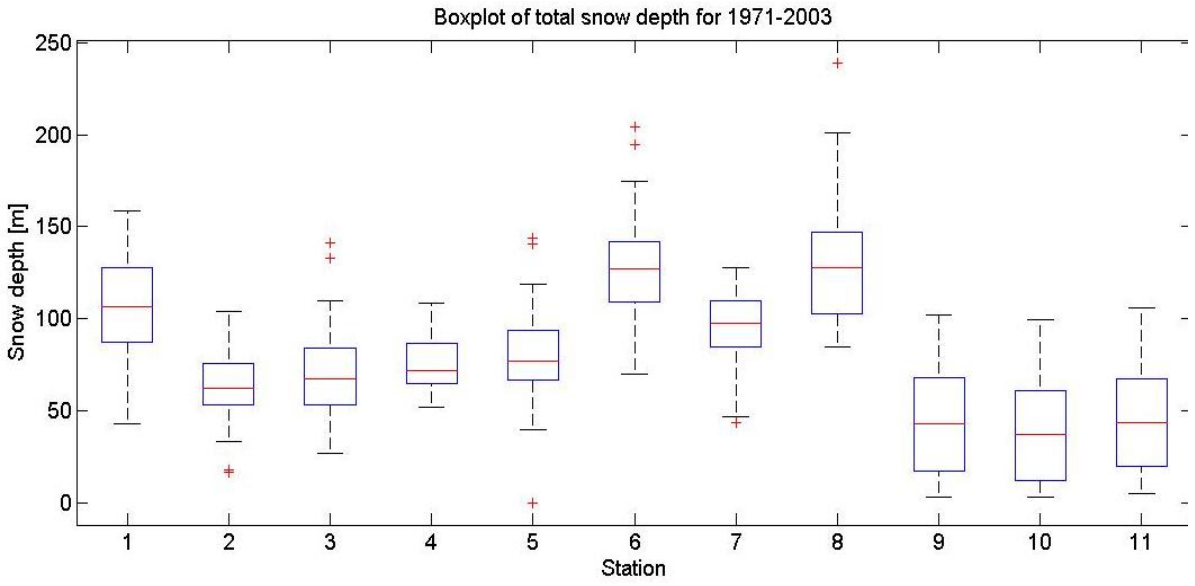

Figure 3.19: Boxplot of total seasonal snow depth (1971-2003) for the eleven stations.

Table 3.3: Statistical results of simulated and observed: Snow depth on four selected dates and 2. Total seasonal snow depth.

Station	**Mean snow depth on a particular date [cm] ± standard deviation**								**Total seasonal snow depth [cm]**	
	Dec-15		**Jan-15**		**Feb-15**		**Mar-15**			
	obs	*sim*	*obs*	*sim*	*obs*	*sim*	*obs*	*sim*	*obs*	*sim*
1.Jotkajavre	29.8 ± 13.5	30.9 ± 12.7	44.6 ± 18.7	42.0 ± 13.0	56.3 ± 17.6	50.9 ± 14.1	73.1 ± 23.5	56.1 ± 14.9	10640 ± 2956	8973 ± 2486
2.Cuovddatmohki	22.4 ± 8.4	18.9 ± 6.9	30.7 ± 9.5	25.3 ± 7.5	39.8 ± 13.4	30.8 ± 8.4	44.5 ± 17.1	32.6 ± 7.8	6248 ± 2068	5032 ± 1500
3.Karasjok	28.0 ± 16.1	15.2 ± 7.9	39.6 ± 19.4	20.7 ± 9.0	48.4 ± 17.4	25.0 ± 8.1	49.2 ± 15.8	25.2 ± 8.4	6996 ± 2516	3690 ± 1321
4.Sihcajavri	28.4 ± 7.6	17.0 ± 5.4	38.1 ± 8.2	23.3 ± 8.3	45.3 ± 8.0	27.9 ± 8.8	48.8 ± 9.5	30.0 ± 9.0	7692 ± 1503	4677 ± 1570
5.Røros	31.3 ± 18.1	29.1 ± 14.4	50.7 ± 26.2	41.0 ± 15.5	64.3 ± 24.6	53.2 ± 14.2	68.0 ± 23.7	58.6 ± 16.0	7983 ± 2541	7867 ± 2428
6.Aursund	46.1 ± 21.3	31.7 ± 19.3	64.5 ± 21.0	44.8 ± 22.8	84.2 ± 21.0	60.2 ± 21.9	95.1 ± 21.1	67.3 ± 24.3	12757 ± 3032	9229 ± 3570
7.Os i Østerdal	33.3 ± 13.8	20.8 ± 11.1	49.1 ± 16.3	28.9 ± 11.5	62.1 ± 17.1	37.5 ± 11.7	70.3 ± 18.0	41.0 ± 12.9	9308 ± 2329	5403 ± 1839
8.Vauldalen	44.2 ± 21.7	48.1 ± 13.6	64.4 ± 22.7	65.8 ± 18.0	83.6 ± 22.1	81.9 ± 16.4	92.9 ± 24.2	90.4 ± 18.3	13116 ± 3381	14079 ± 2692
9.Gardermoen	16.1 ± 14.5	15.5 ± 11.4	26.6 ± 23.8	26.3 ± 15.6	39.8 ± 27.3	34.8 ± 18.5	43.8 ± 28.6	37.4 ± 21.6	4521 ± 2913	4108 ± 2214
10.Ukkestad	12.6 ± 12.0	13.7 ± 10.6	21.4 ± 22.7	23.3 ± 15.0	33.8 ± 27.5	31.0 ± 18.7	38.7 ± 30.3	33.1 ± 20.9	3991 ± 2777	3554 ± 2051
11.Eidsvoll-verk	16.4 ± 14.8	13.5 ± 10.2	29.1 ± 23.3	22.8 ± 15.1	41.5 ± 26.8	30.3 ± 18.1	45.1 ± 28.9	31.7 ± 20.4	4803 ± 2981	3512 ± 2035

Table 3.4: Correlation between simulations and observations of: 1.Snow depth on four selected dates and 2. Total seasonal snow depth.

Station	**Coefficient of determination R^2 between observations and simulations**				
	Dec-15	**Jan-15**	**Feb-15**	**Mar-15**	**Total seasonal snow depth**
1.Jotkajavre	0.60	0.42	0.24	0.61	0.47
2.Cuovddatmohki	0.47	0.30	0.44	0.33	0.14
3.Karasjok	0.61	0.66	0.53	0.52	0.63
4.Sihcajavri	0.13	0.30	0.14	0.11	0.24
5.Røros	0.76	0.68	0.50	0.36	0.61
6.Aursund	0.90	0.87	0.65	0.63	0.70
7.Os i Østerdal	0.53	0.56	0.62	0.56	0.51
8.Vauldalen	0.69	0.50	0.33	0.41	0.33
9.Gardermoen	0.59	0.69	0.71	0.79	0.78
10.Ukkestad	0.59	0.71	0.69	0.62	0.71
11.Eidsvoll-verk	0.74	0.83	0.81	0.83	0.83

Table 3.5: Cluster averages of correlations shown in Table 3.4, for our three regions.

Region	**Coefficient of determination R^2 between observations and simulations**				
	Dec-15	**Jan-15**	**Feb-15**	**Mar-15**	**Total seasonal snow depth**
1. Finnmarks-vidda	0.45	0.42	0.34	0.39	0.37
2. Røros	0.72	0.65	0.53	0.49	0.54
3. Romerike	0.64	0.74	0.74	0.75	0.77

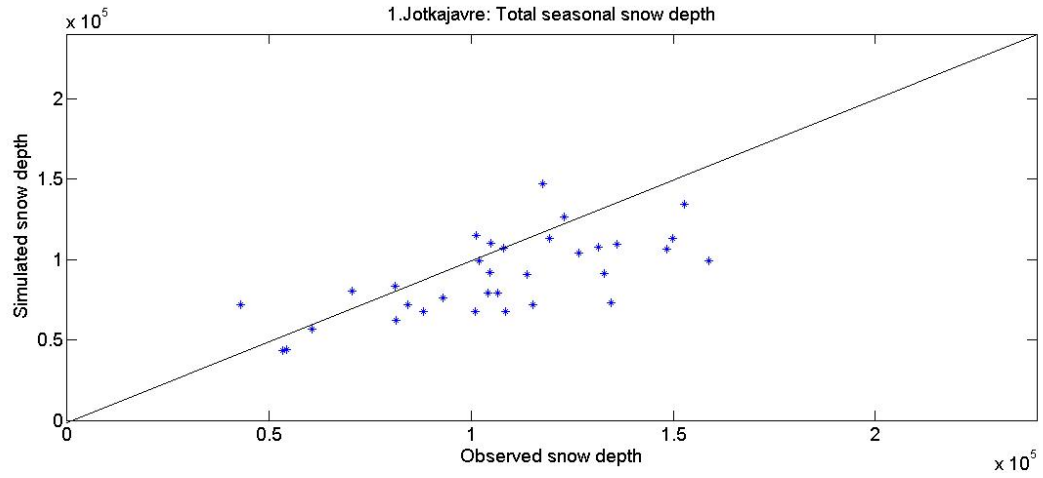

Figure 3.20: Scatteplot of observed versus simulated total snow depth for the winter season at station 1 Jotkajavre.

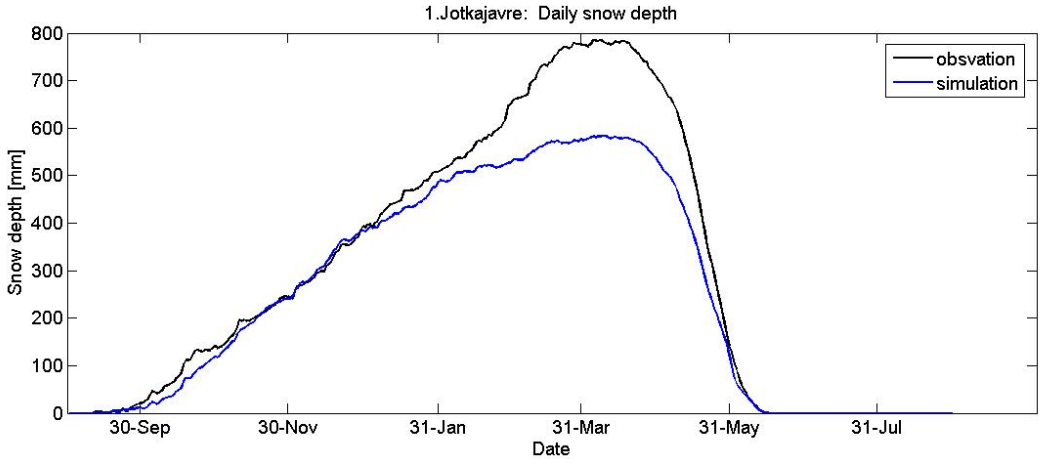

Figure 3.21: Mean daily snow depth (1971-2003) at station 1 Jotkajavre.

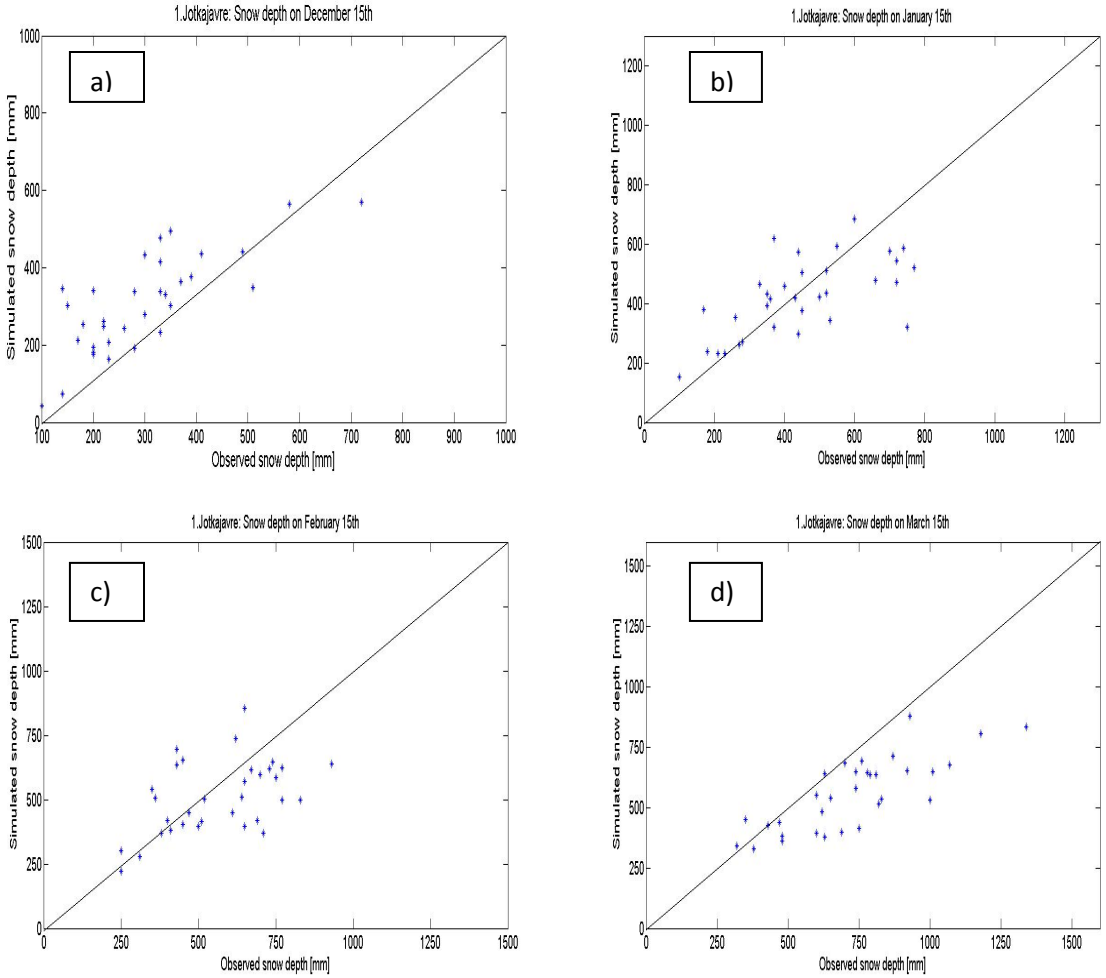

Figure 3.22: Station 1 Jotkajavre: Scatter plots of observed and simulated snow depth on a) December 15th b) January 15th c) February 15th d) March 15th.

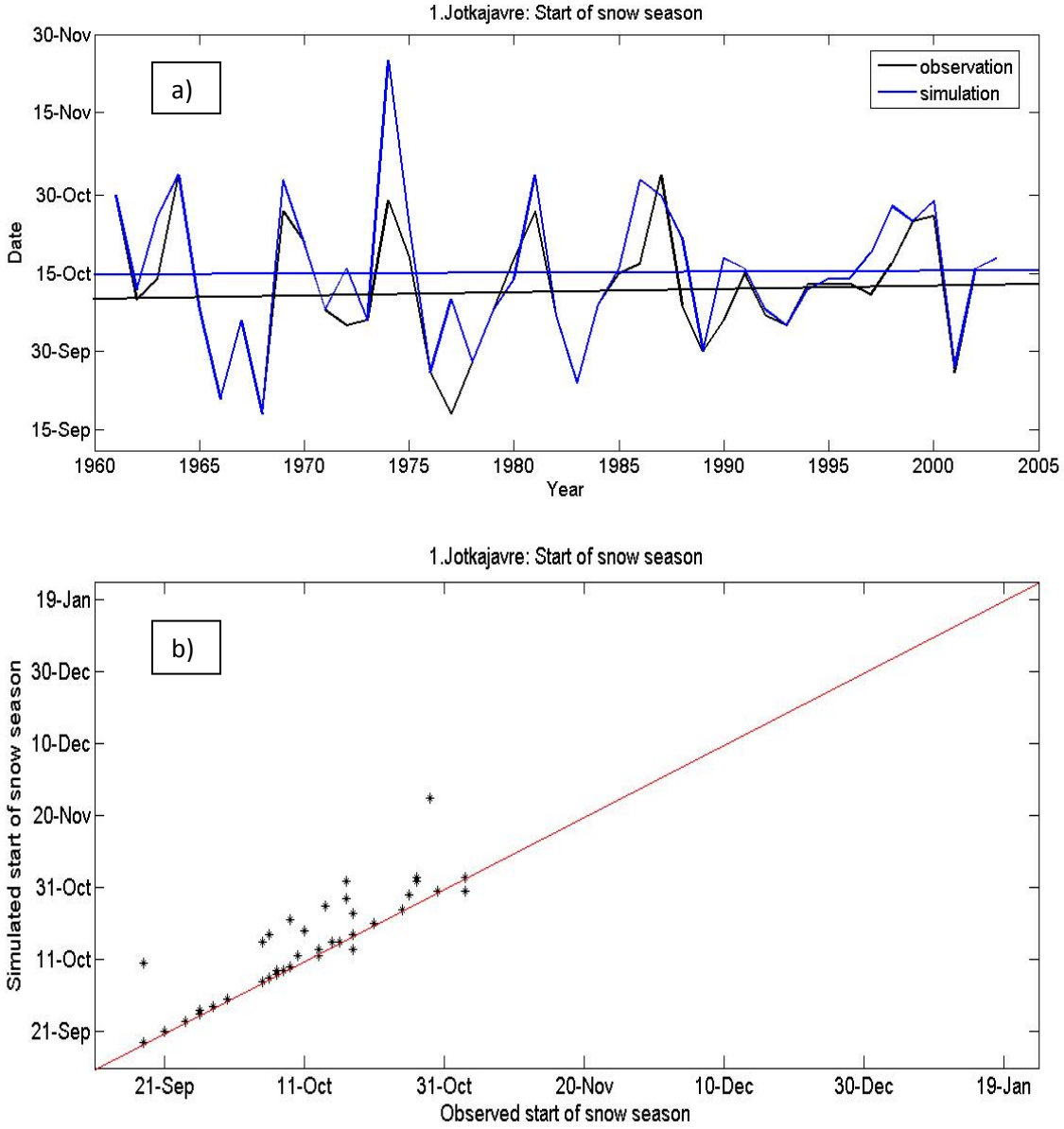

Figure 3.23: Observed and simulated start of snow season at station1 Jotkajavre: a) Time series b) Scatter plot.

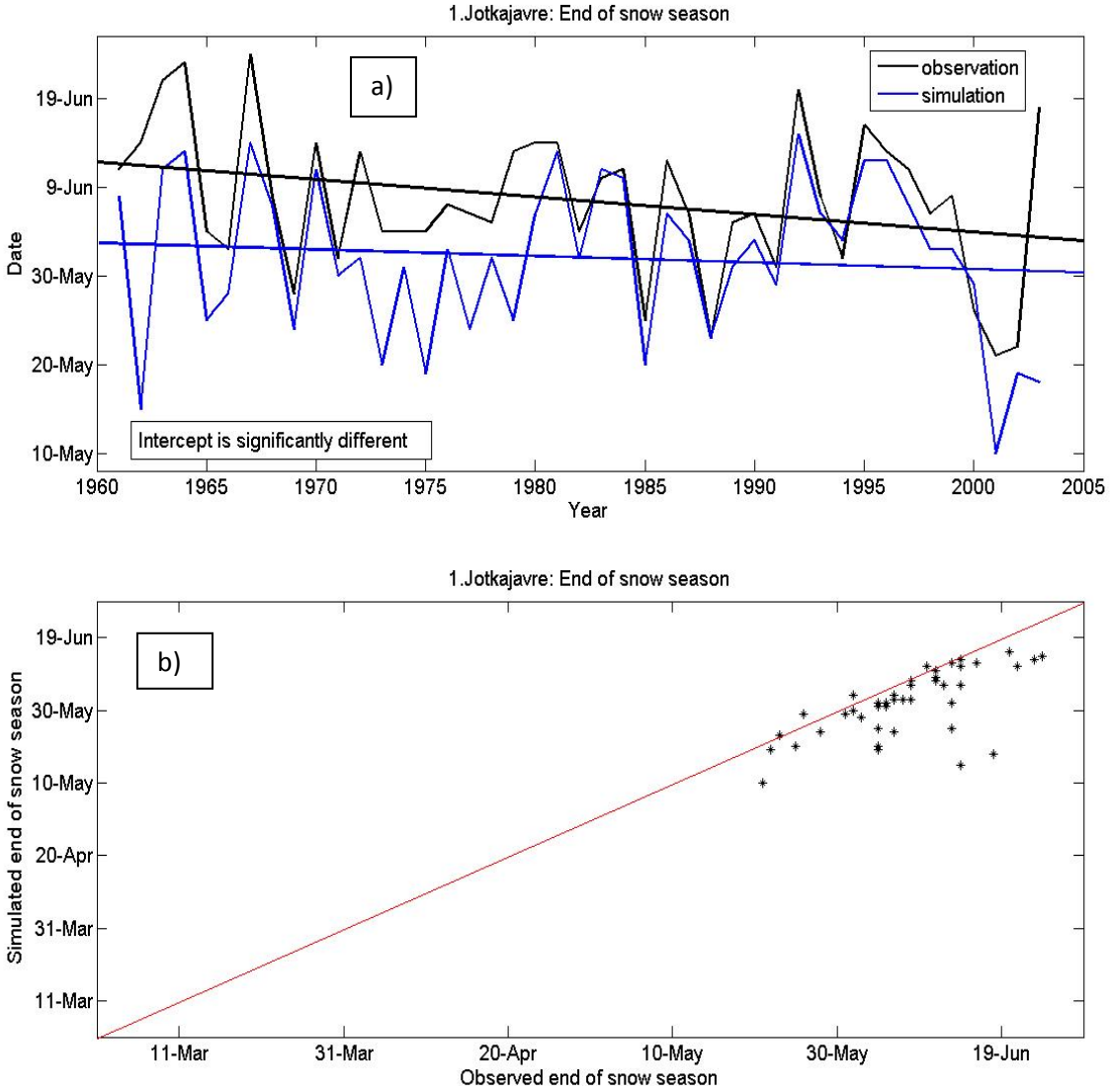

Figure 3.24: Observed and simulated end of snow season at station1 Jotkajavre: a) Time series b) Scatter plot.

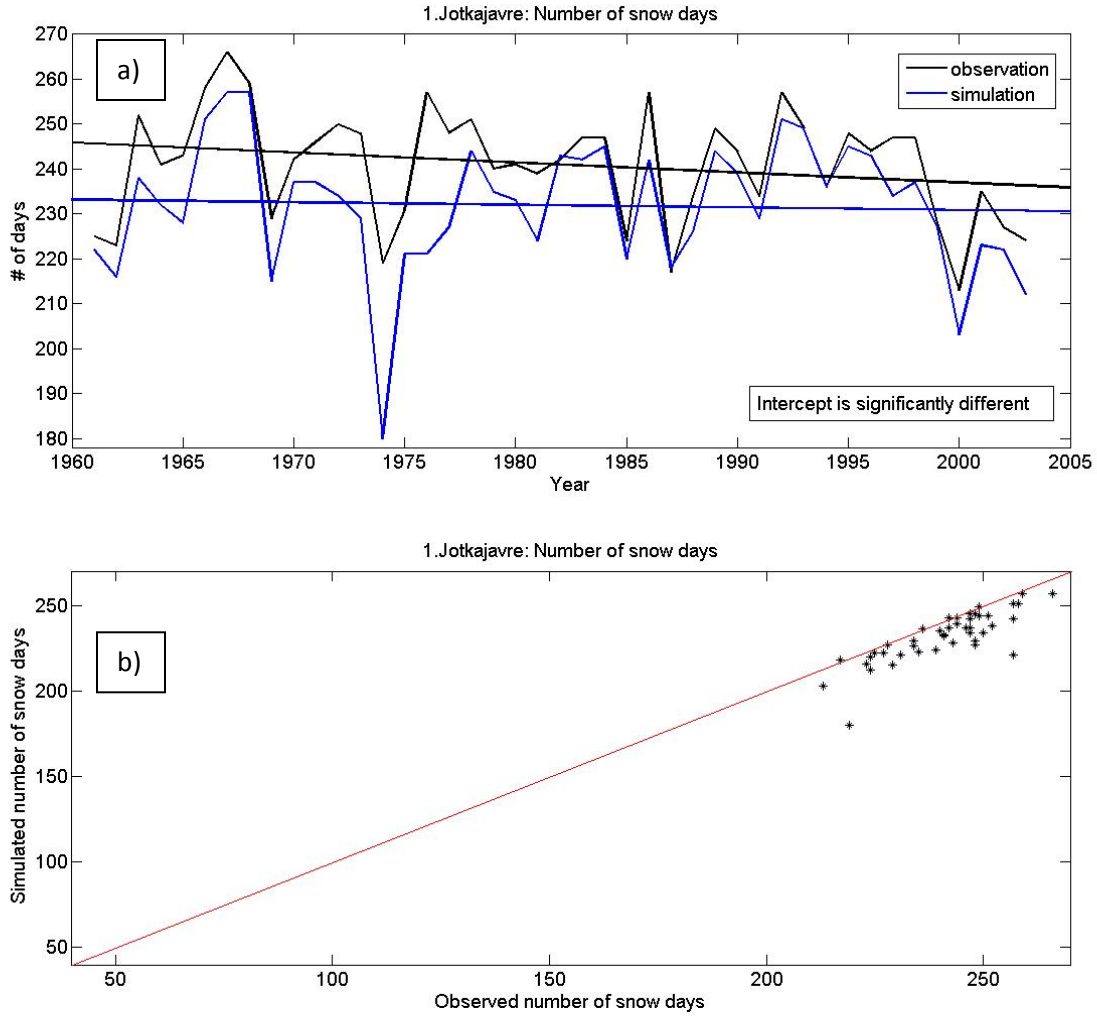

Figure 3.25: Observed and simulated number of snow days per winter season at station 1 Jotkajavre: a) Time series b) Scatter plot.

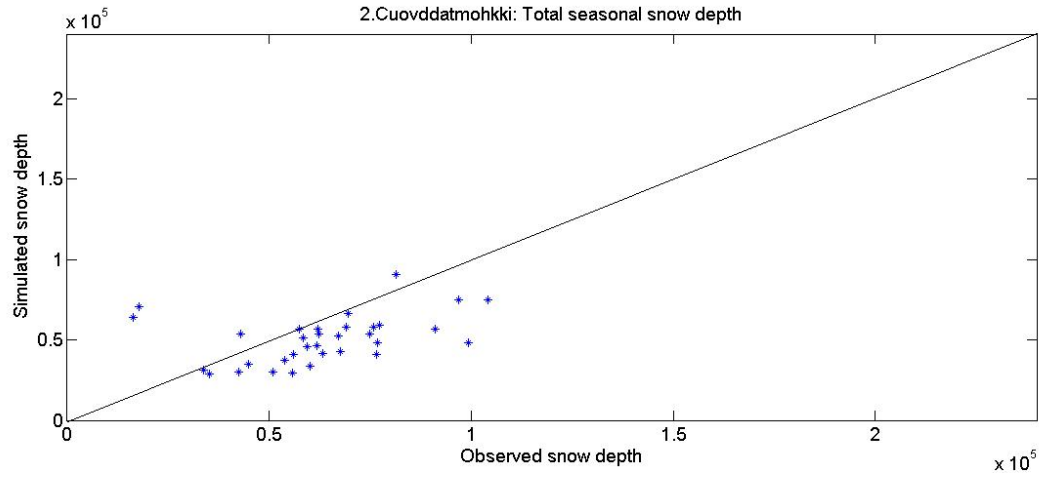

Figure 3.26: Scatteplot of observed versus simulated total snow depth for the winter season at station 2 Cuovddatmohkki.

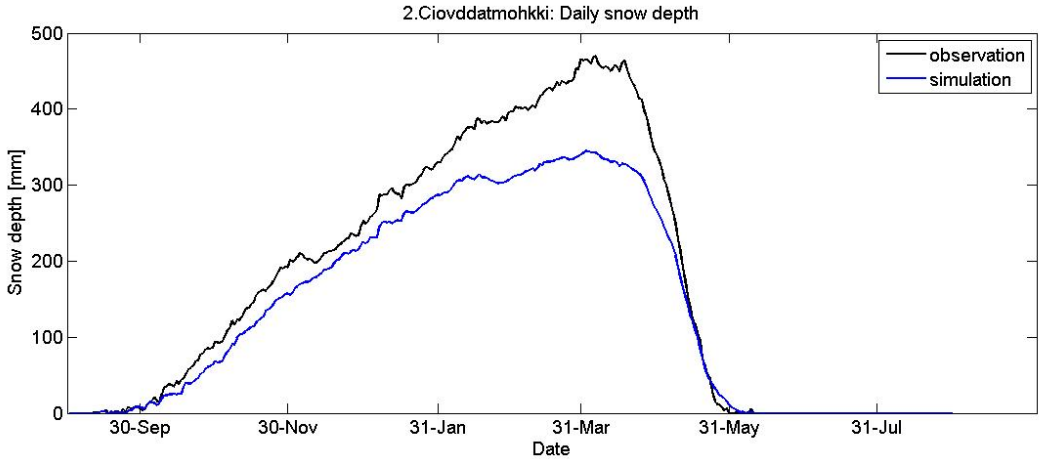

Figure 3.27: Mean daily snow depth (1971-2003) at station 2 Cuovddatmohkki.

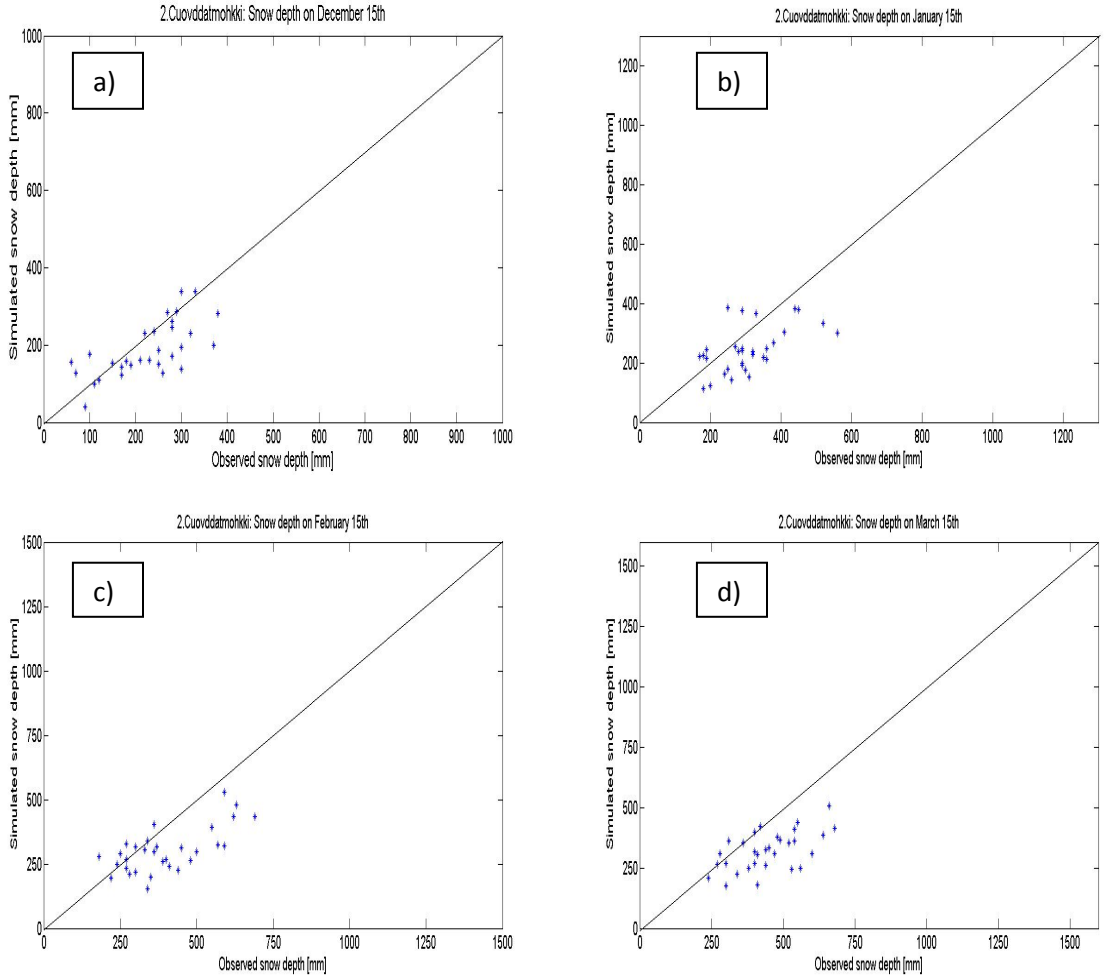

Figure 3.28: Station 2 Cuovddatmohkki: Scatter plots of observed and simulated snow depth on a) December 15th b) January 15th c) February 15th d) March 15th.

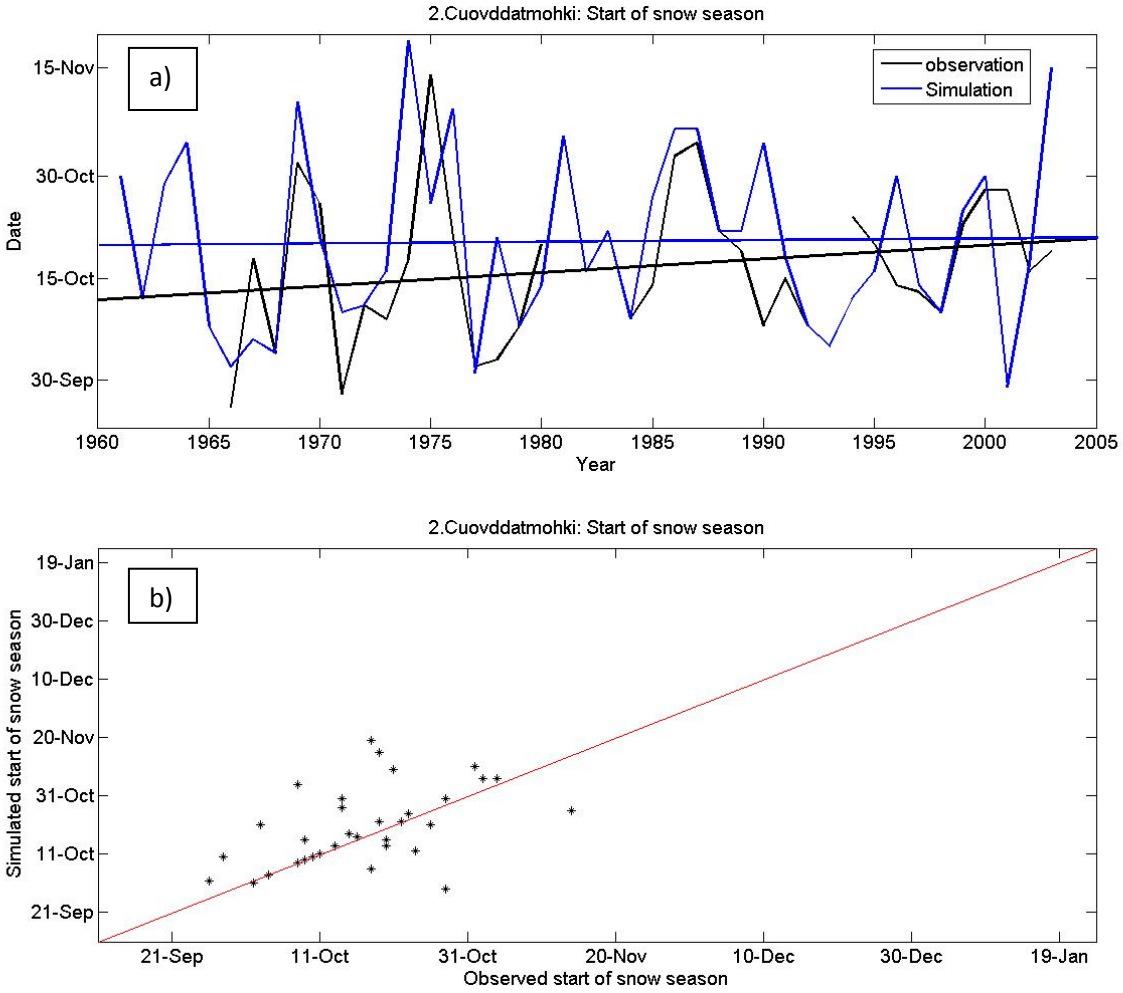

Figure 3.29: Observed and simulated start of snow season at station 2 Cuovddatmohkki: a) Time series b) Scatter plot.

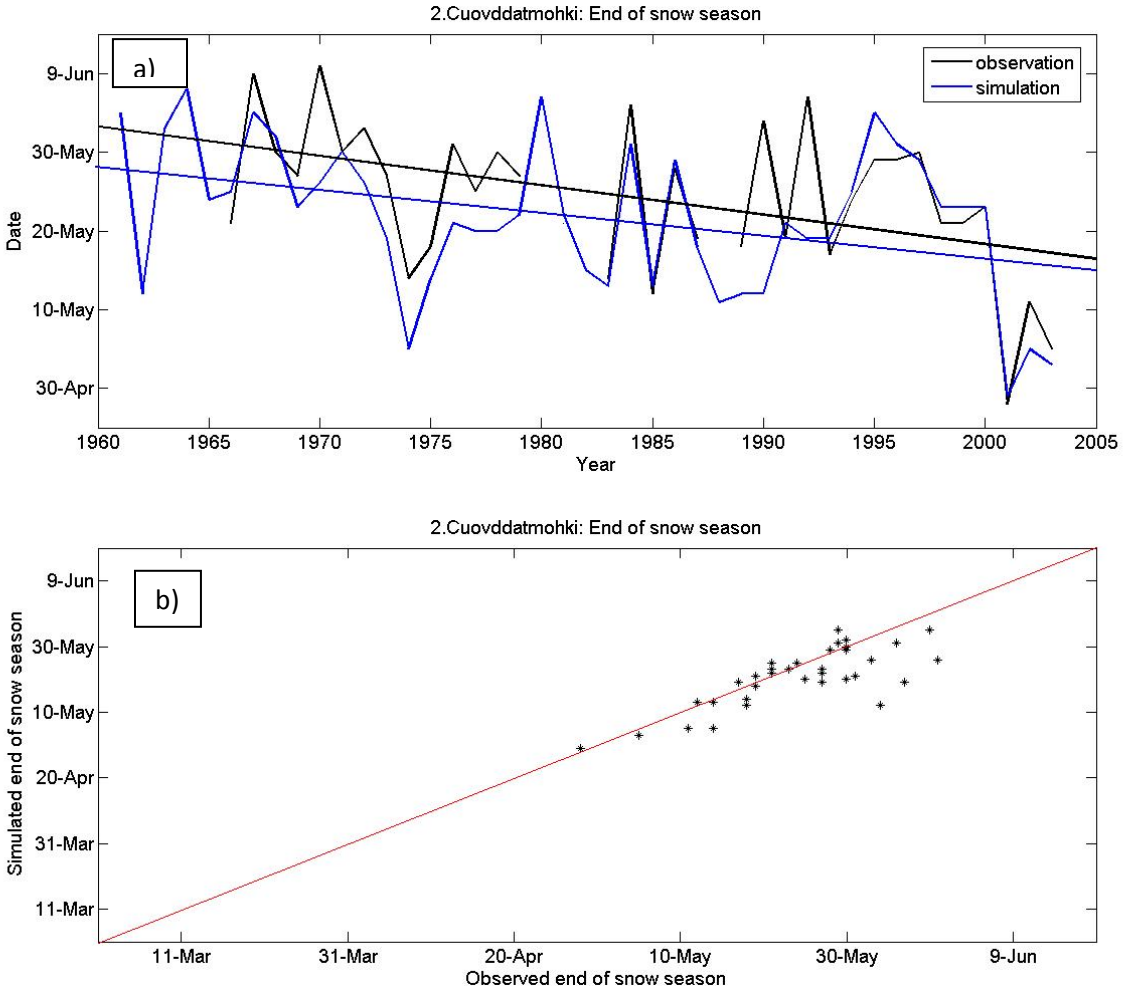

Figure 3.30: Observed and simulated end of snow season at station 2 Cuovddatmohkki: a) Time series b) Scatter plot.

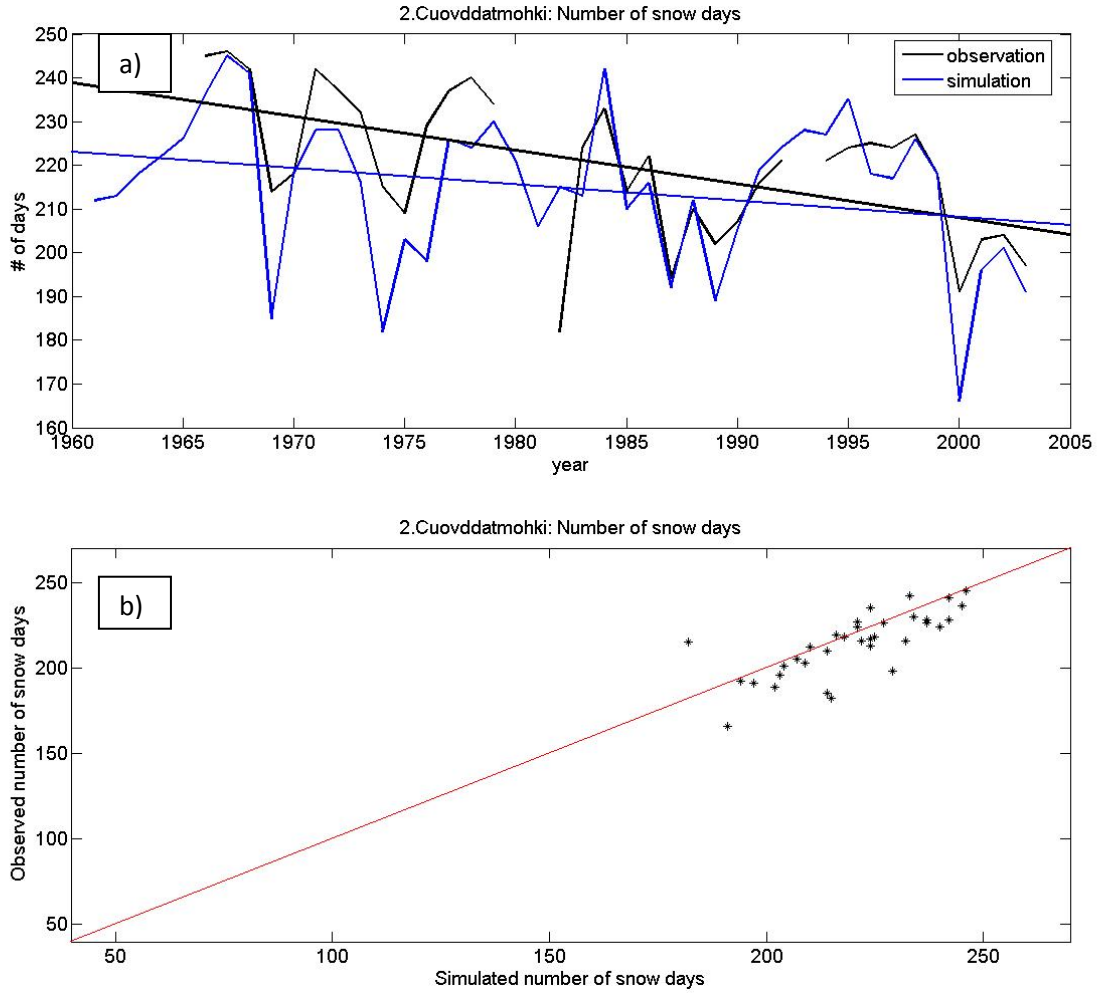

Figure 3.31: Observed and simulated number of snow days per winter season at station 2 Cuovddatmohkki: a) Time series b) Scatter plot.

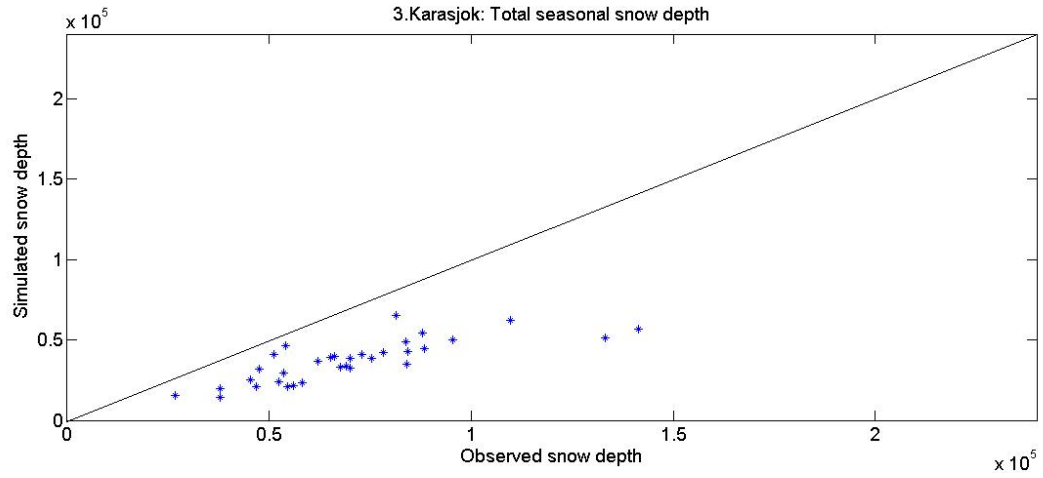

Figure 3.32: Scatteplot of observed versus simulated total snow depth for the winter season at station 3 Karasjok.

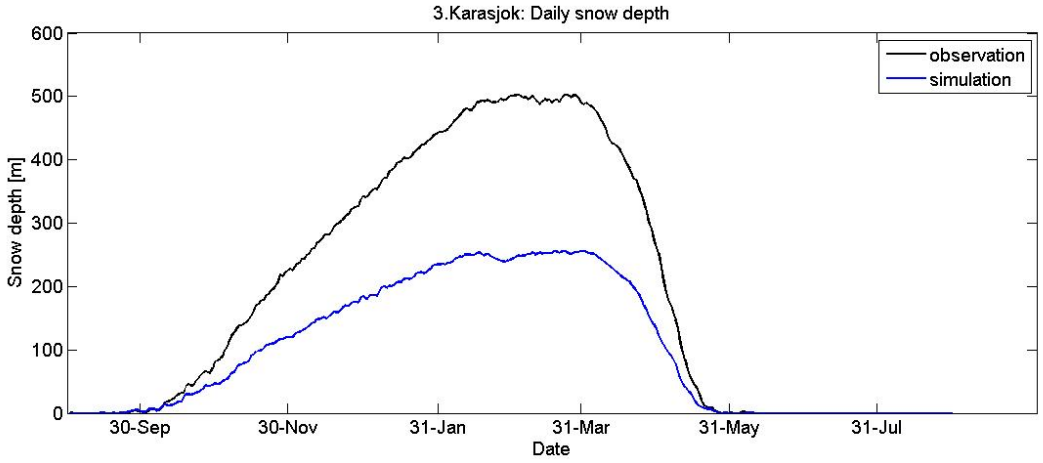

Figure 3.33: Mean daily snow depth (1971-2003) at station 3 Karasjok.

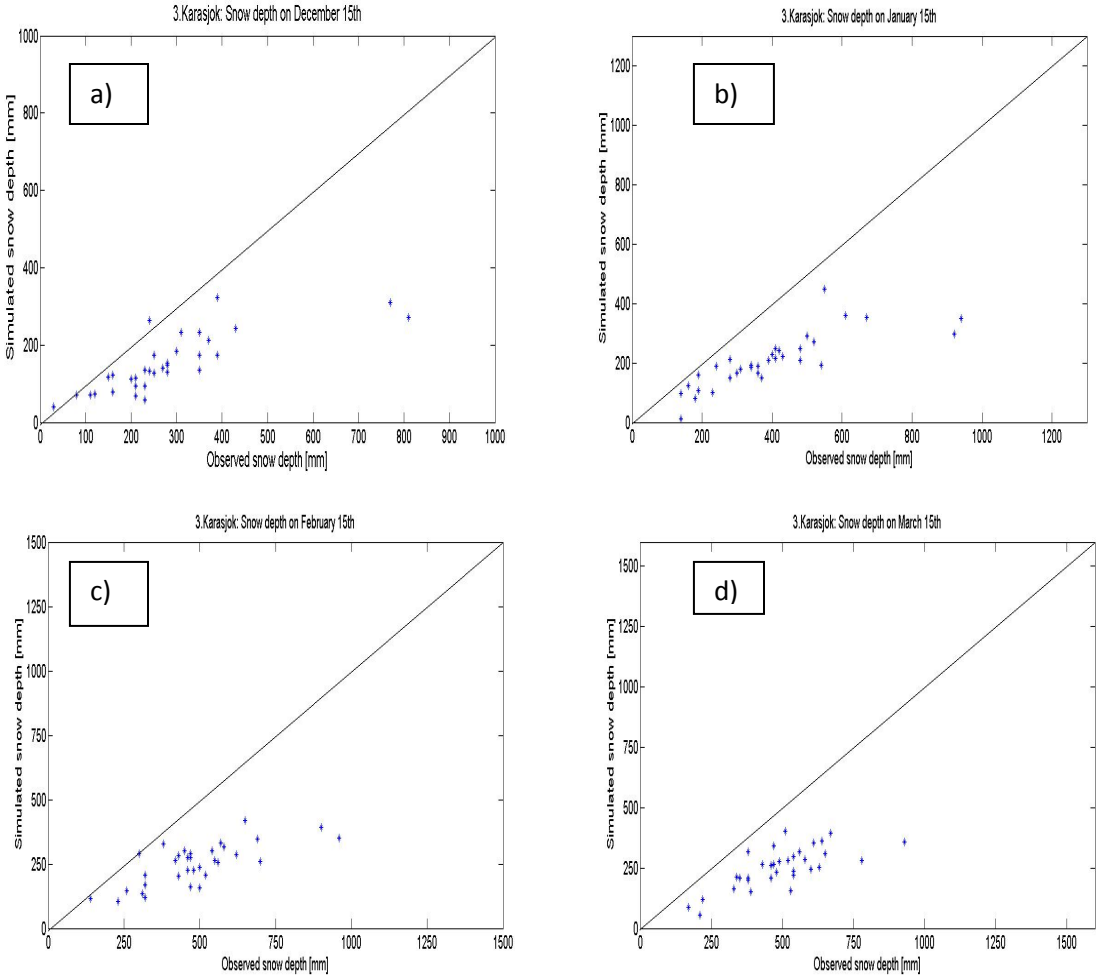

Figure 3.34: Station 3 Karasjok: Scatter plots of observed and simulated snow depth on a) December 15th b) January 15th c) February 15th d) March 15th.

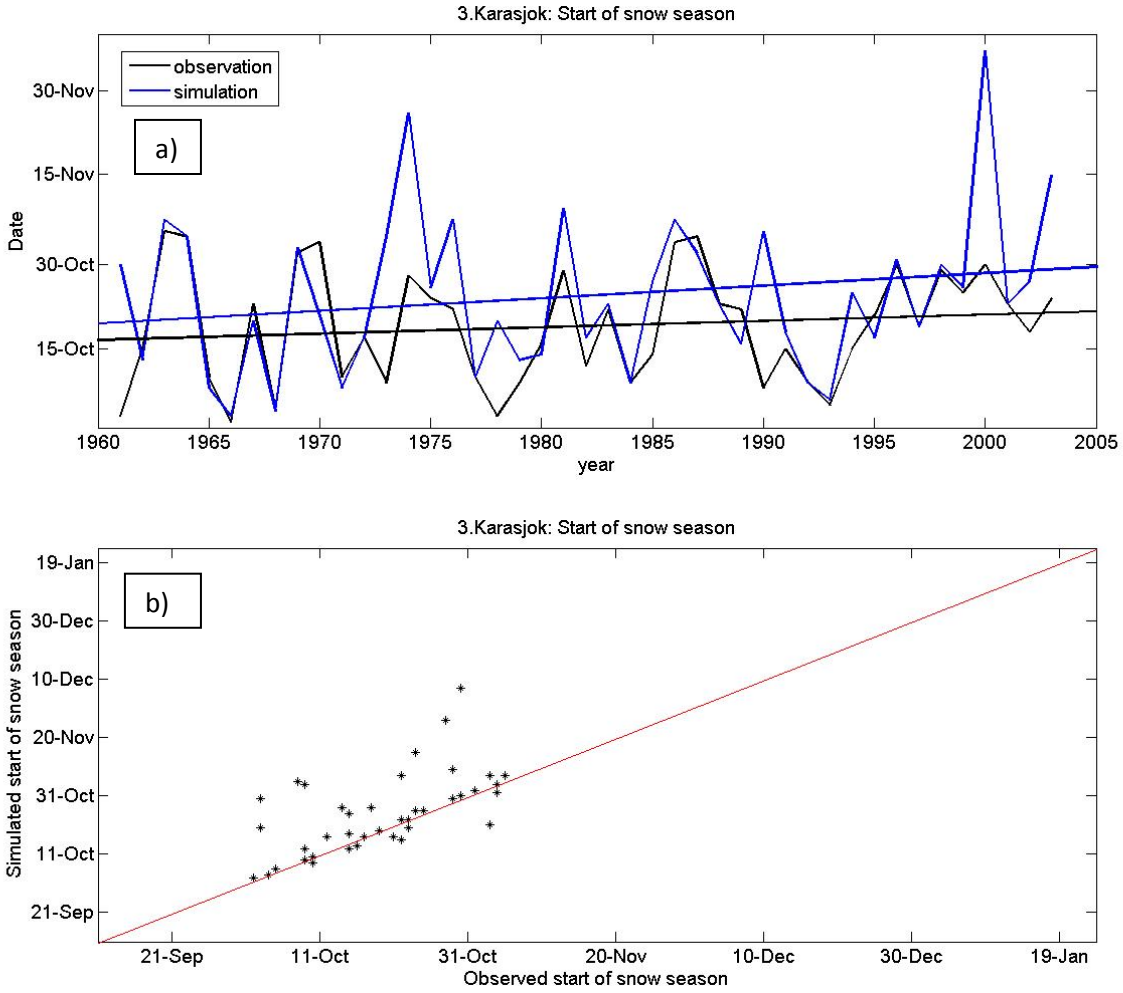

Figure 3.35: Observed and simulated start of snow season at station 3 Karasjok: a) Time series b) Scatter plot.

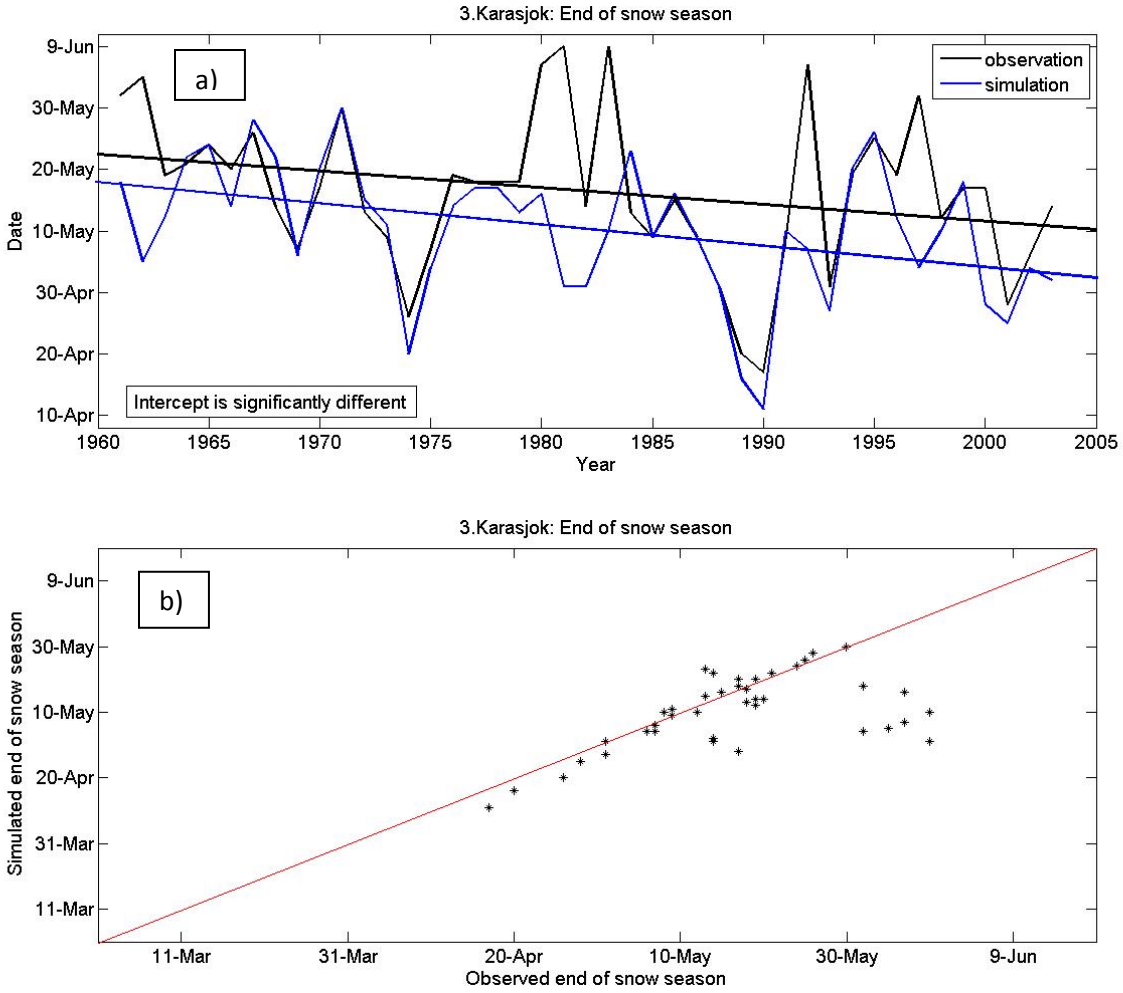

Figure 3.36: Observed and simulated end of snow season at station 3 Karasjok: a) Time series b) Scatter plot.

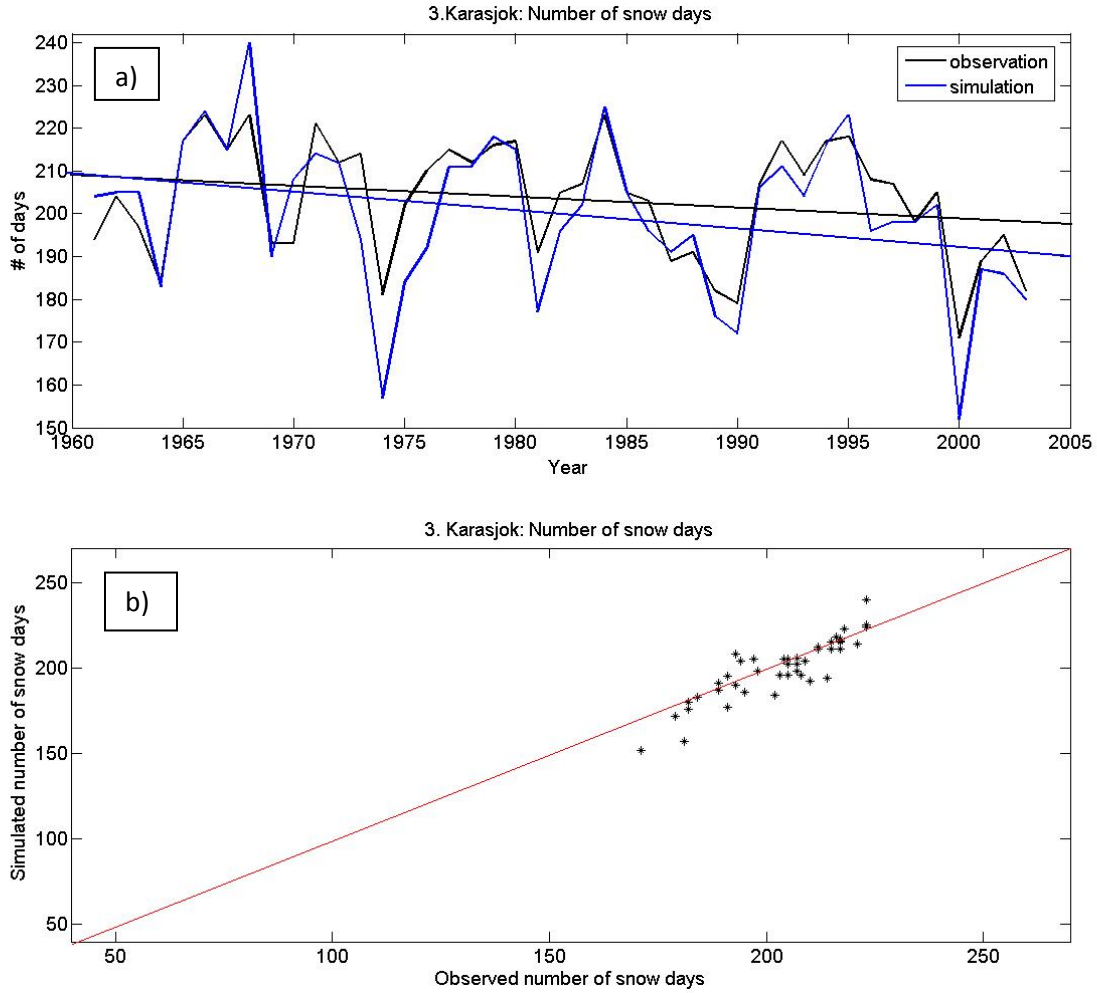

Figure 3.37: Observed and simulated number of snow days per winter season at station 3 Karasjok: a) Time series b) Scatter plot.

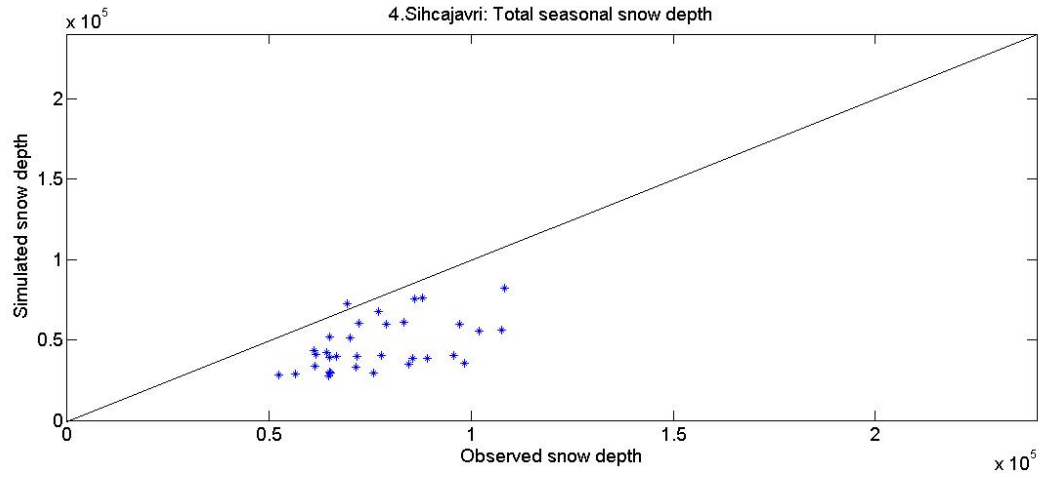

Figure 3.38: Scatteplot of observed versus simulated total snow depth for the winter season at station 4 Sihcajavri.

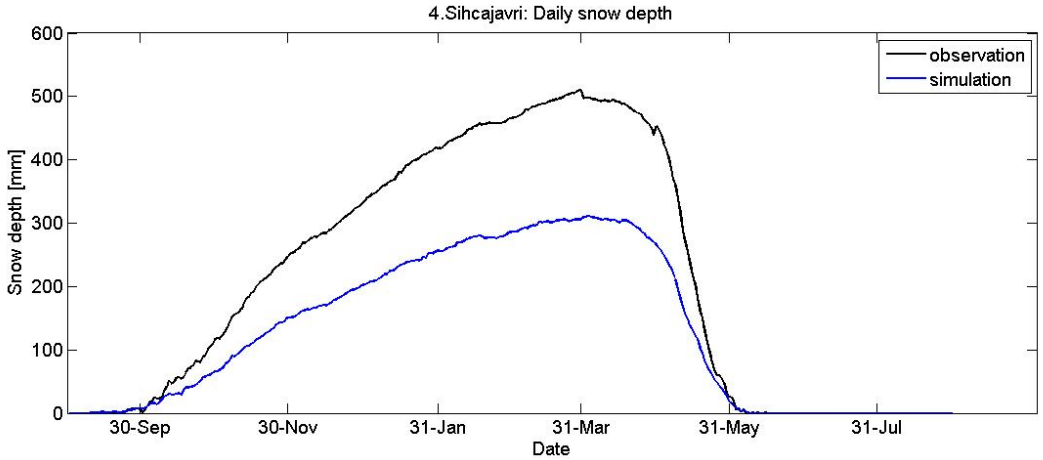

Figure 3.39: Mean daily snow depth (1971-2003) at station 4 Sihcajavri.

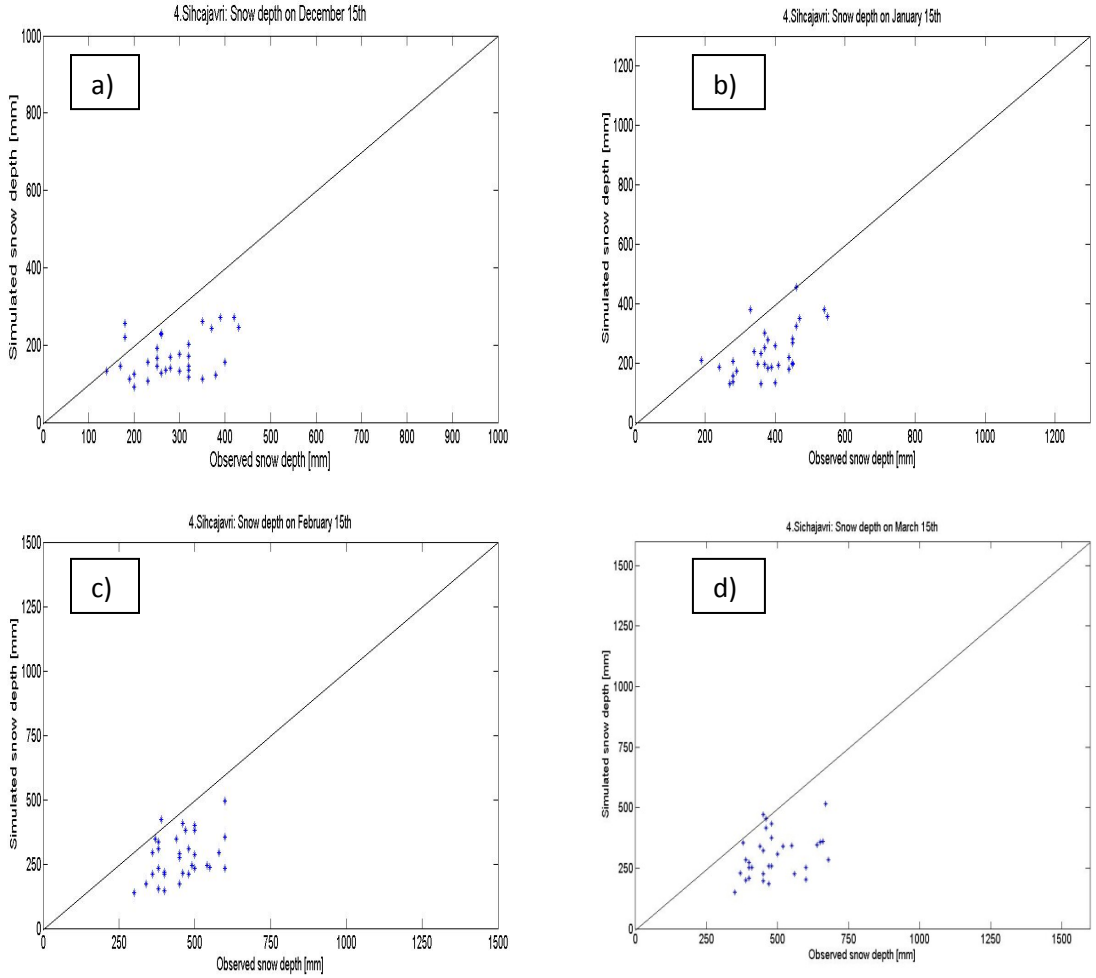

Figure 3.40: Station 4 Sihcajavri: Scatter plots of observed and simulated snow depth on a) December 15th b) January 15th c) February 15th d) March 15th.

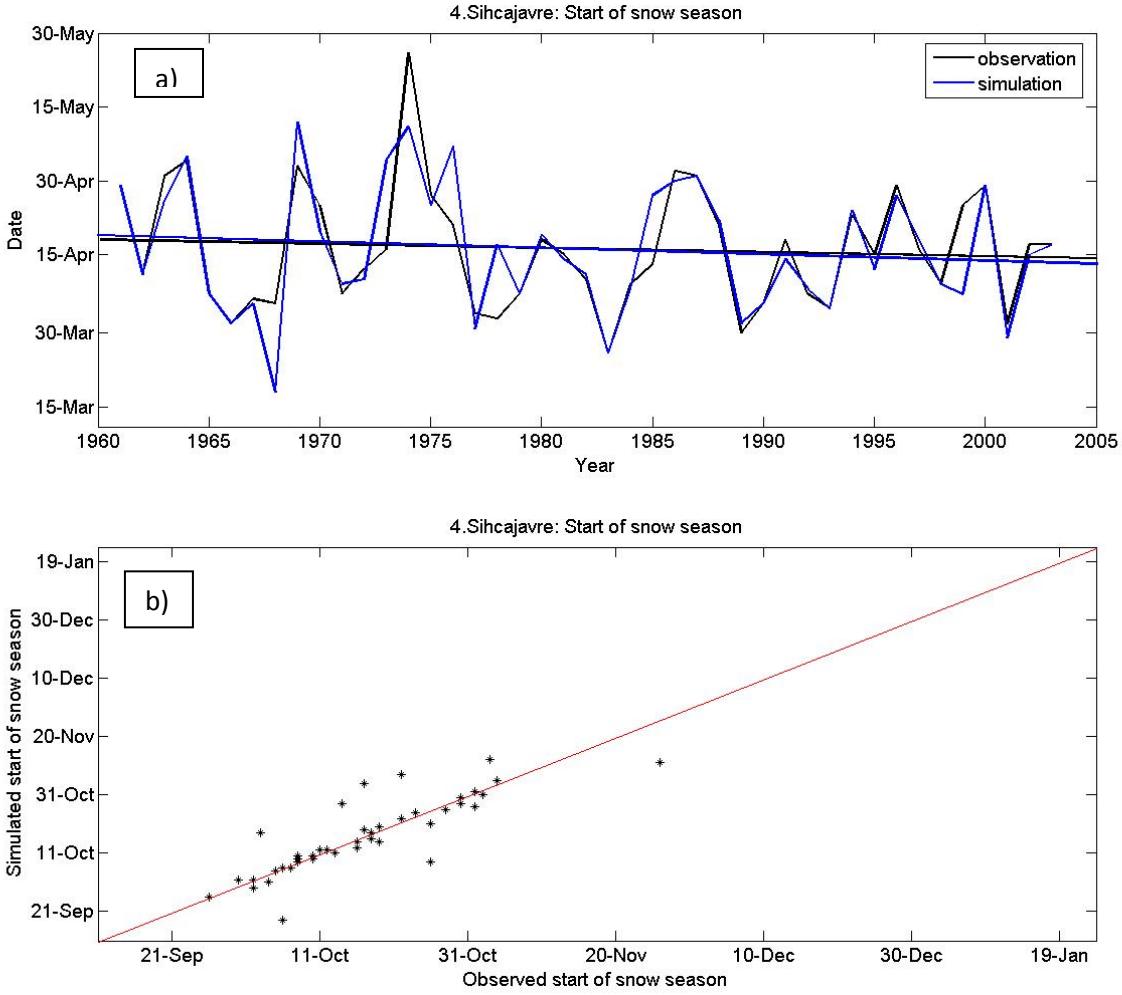

Figure 3.41: Observed and simulated start of snow season at station 4 Sihcajavri: a) Time series b) Scatter plot.

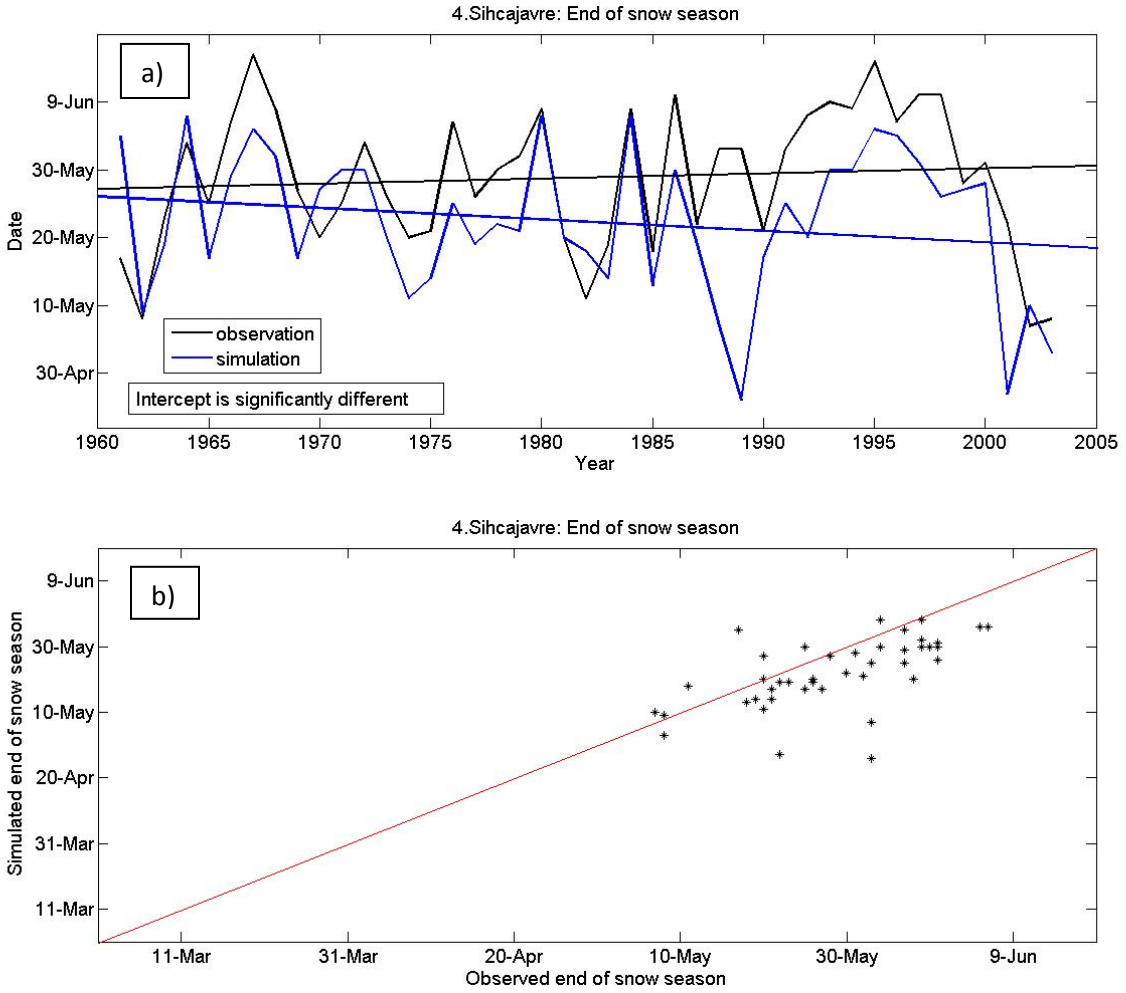

Figure 3.42: Observed and simulated end of snow season at station 4 Sihcajavri: a) Time series b) Scatter plot.

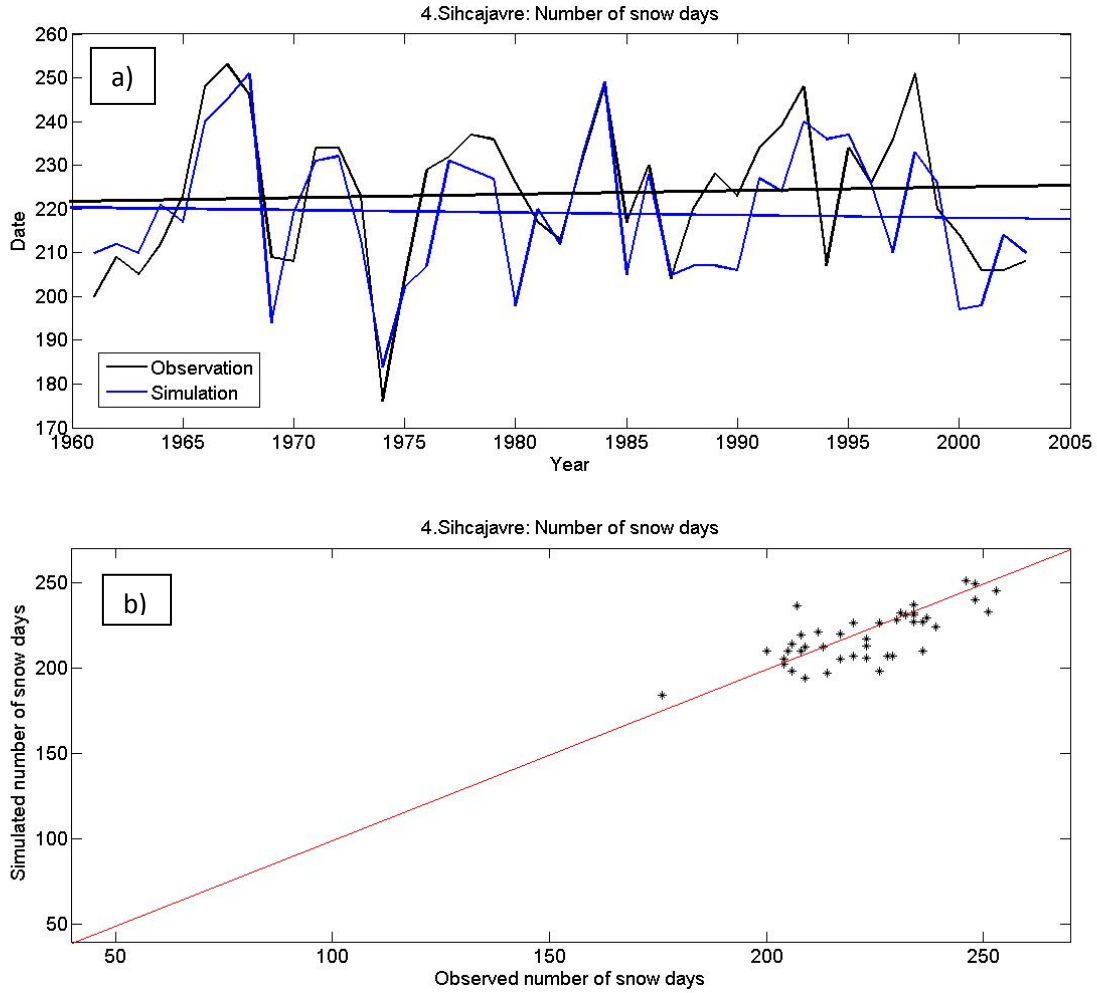

Figure 3.43: Observed and simulated number of snow days per winter season at station 4 Sihcajavri: a) Time series b) Scatter plot.

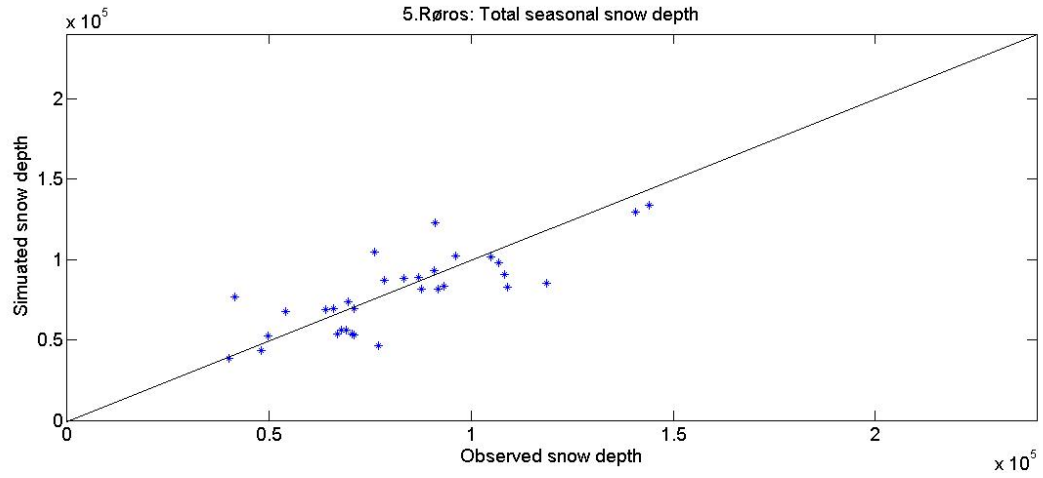

Figure 3.44: Scatteplot of observed versus simulated total snow depth for the winter season at station 5 Røros.

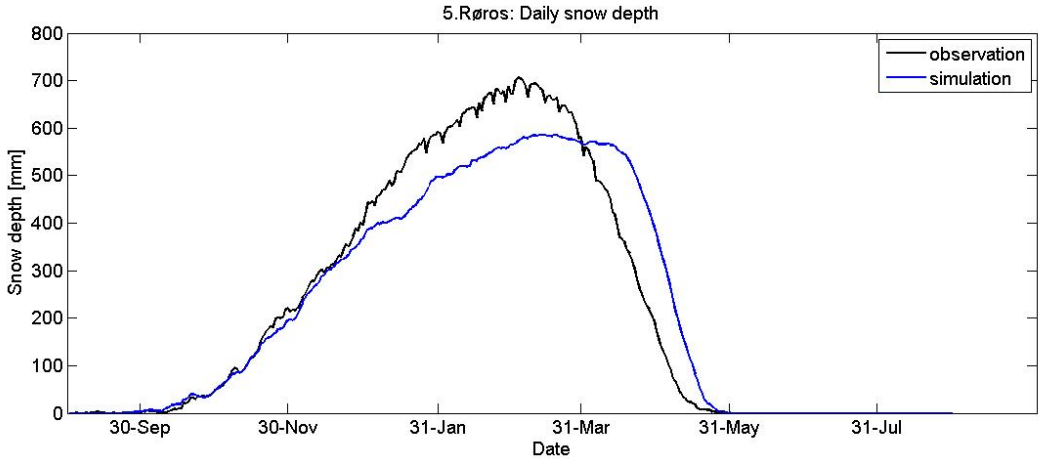

Figure 3.45: Mean daily snow depth (1971-2003) at station 5 Røros.

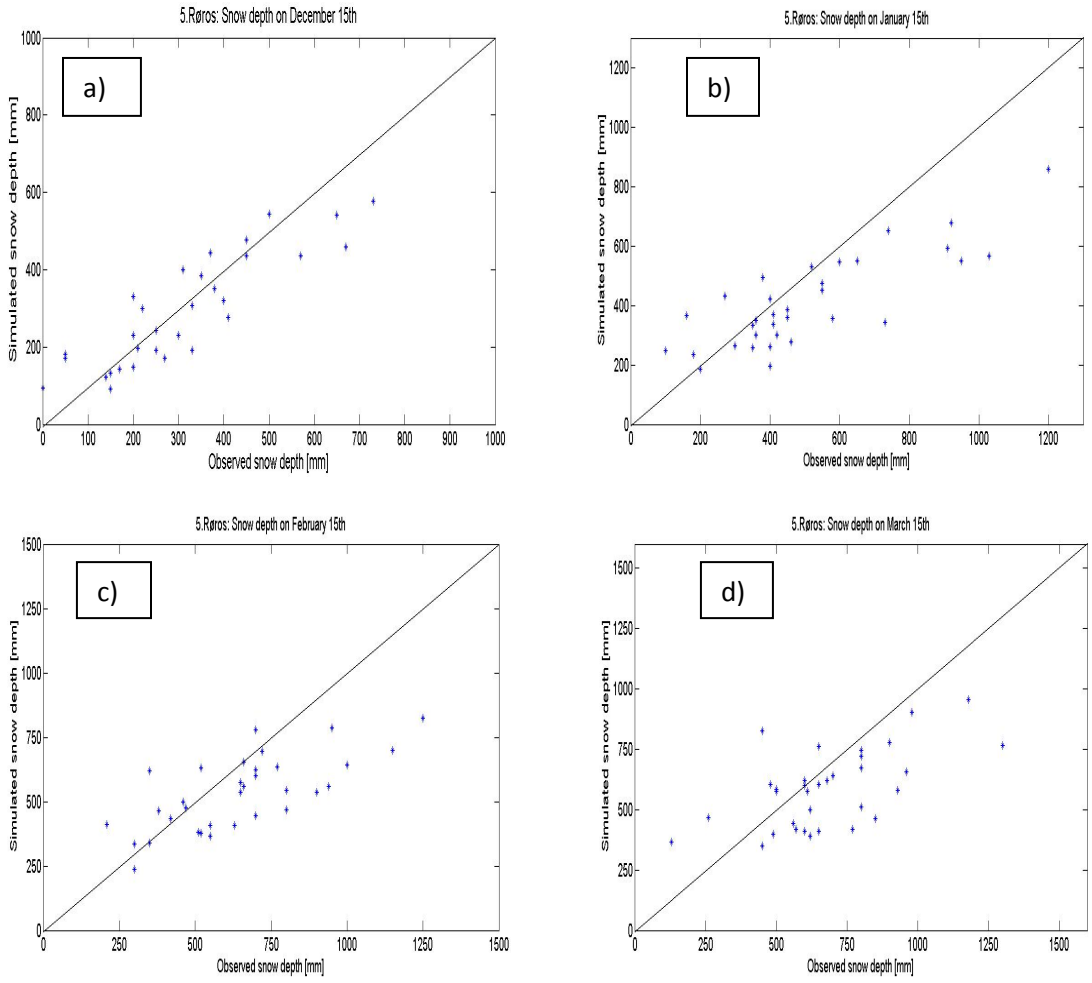

Figure 3.46: Station 5 Røros: Scatter plots of observed and simulated snow depth on a) December 15th b) January 15th c) February 15th d) March 15th.

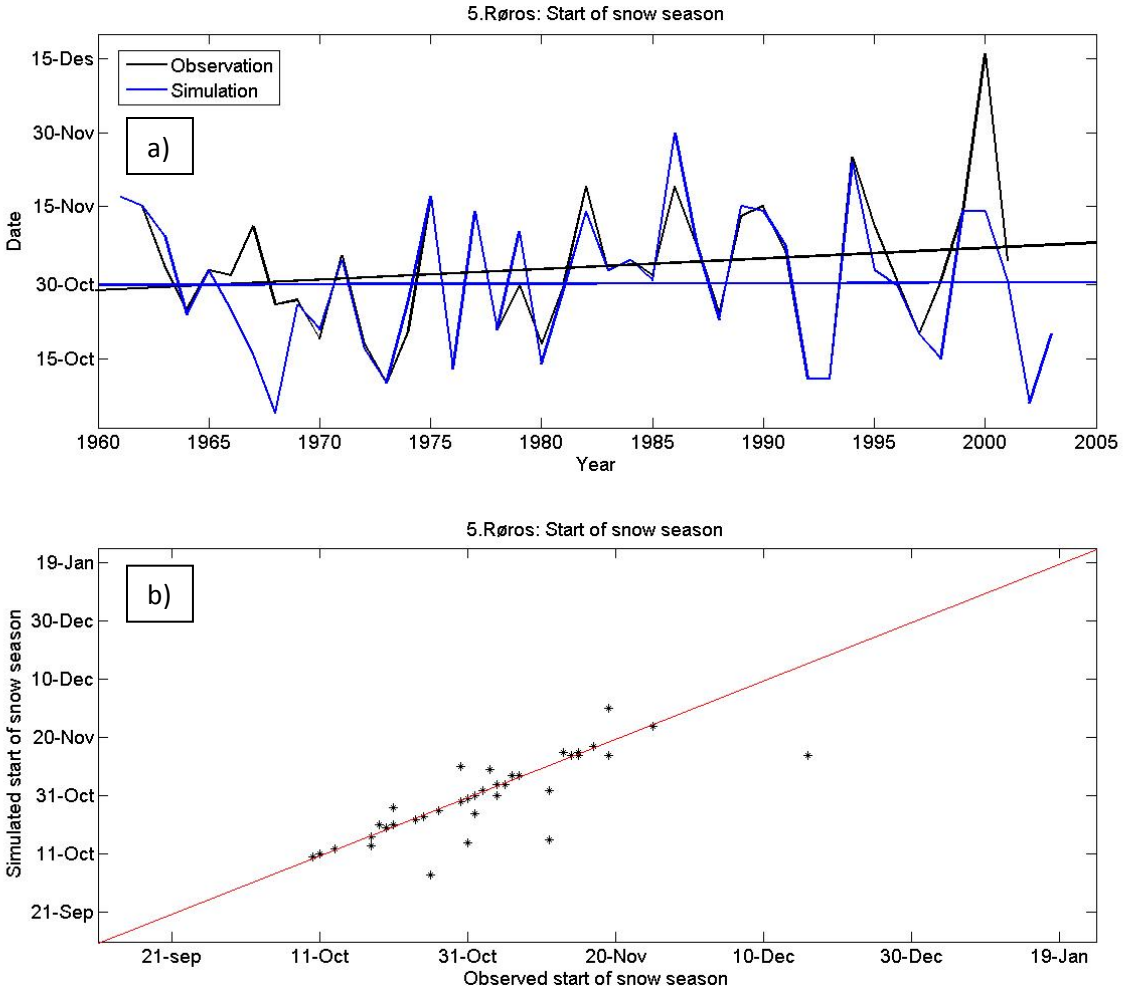

Figure 3.47: Observed and simulated start of snow season at station 5 Røros: a) Time series b) Scatter plot.

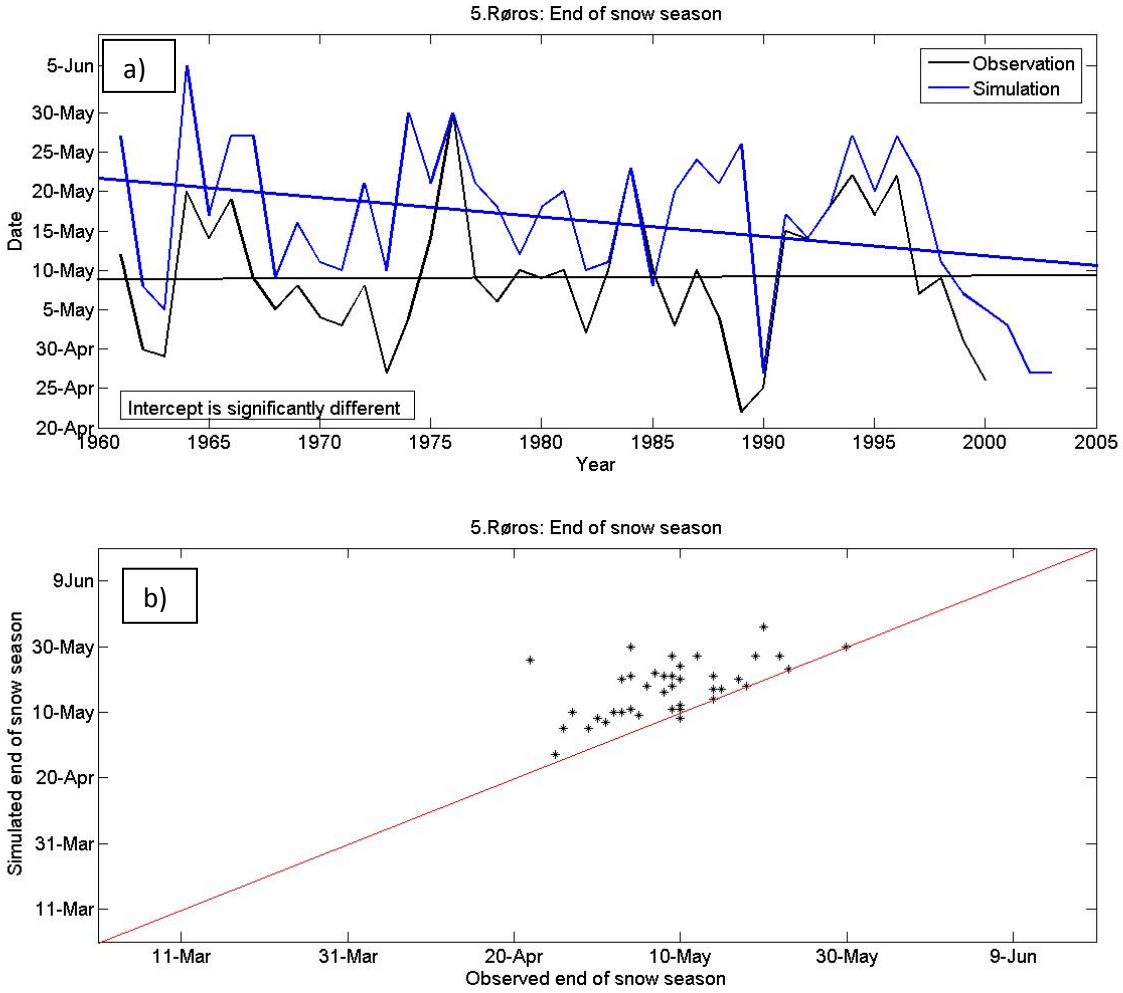

Figure 3.48: Observed and simulated end of snow season at station 5 Røros: a) Time series b) Scatter plot.

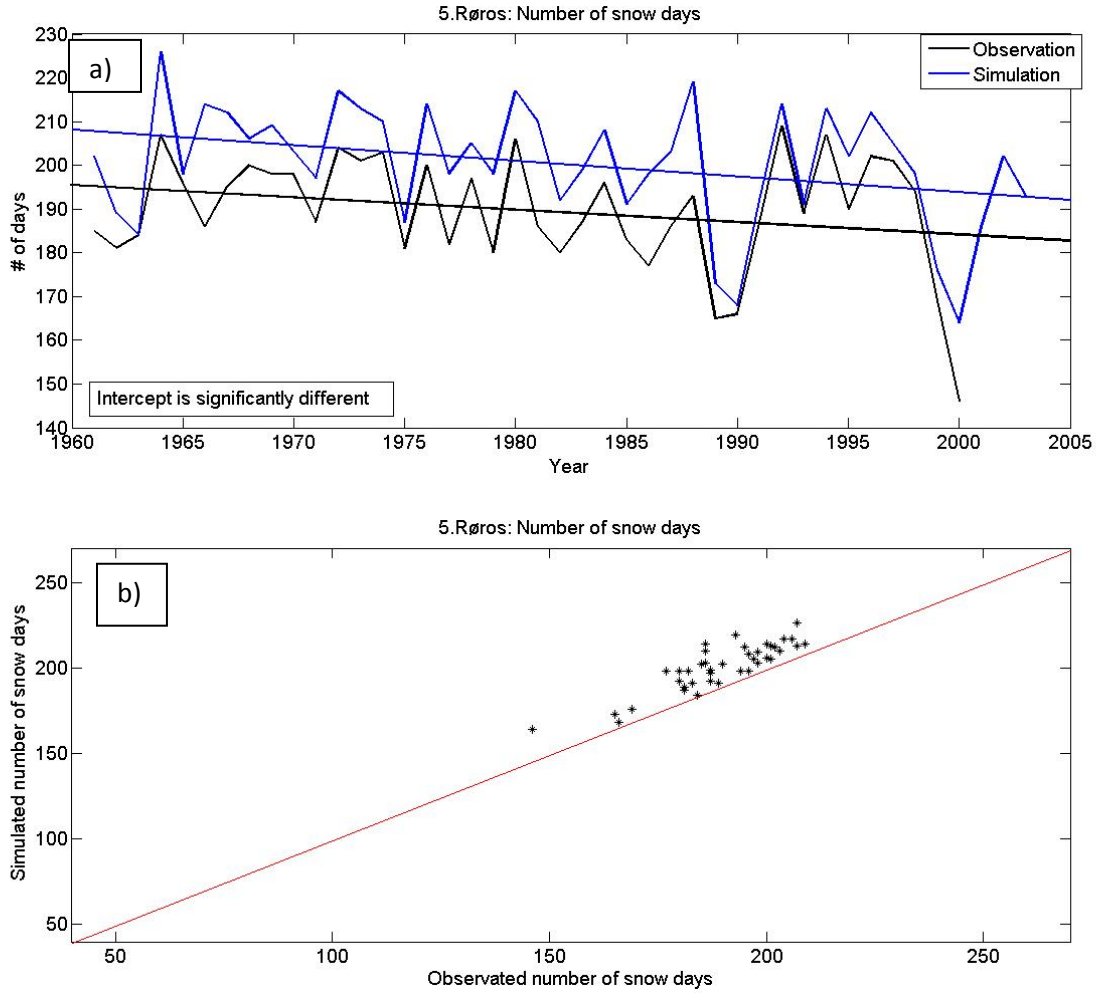

Figure 3.49: Observed and simulated number of snow days per winter season at station 5 Røros: a) Time series b) Scatter plot.

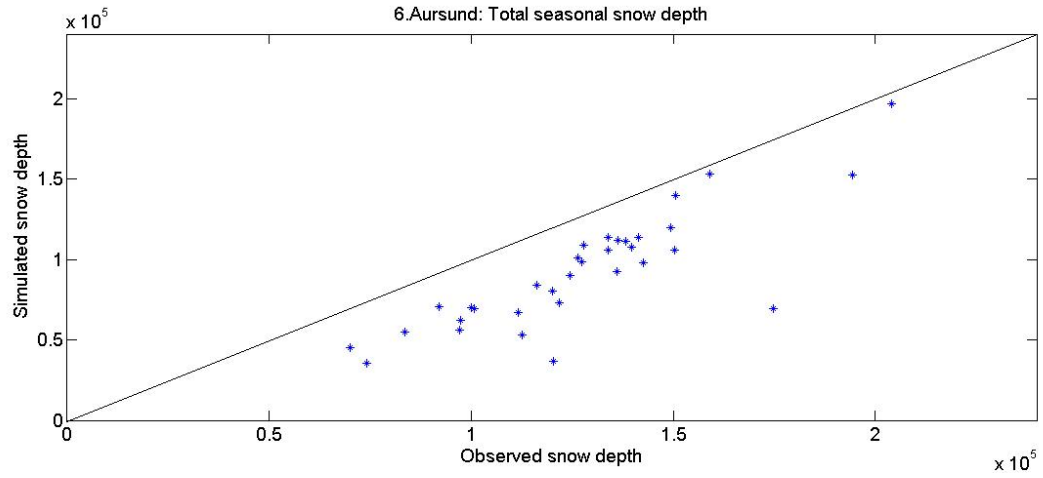

Figure 3.50: Scatteplot of observed versus simulated total snow depth for the winter season at station 6 Aursund.

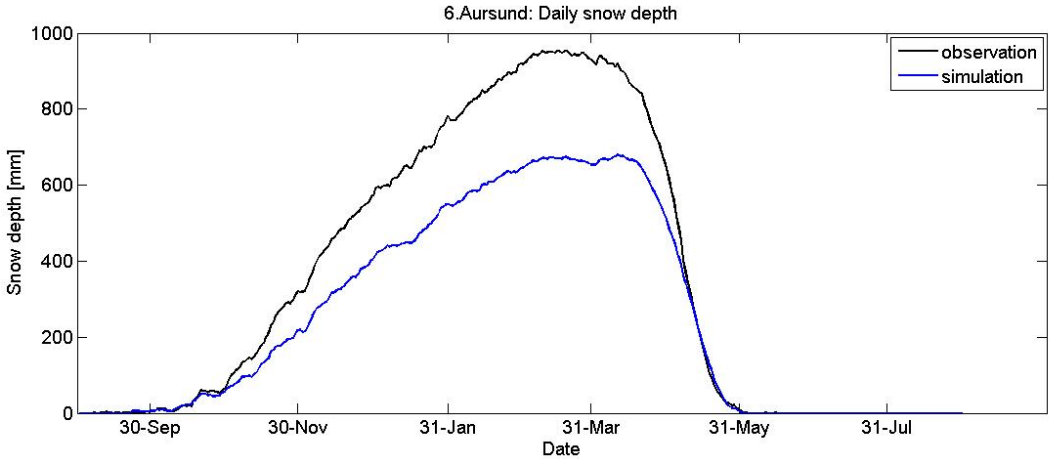

Figure 3.51: Mean daily snow depth (1971-2003) at station 6 Aursund.

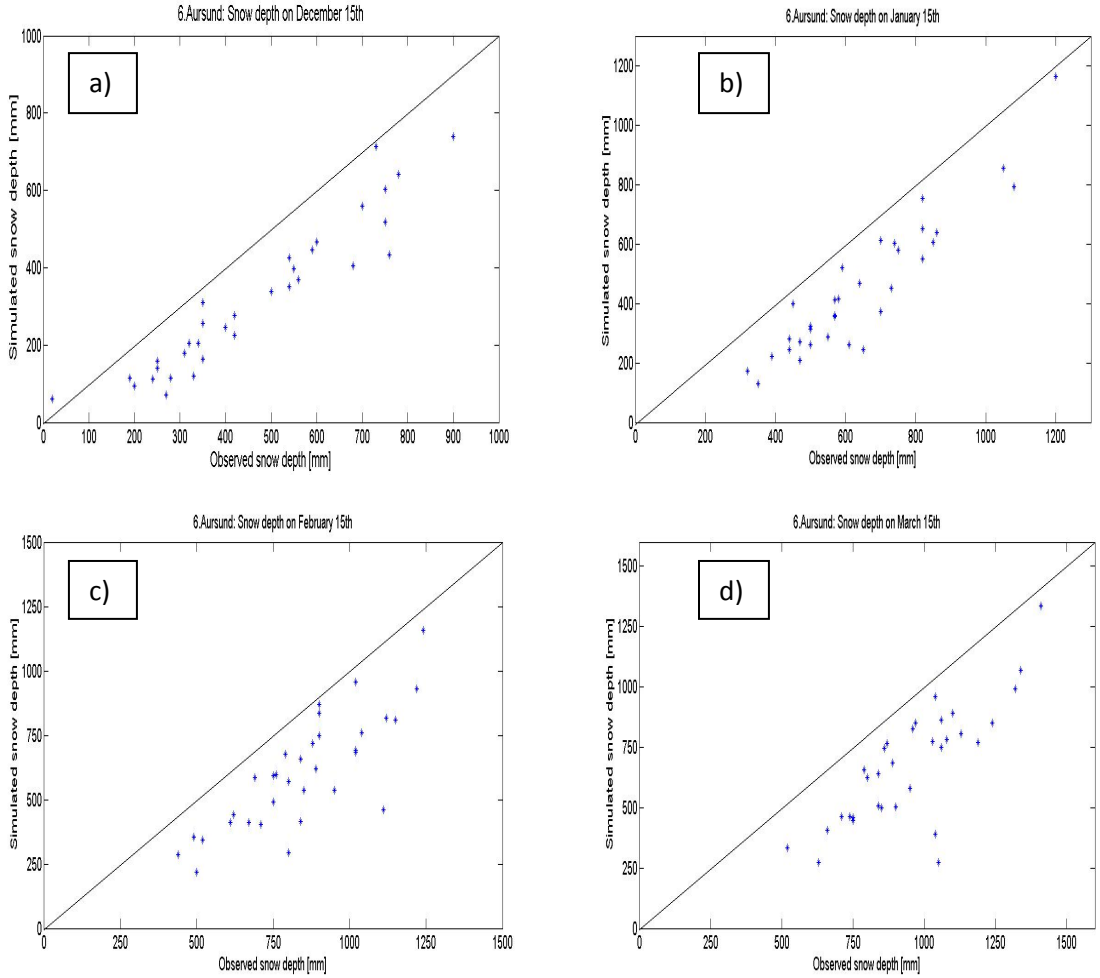

Figure 3.52: Station 6 Aursund: Scatter plots of observed and simulated snow depth on a) December 15th b) January 15th c) February 15th d) March 15th.

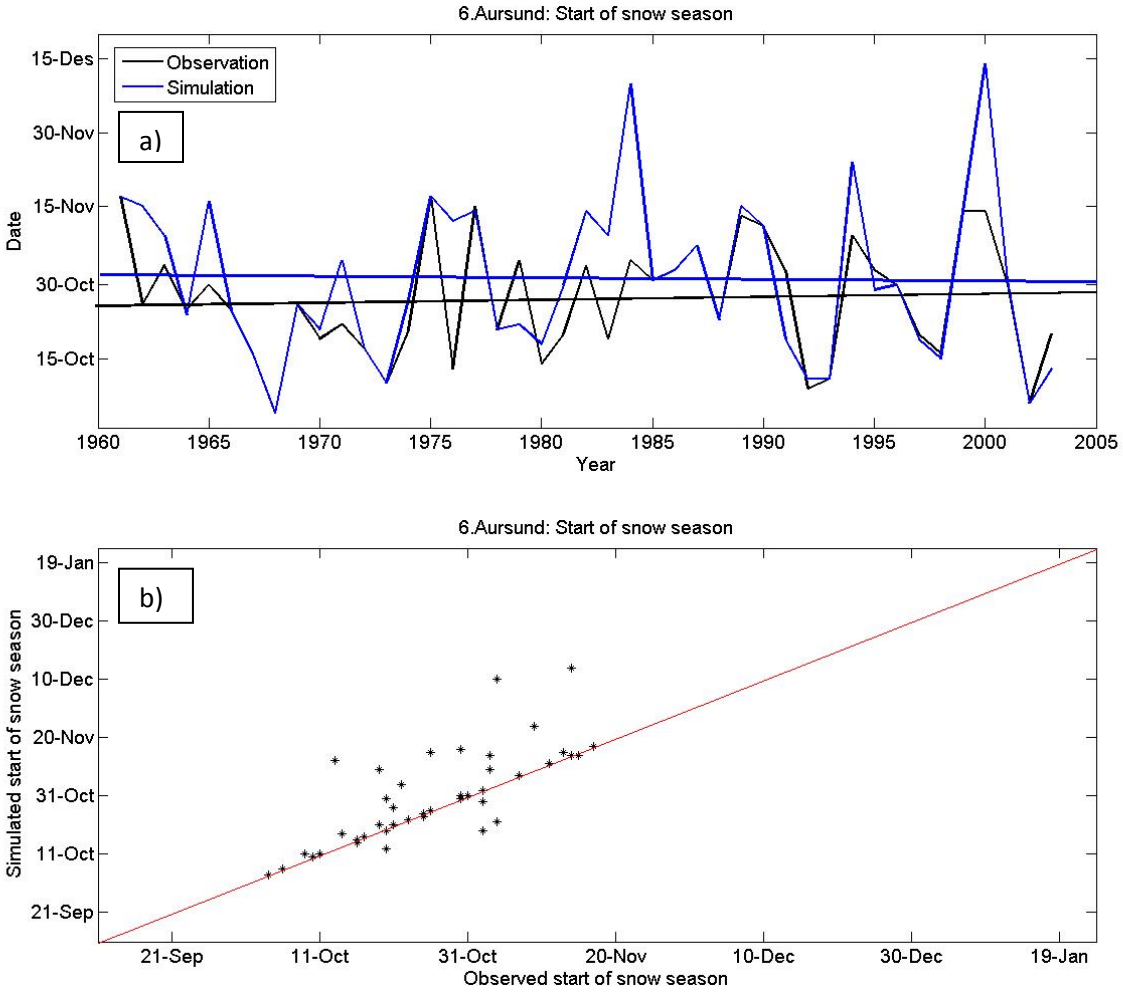

Figure 3.53: Observed and simulated start of snow season at station 6 Aursund: a) Time series b) Scatter plot.

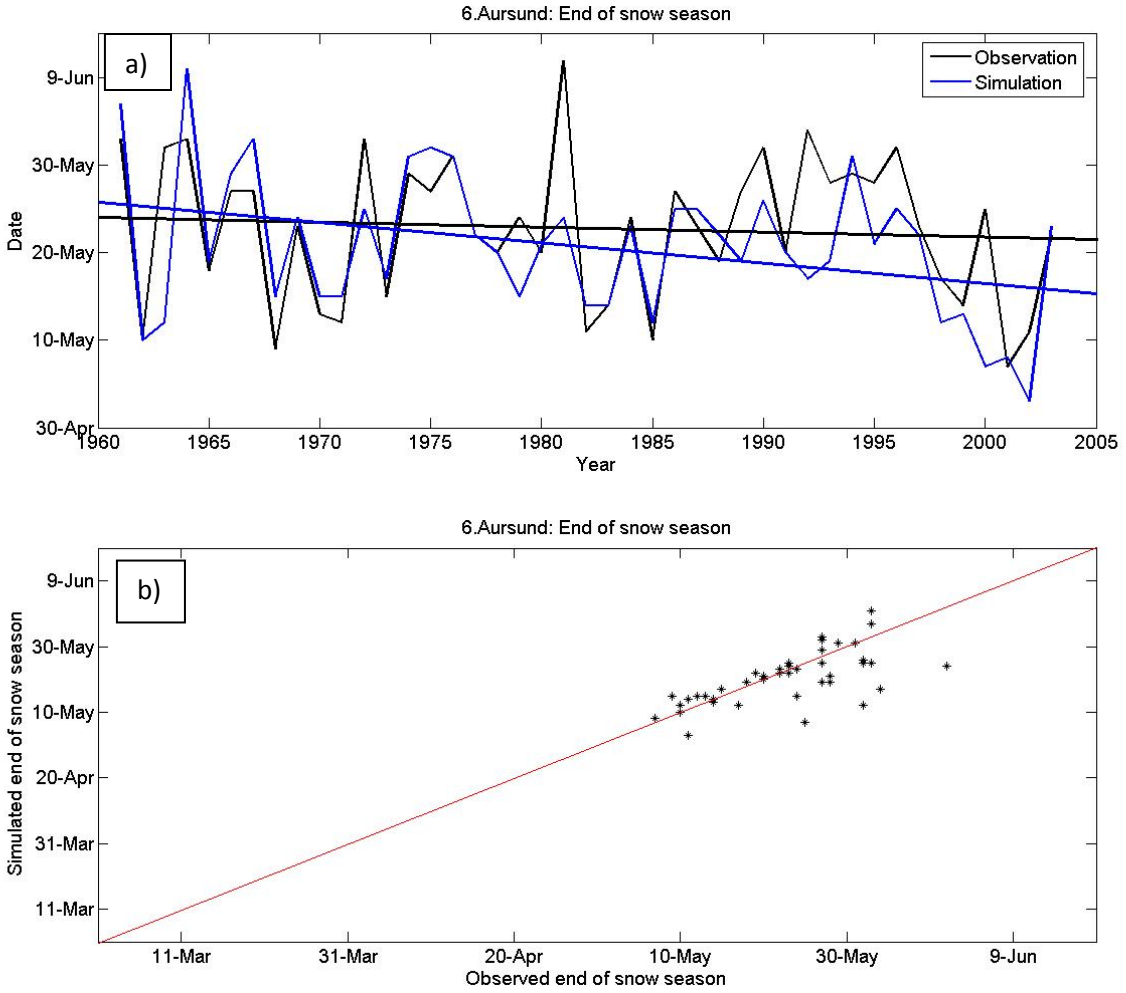

Figure 3.54: Observed and simulated end of snow season at station 6 Aursund: a) Time series b) Scatter plot.

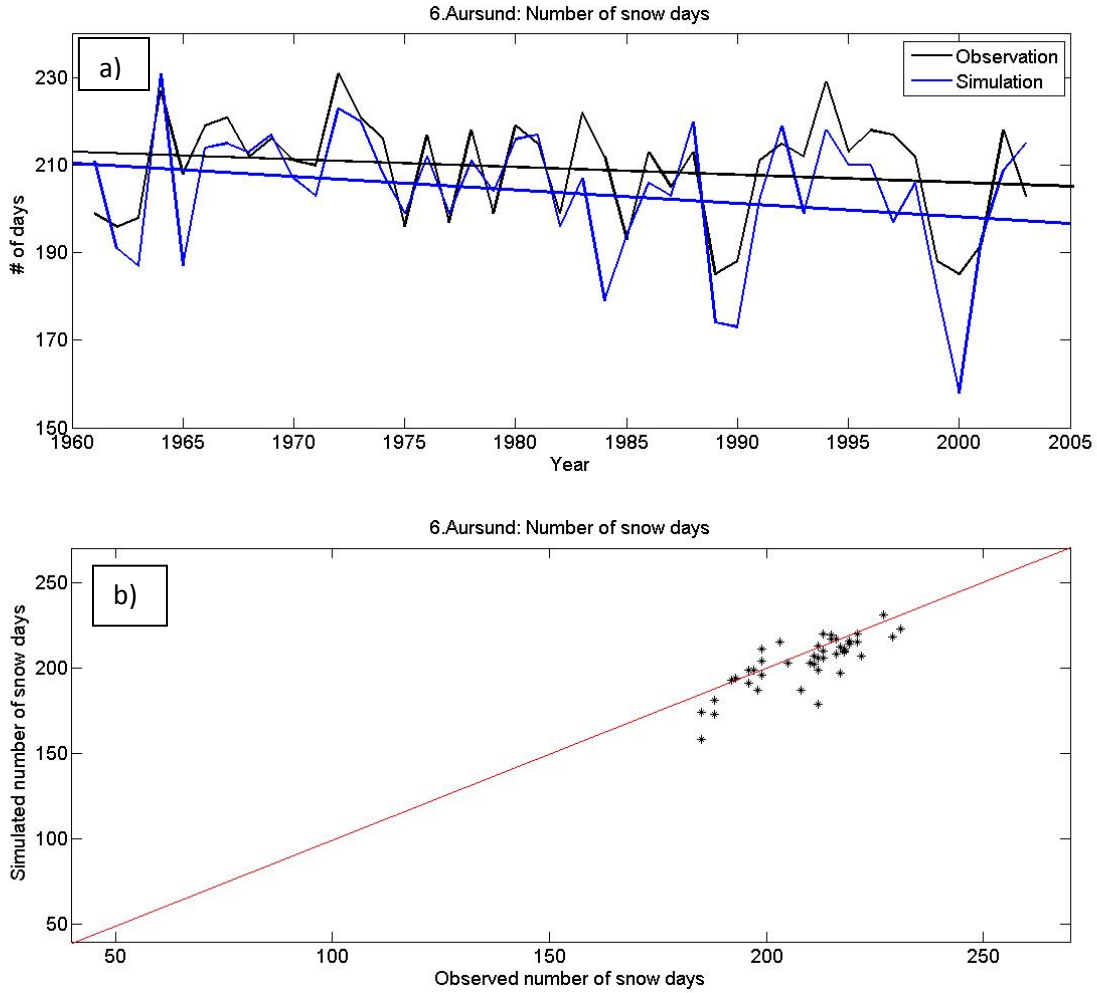

Figure 3.55: Observed and simulated number of snow days per winter season at station 6 Aursund: a) Time series b) Scatter plot.

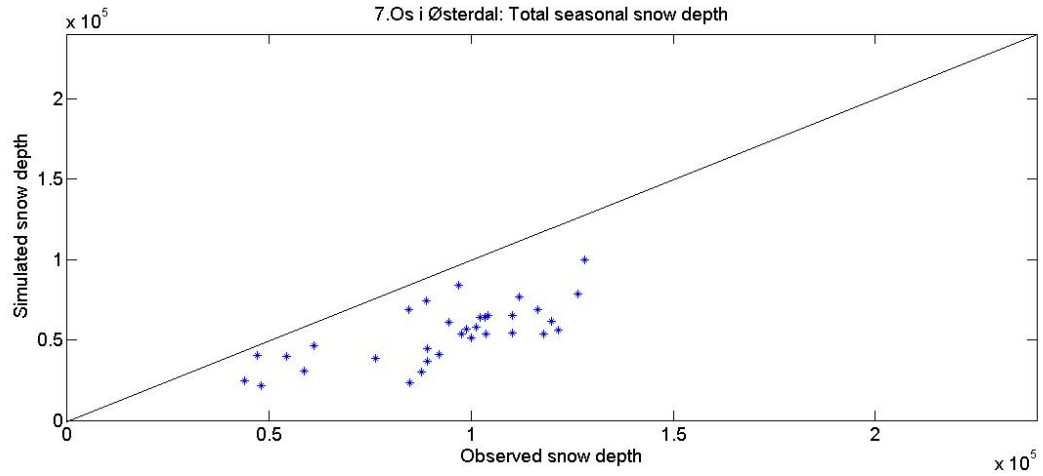

Figure 3.56: Scatteplot of observed versus simulated total snow depth for the winter season at station 7 Os i Østerdal.

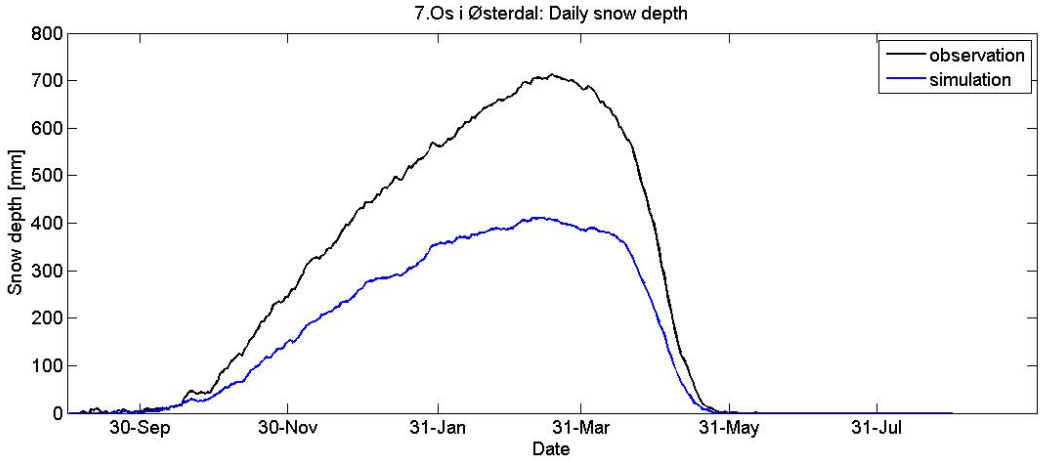

Figure 3.57: Mean daily snow depth (1971-2003) at station 7 Os i Østerdal.

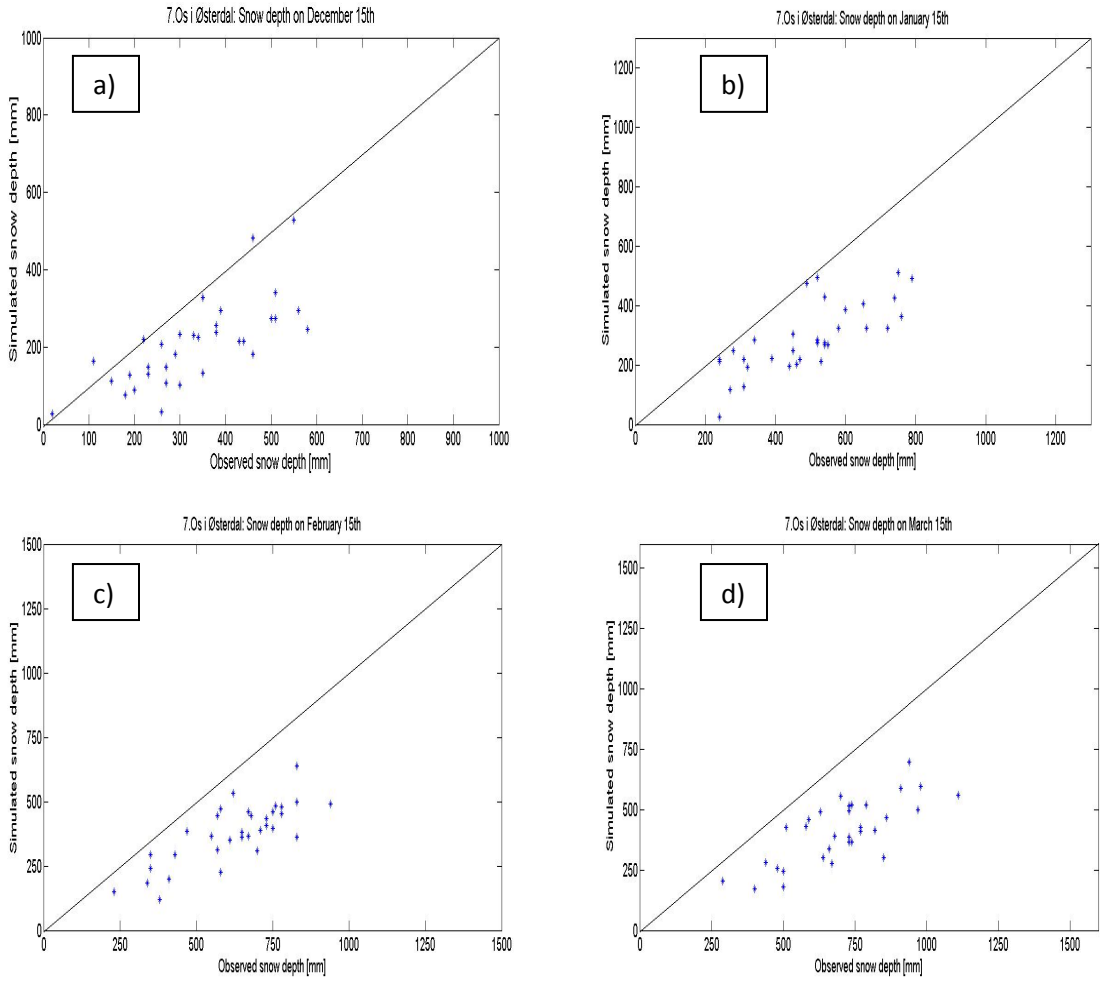

Figure 3.58: Station 7 Os i Østerdal: Scatter plots of observed and simulated snow depth on a) December 15th b) January 15th c) February 15th d) March 15th.

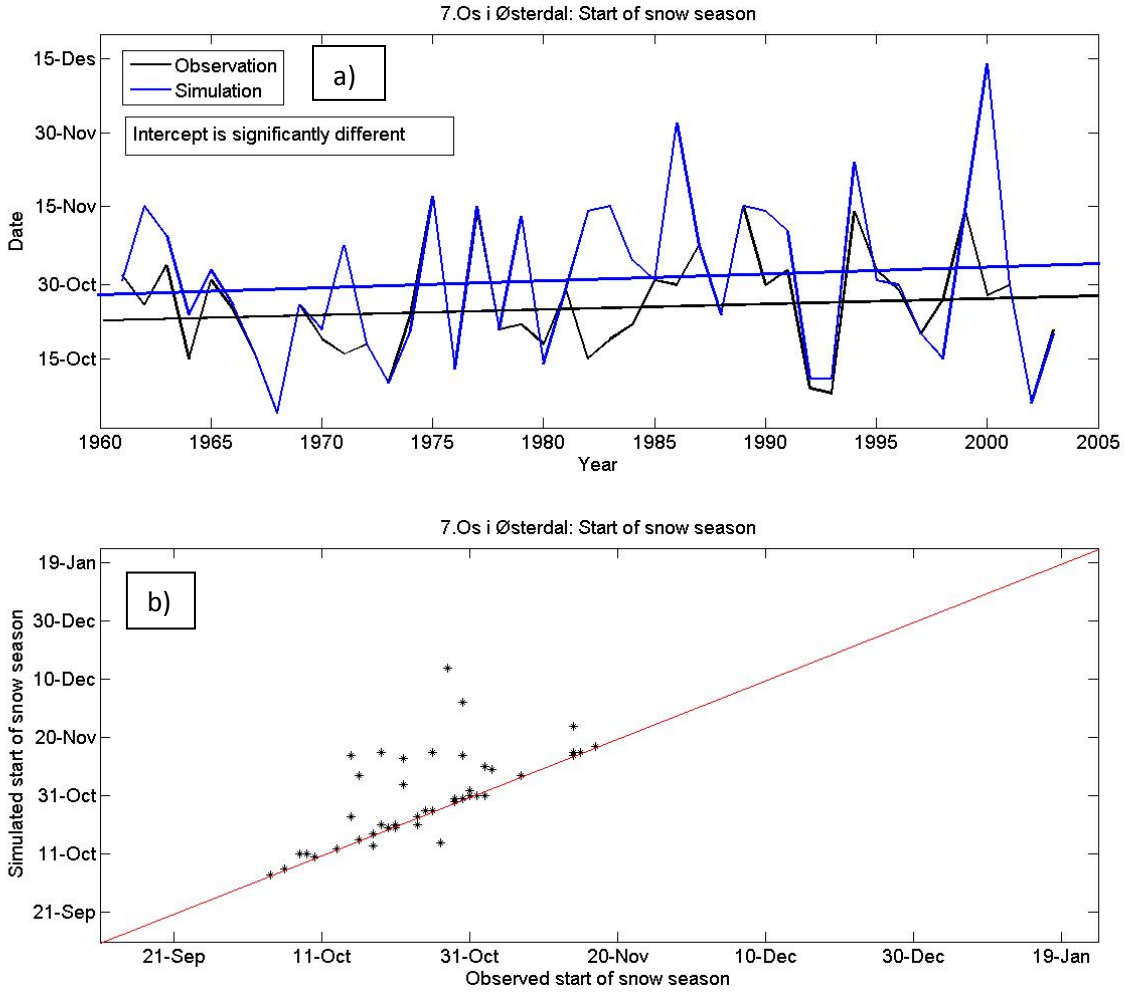

Figure 3.59: Observed and simulated start of snow season at station 7 Os i Østerdal: a) Time series b) Scatter plot.

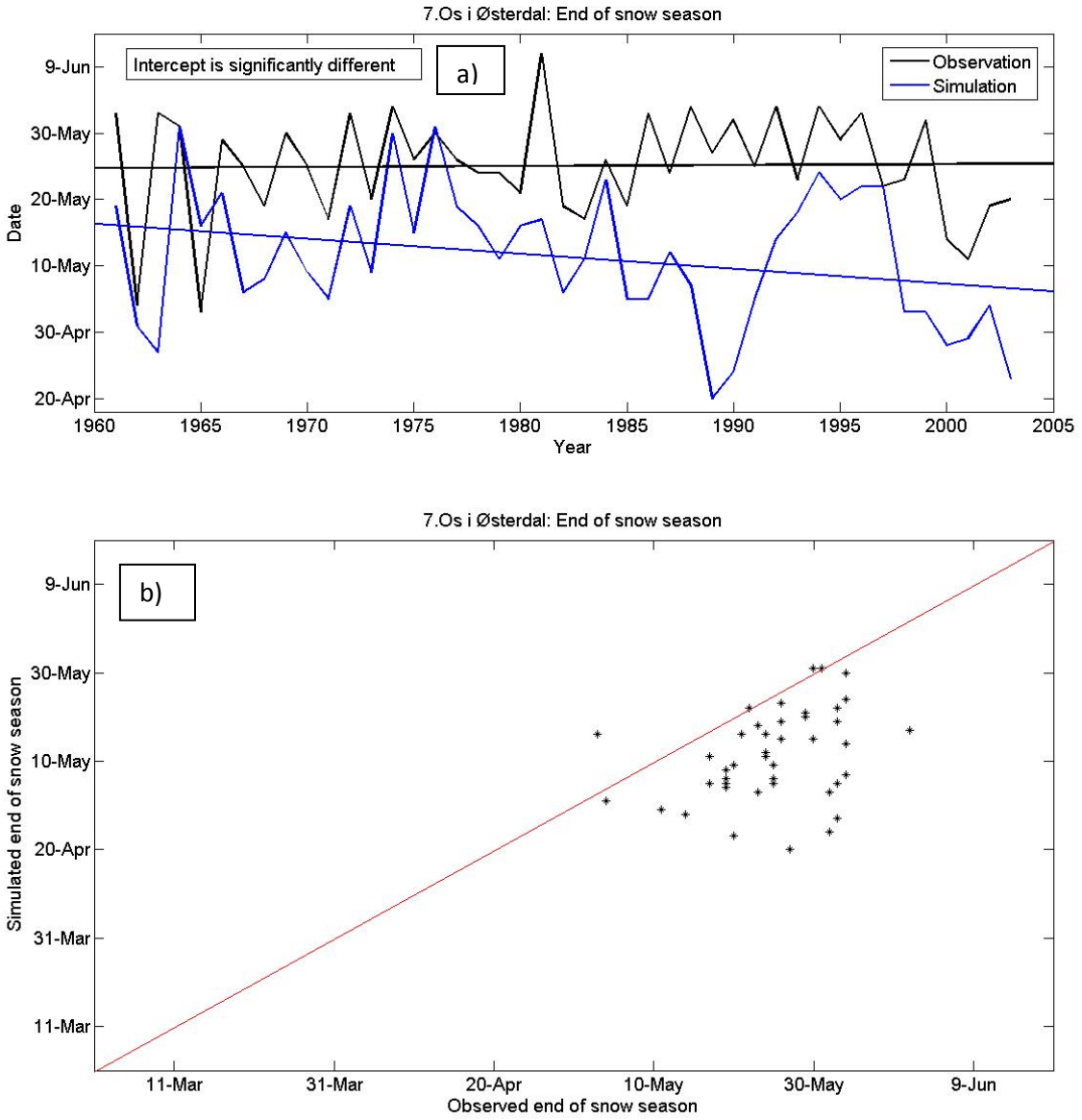

Figure 3.60: Observed and simulated end of snow season at station 7 Os i Østerdal: a) Time series b) Scatter plot.

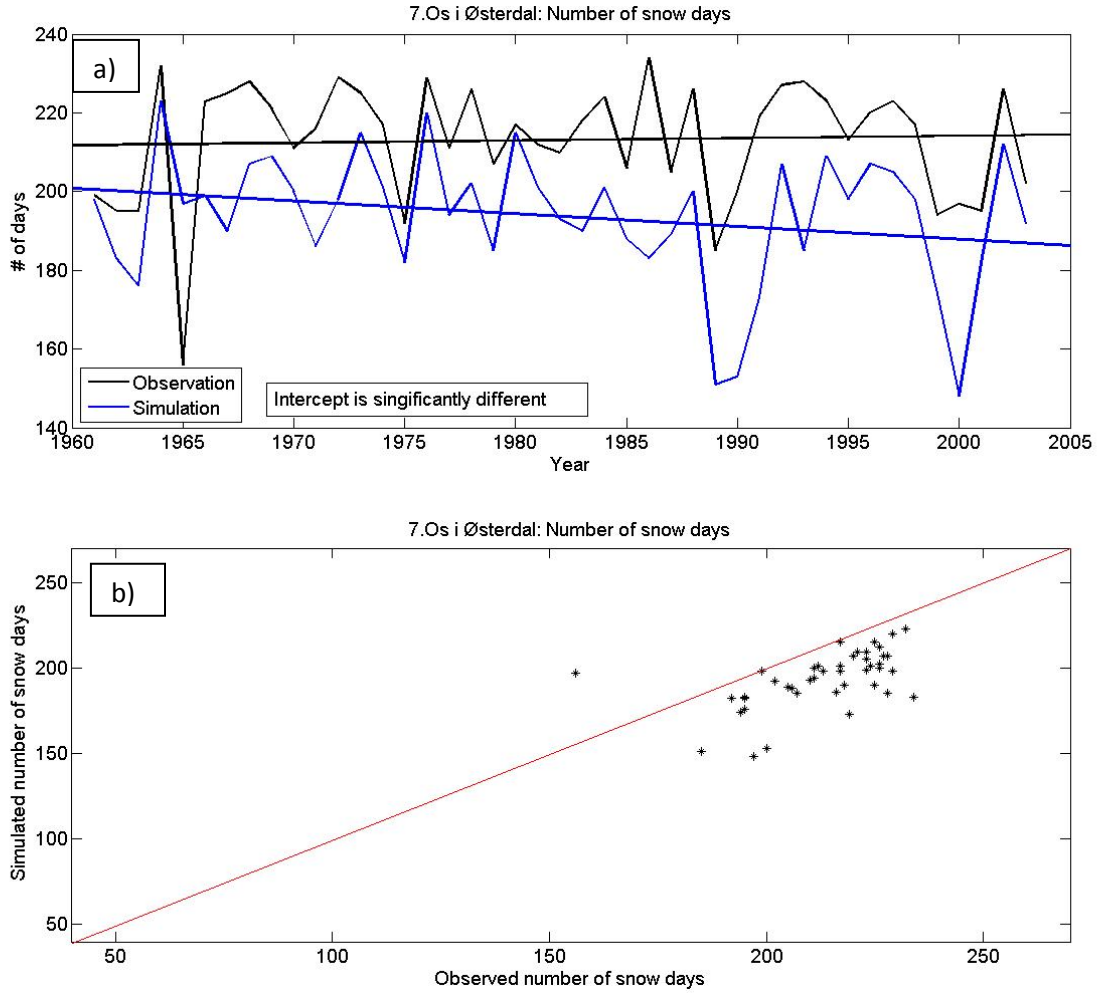

Figure 3.61: Observed and simulated number of snow days per winter season at station 7 Os i Østerdal: a) Time series b) Scatter plot.

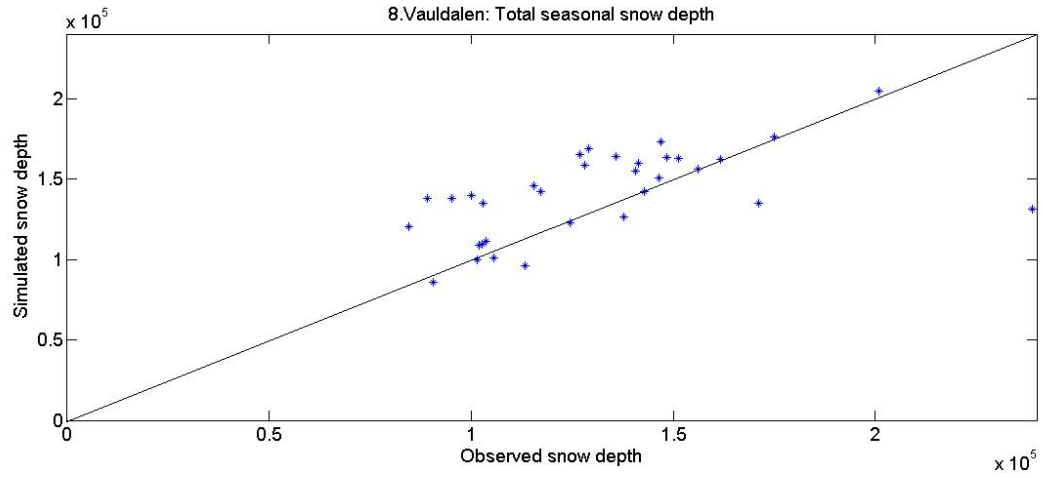

Figure 3.62: Scatteplot of observed versus simulated total snow depth for the winter season at station 8 Vauldalen.

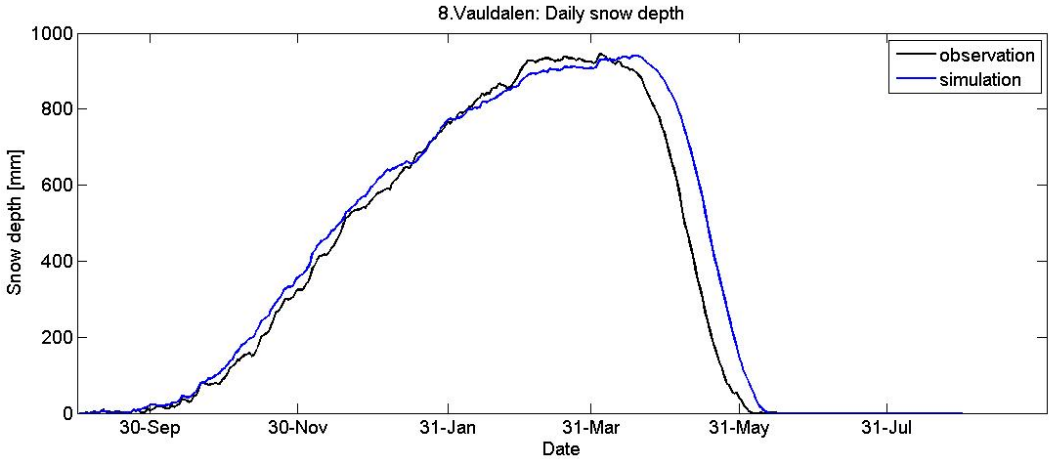

Figure 3.63: Mean daily snow depth (1971-2003) at station 8 Aursund.

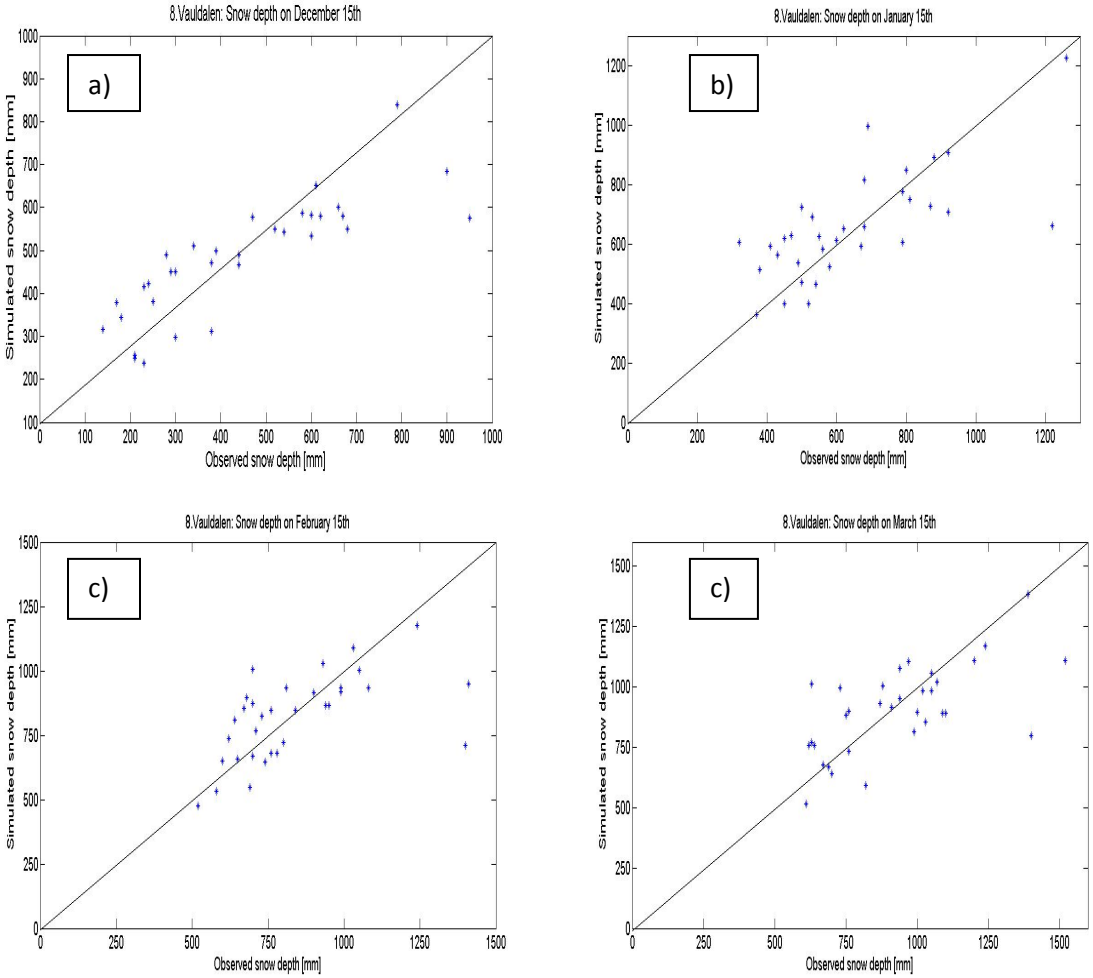

Figure 3.64: Station 8 Vauldalen: Scatter plots of observed and simulated snow depth on a) December 15th b) January 15th c) February 15th d) March 15th.

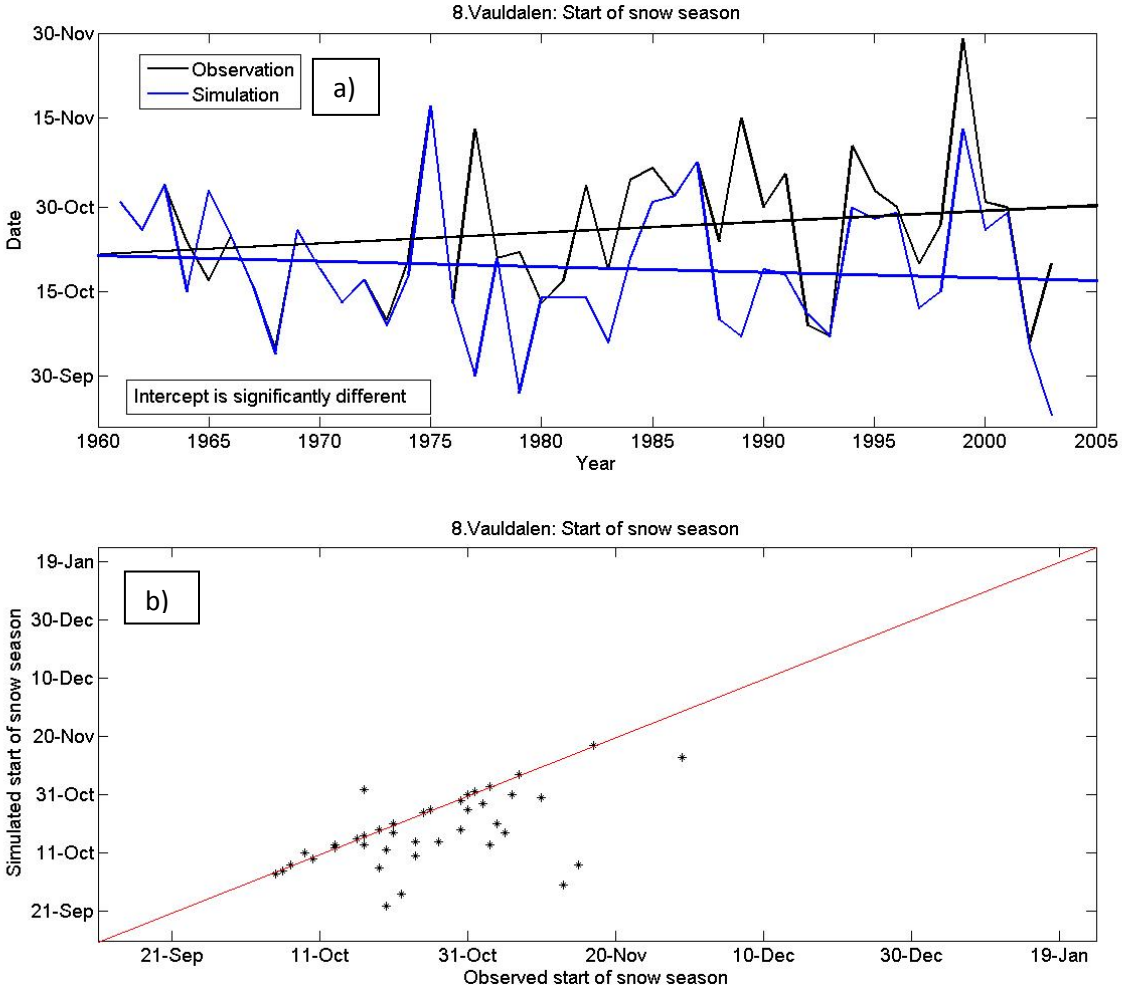

Figure 3.65: Observed and simulated start of snow season at station 8 Vauldalen: a) Time series b) Scatter plot.

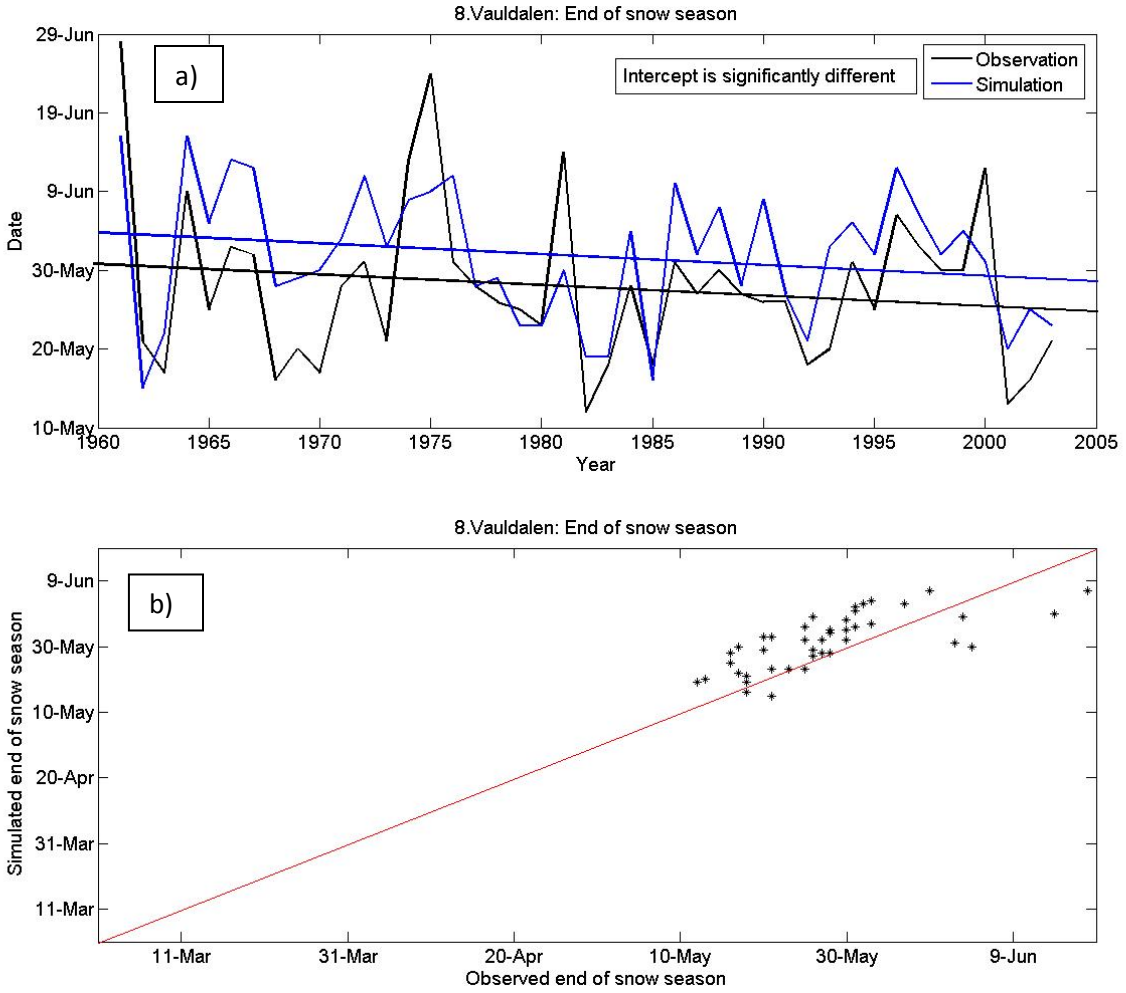

Figure 3.66: Observed and simulated end of snow season at station 8 Vauldalen: a) Time series b) Scatter plot.

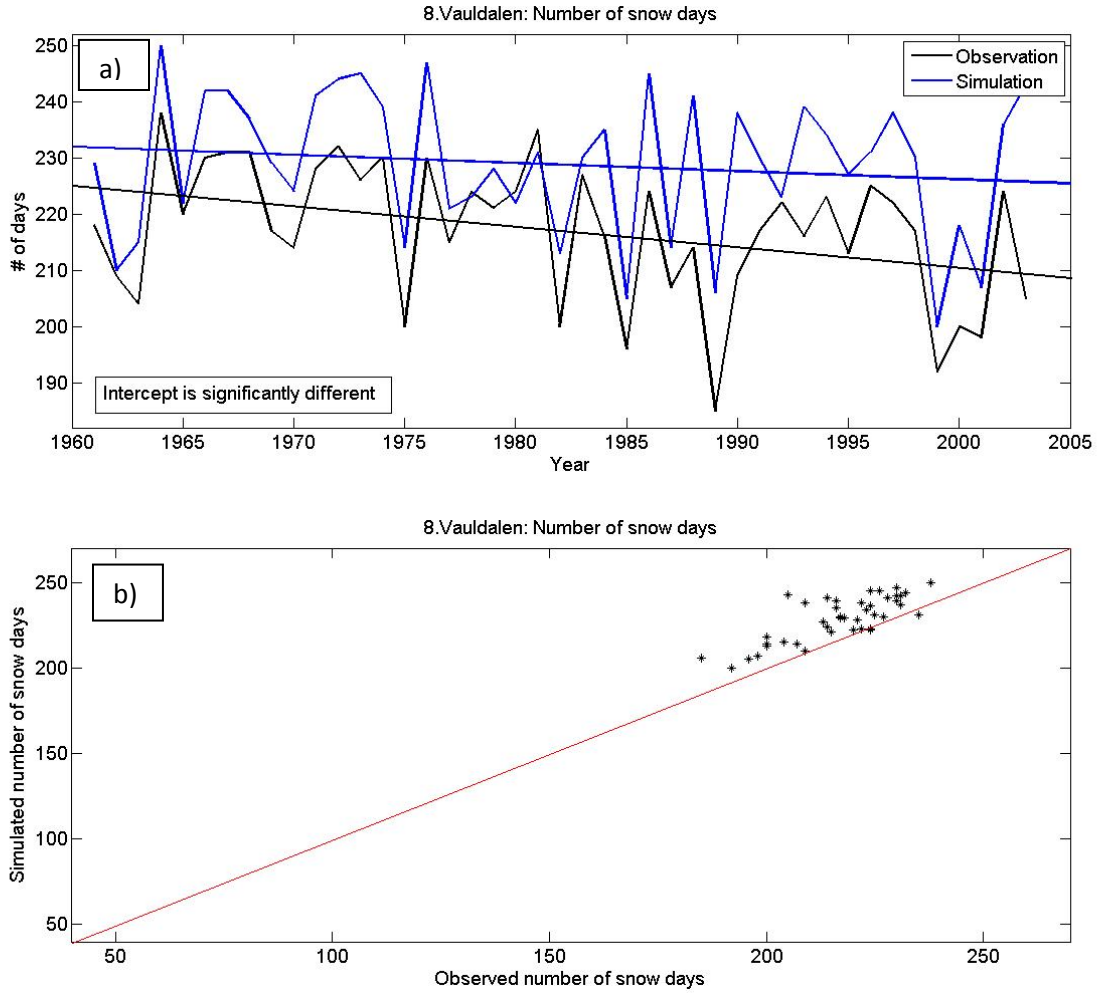

Figure 3.67: Observed and simulated number of snow days per winter season at station 8 Vauldalen: a) Time series b) Scatter plot.

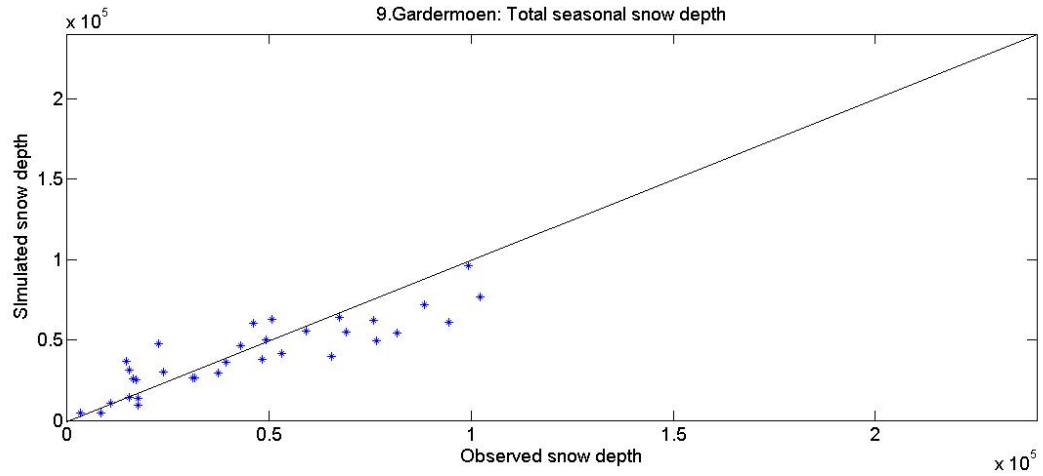

Figure 3.68: Scatteplot of observed versus simulated total snow depth for the winter season at station 9 Gardermoen.

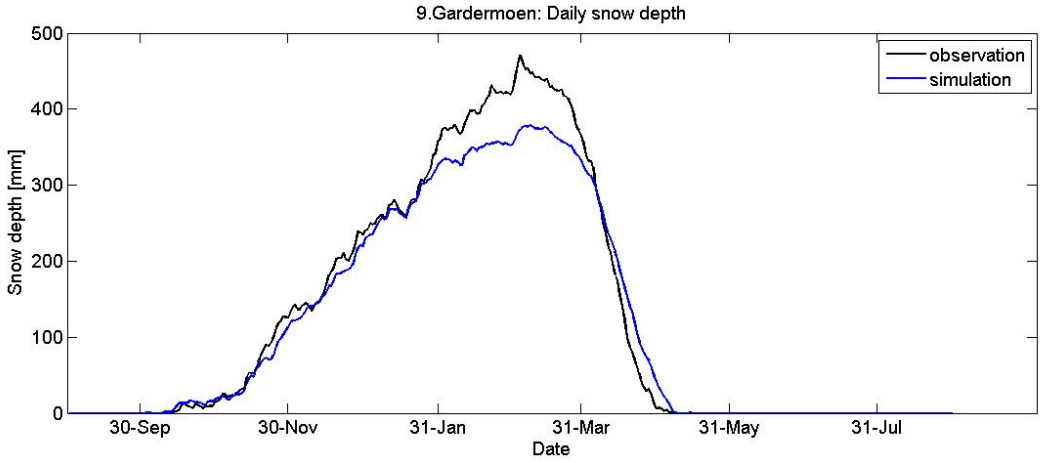

Figure 3.69: Mean daily snow depth (1971-2003) at station 9 Gardermoen.

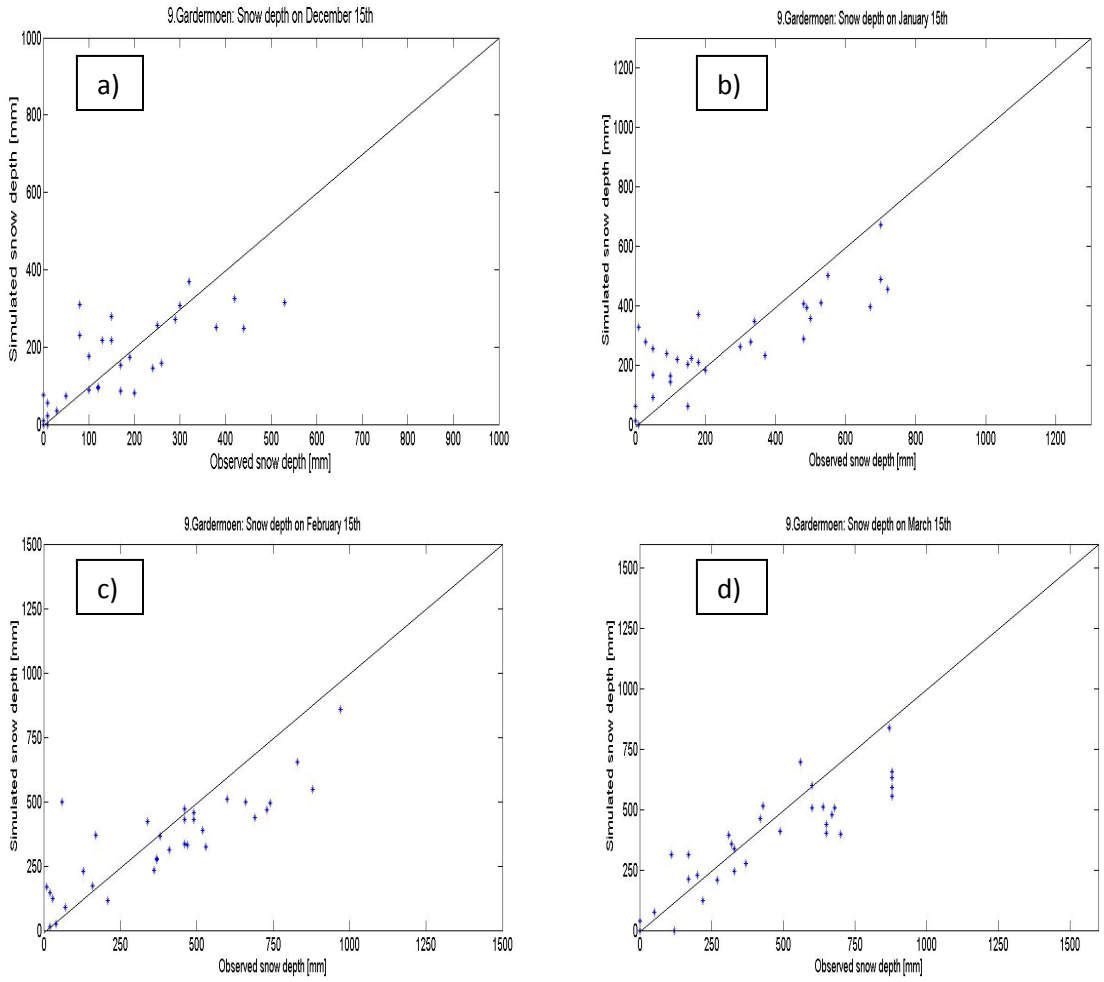

Figure 3.70: Station 9 Gardermoen: Scatter plots of observed and simulated snow depth on a) December 15th b) January 15th c) February 15th d) March 15th.

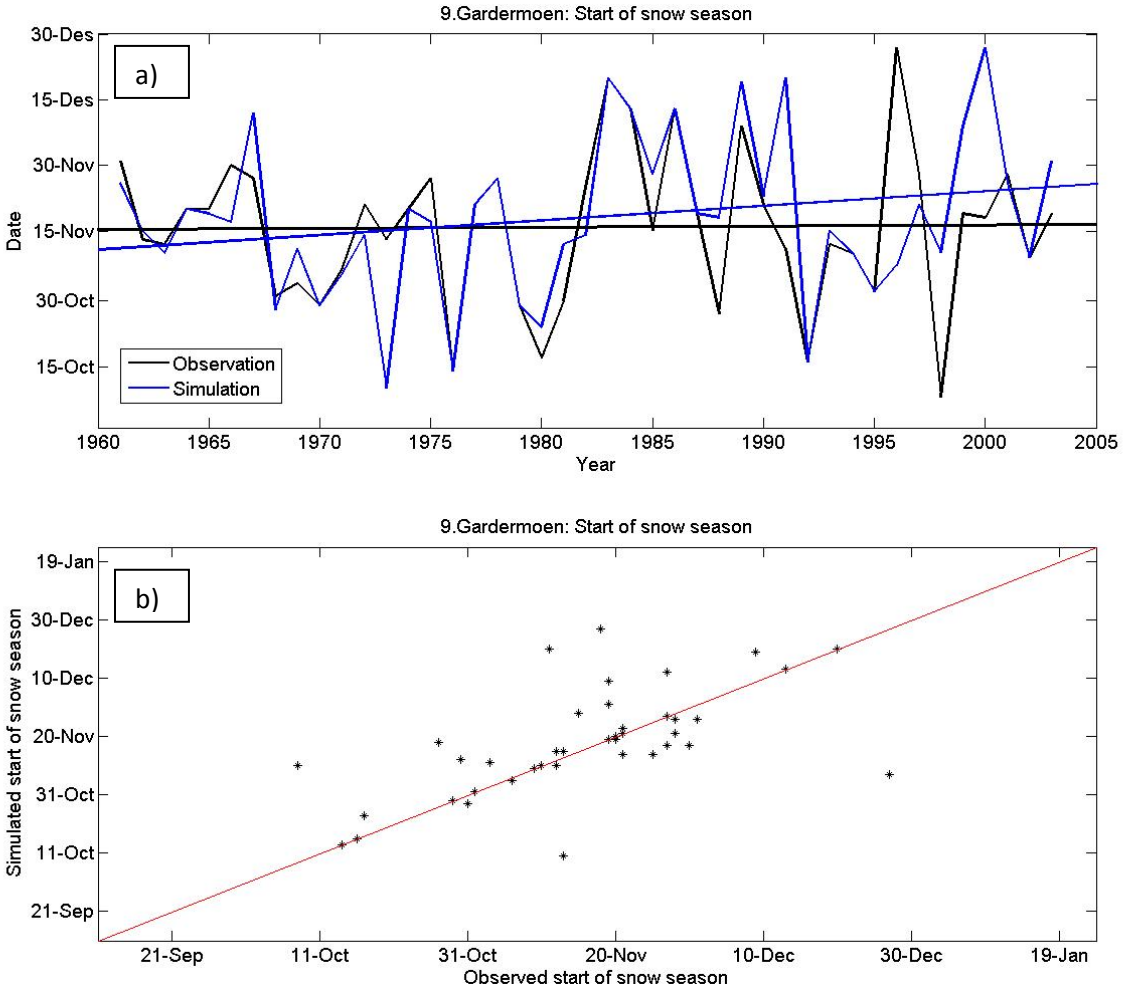

Figure 3.71: Observed and simulated start of snow season at station 9 Gardermoen: a) Time series b) Scatter plot.

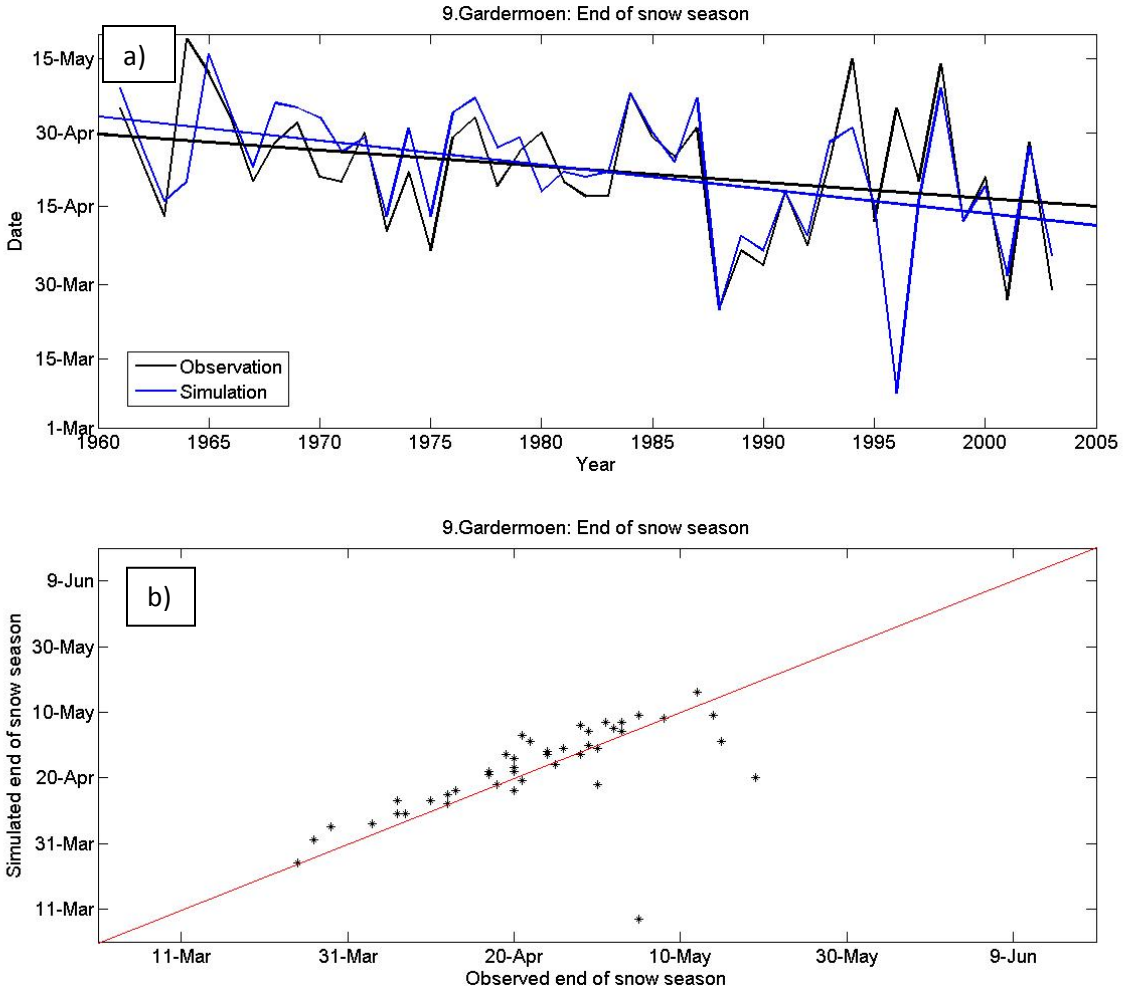

Figure 3.72: Observed and simulated end of snow season at station 9 Gardermoen: a) Time series b) Scatter plot.

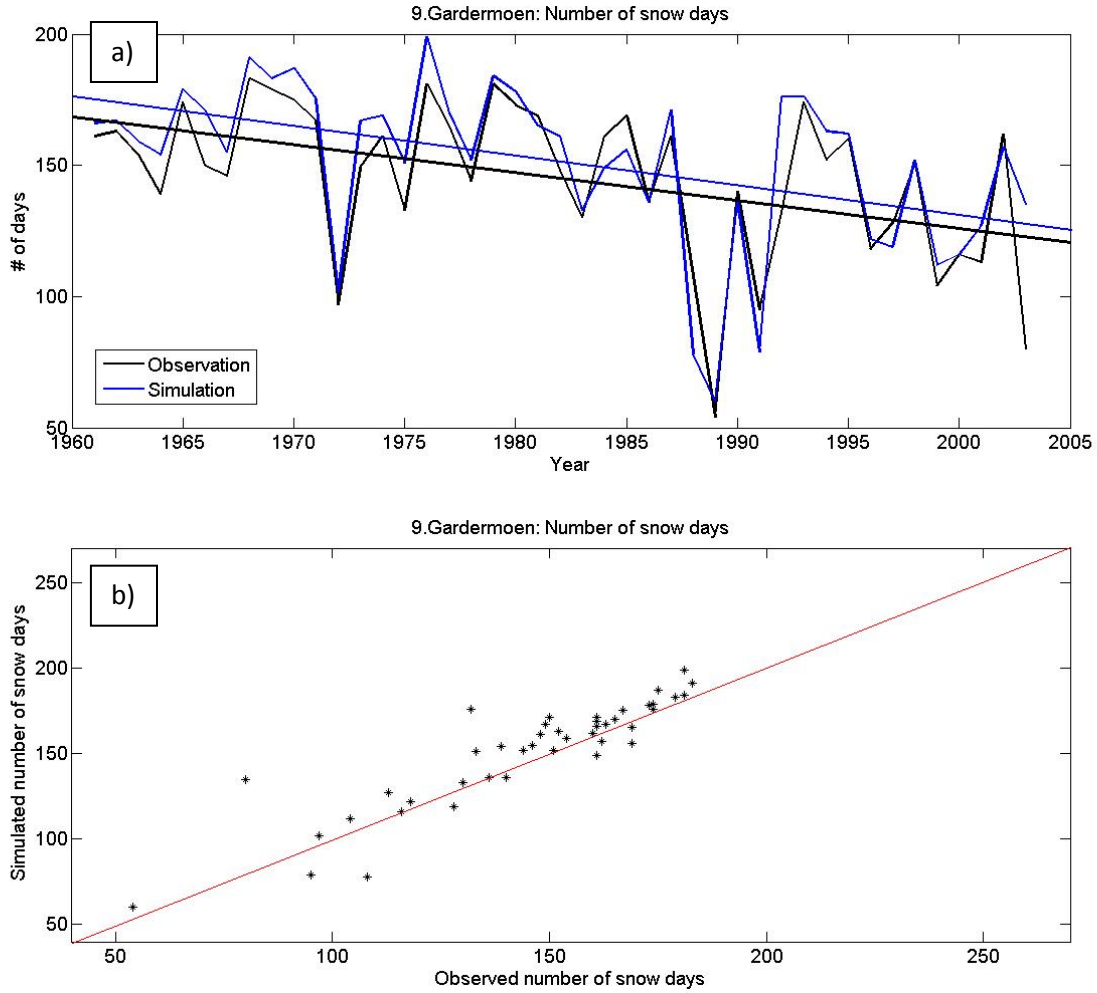

Figure 3.73: Observed and simulated number of snow days per winter season at station 9 Gardermoen: a) Time series b) Scatter plot.

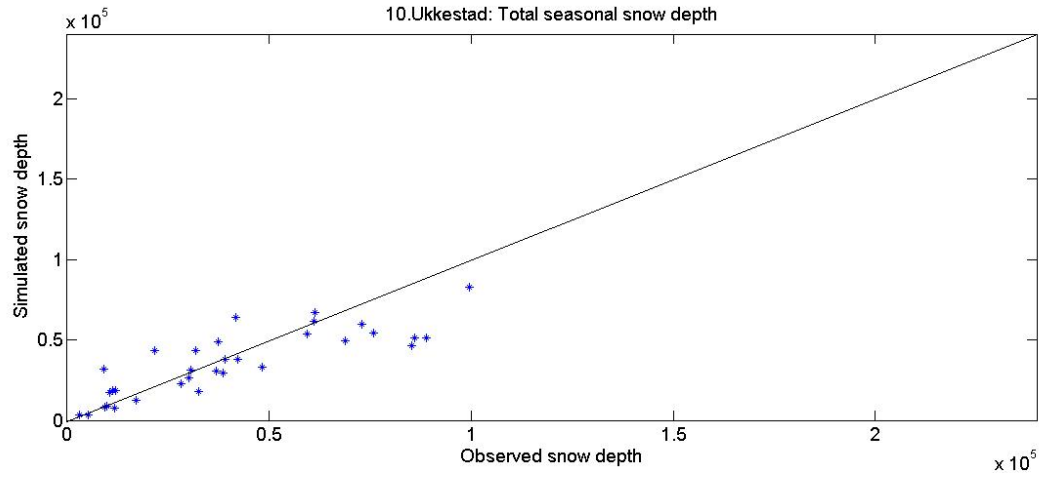

Figure 3.74: Scatteplot of observed versus simulated total snow depth for the winter season at station 10 Ukkestad.

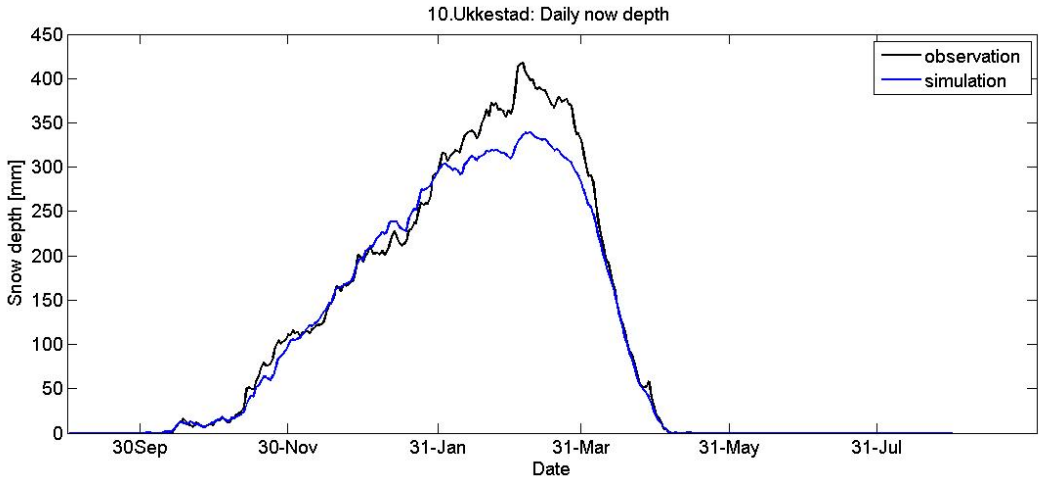

Figure 3.75: Mean daily snow depth (1971-2003) at station 10 Ukkestad.

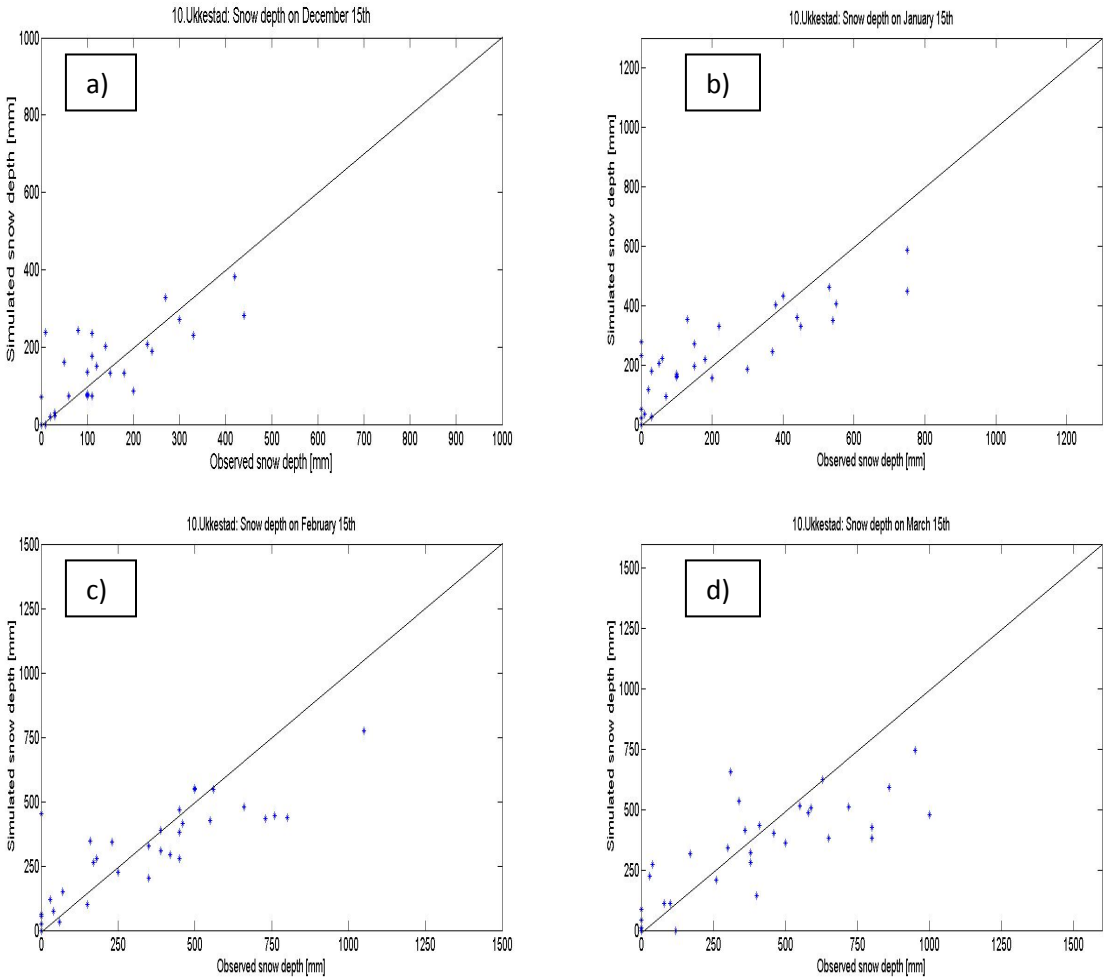

Figure 3.76: Station 10 Ukkestad: Scatter plots of observed and simulated snow depth on a) December 15th b) January 15th c) February 15th d) March 15th.

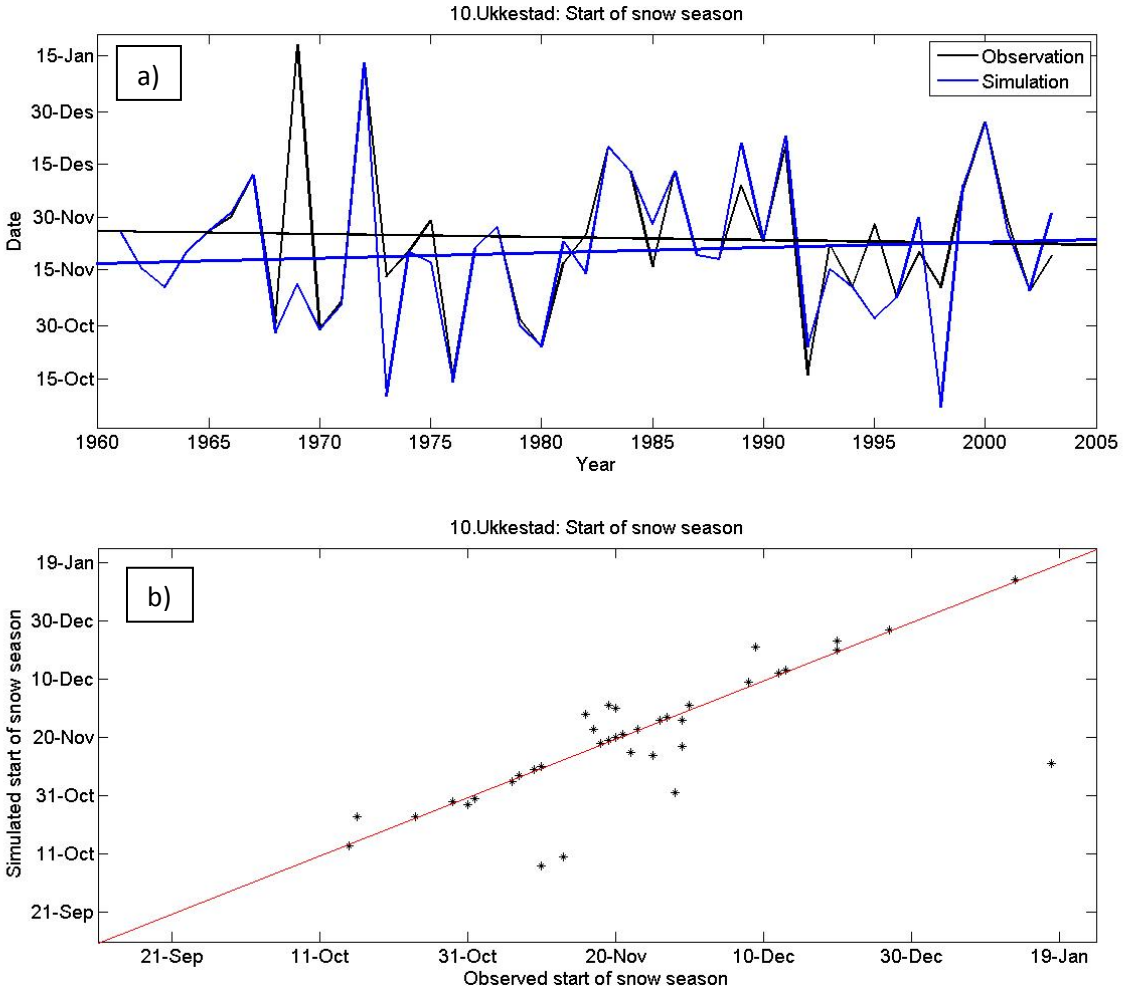

Figure 3.77: Observed and simulated start of snow season at station l0 Ukkestad: a) Time series b) Scatter plot.

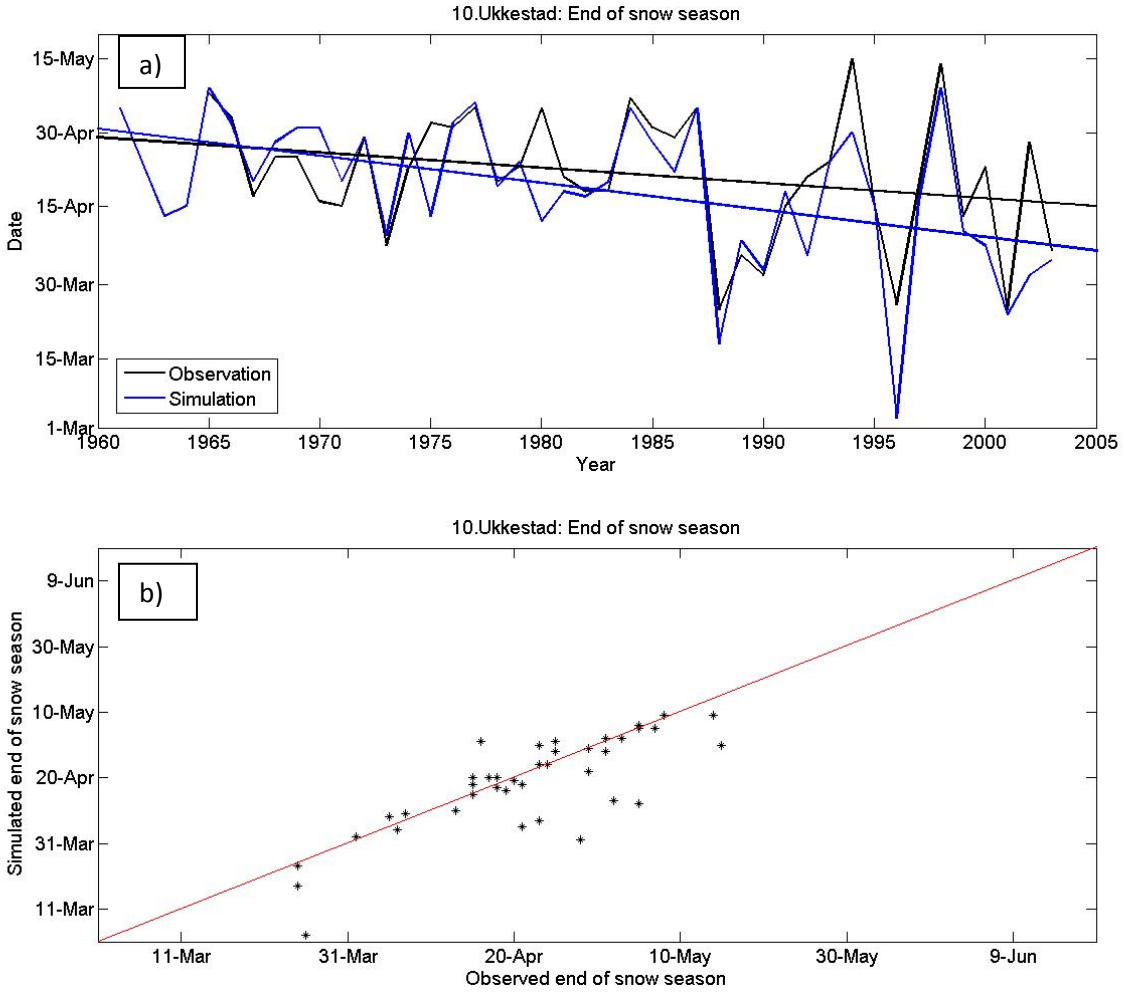

Figure 3.78: Observed and simulated end of snow season at station 10 Ukkestad: a) Time series b) Scatter plot.

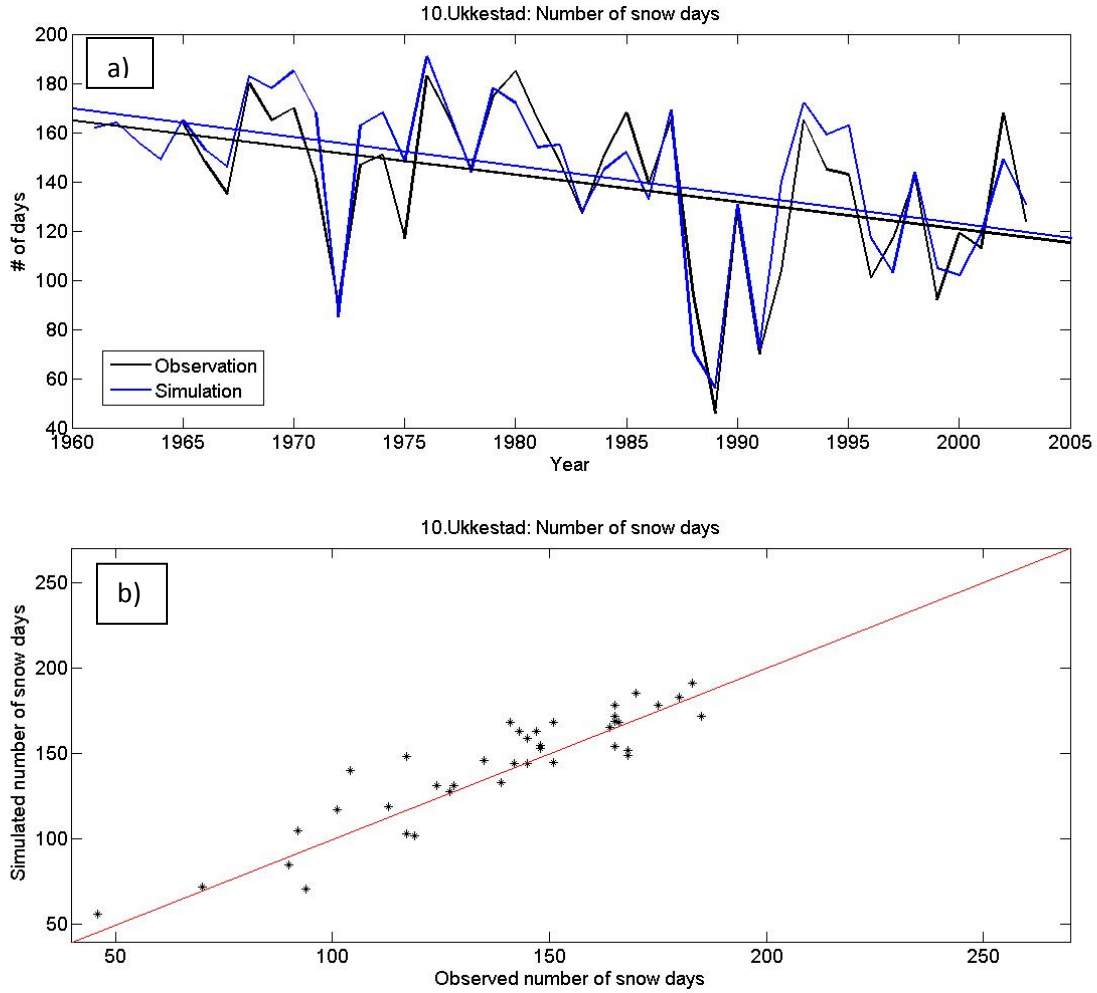

Figure 3.79: Observed and simulated number of snow days per winter season at station 10 Ukkestad: a) Time series b) Scatter plot.

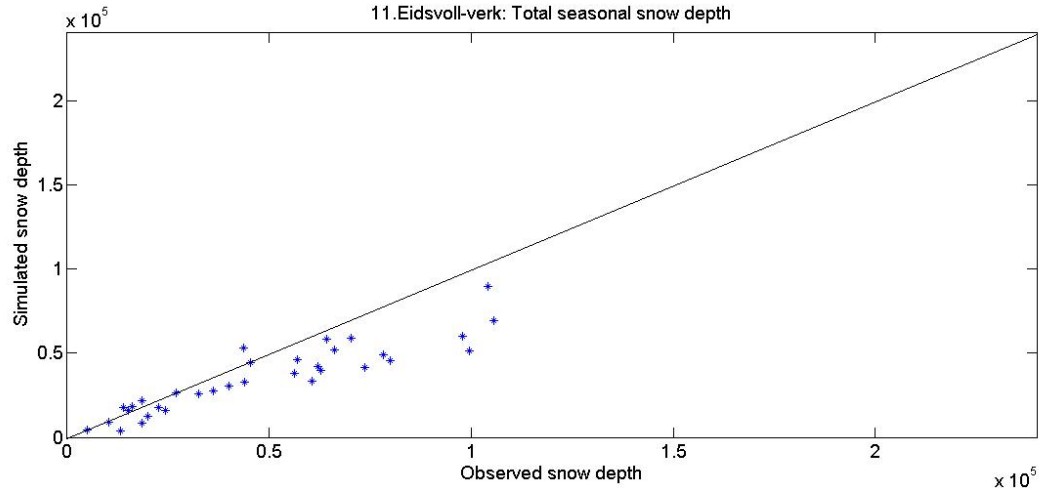

Figure 3.80: Scatteplot of observed versus simulated total snow depth for the winter season at station 11 Eidsvoll-verk.

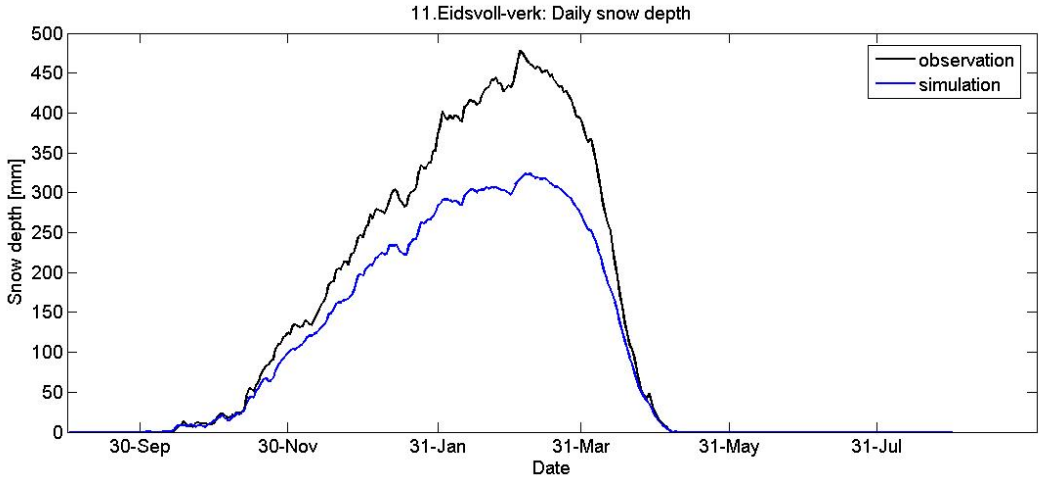

Figure 3.81: Mean daily snow depth (1971-2003) at station 11 Eidsvoll-verk.

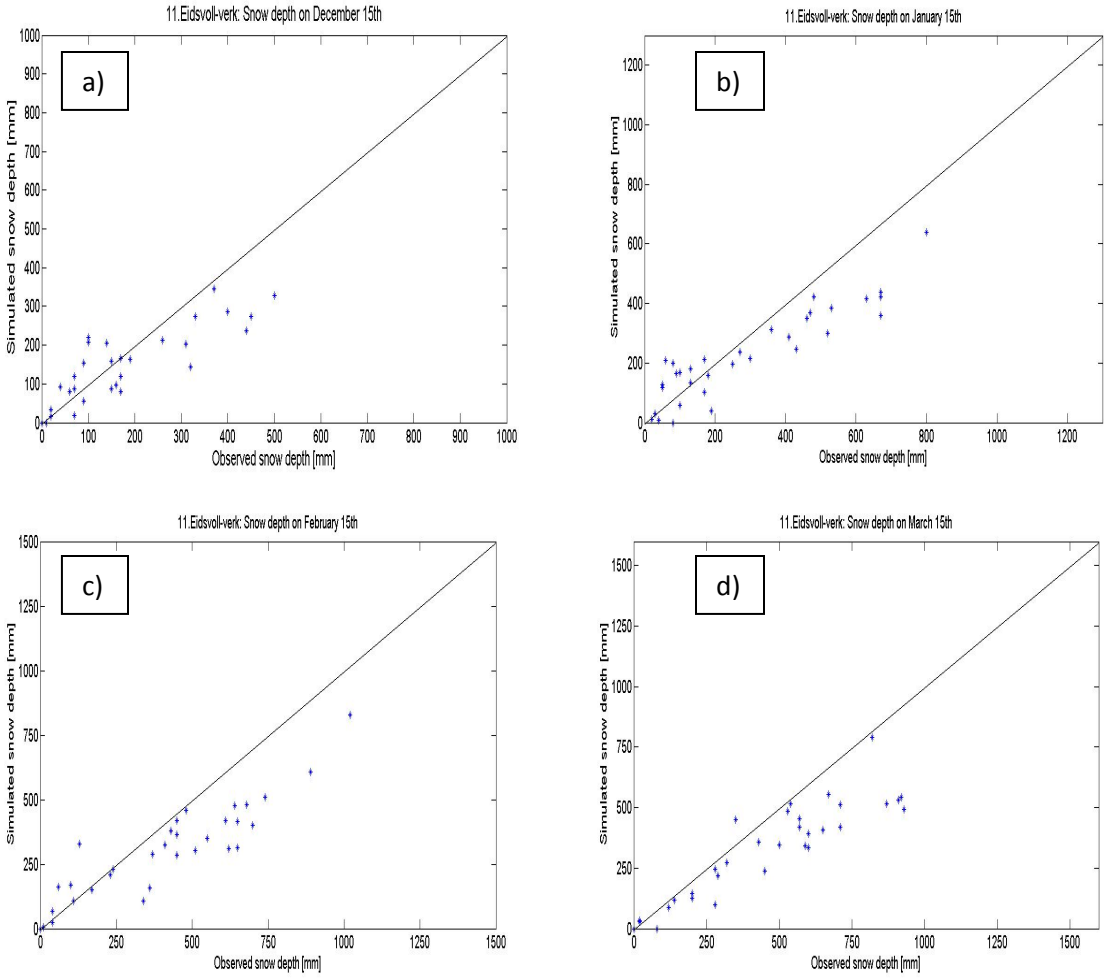

Figure 3.82: Station 11 Eidsvoll-verk: Scatter plots of observed and simulated snow depth on a) December 15th b) January 15th c) February 15th d) March 15th.

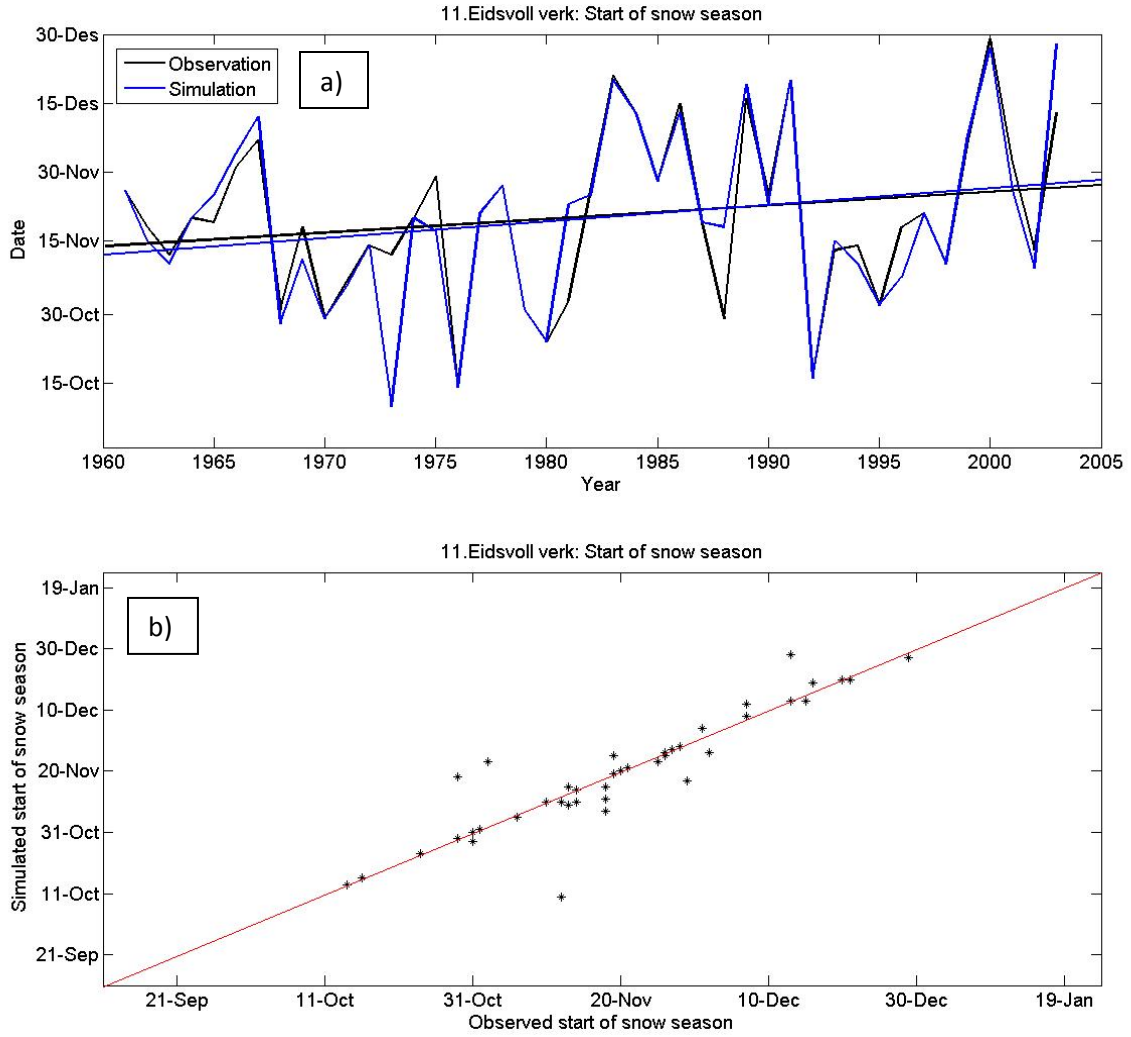

Figure 3.83: Observed and simulated start of snow season at station 11 Eidsvoll-verk: a) Time series b) Scatter plot.

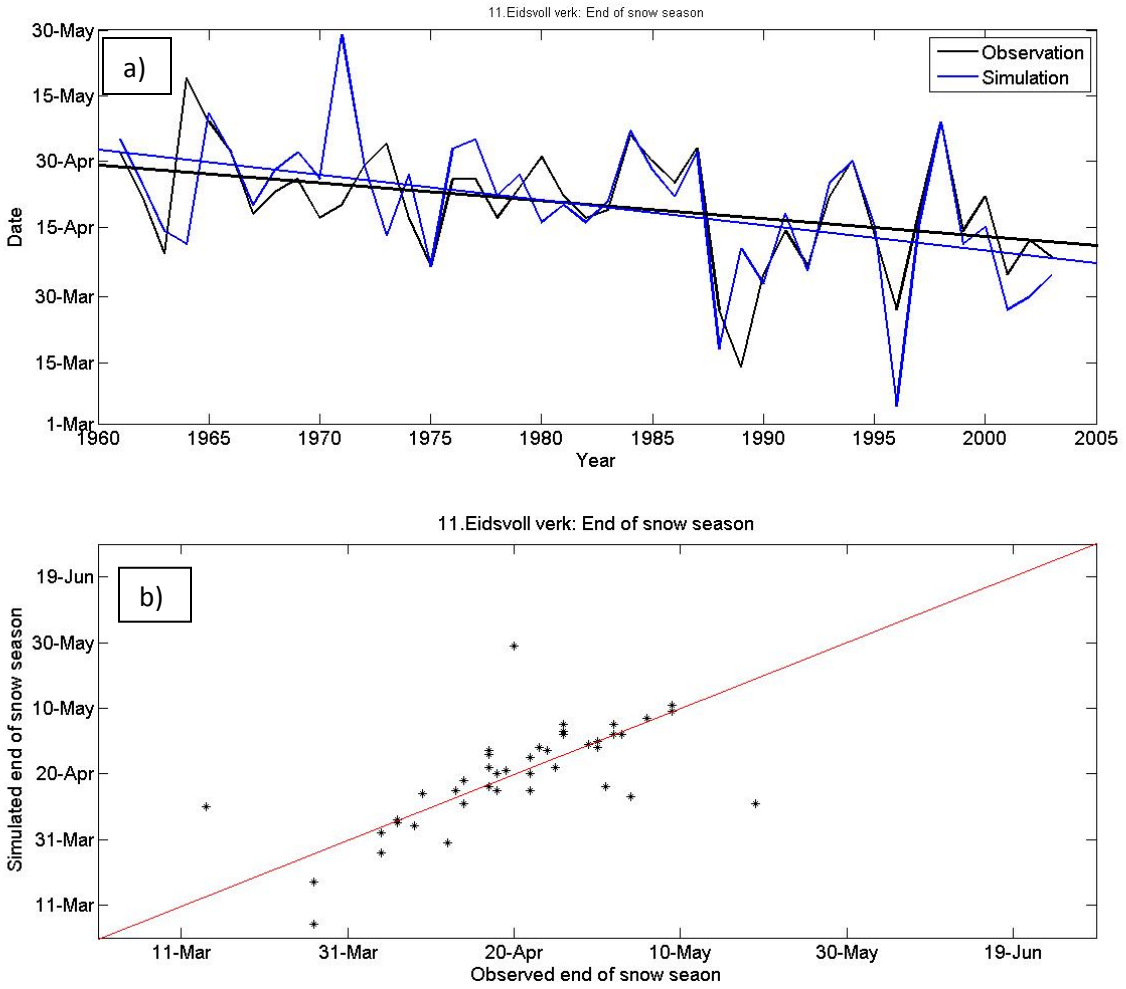

Figure 3.84: Observed and simulated end of snow season at station 11 Eidsvoll-verk: a) Time series b) Scatter plot.

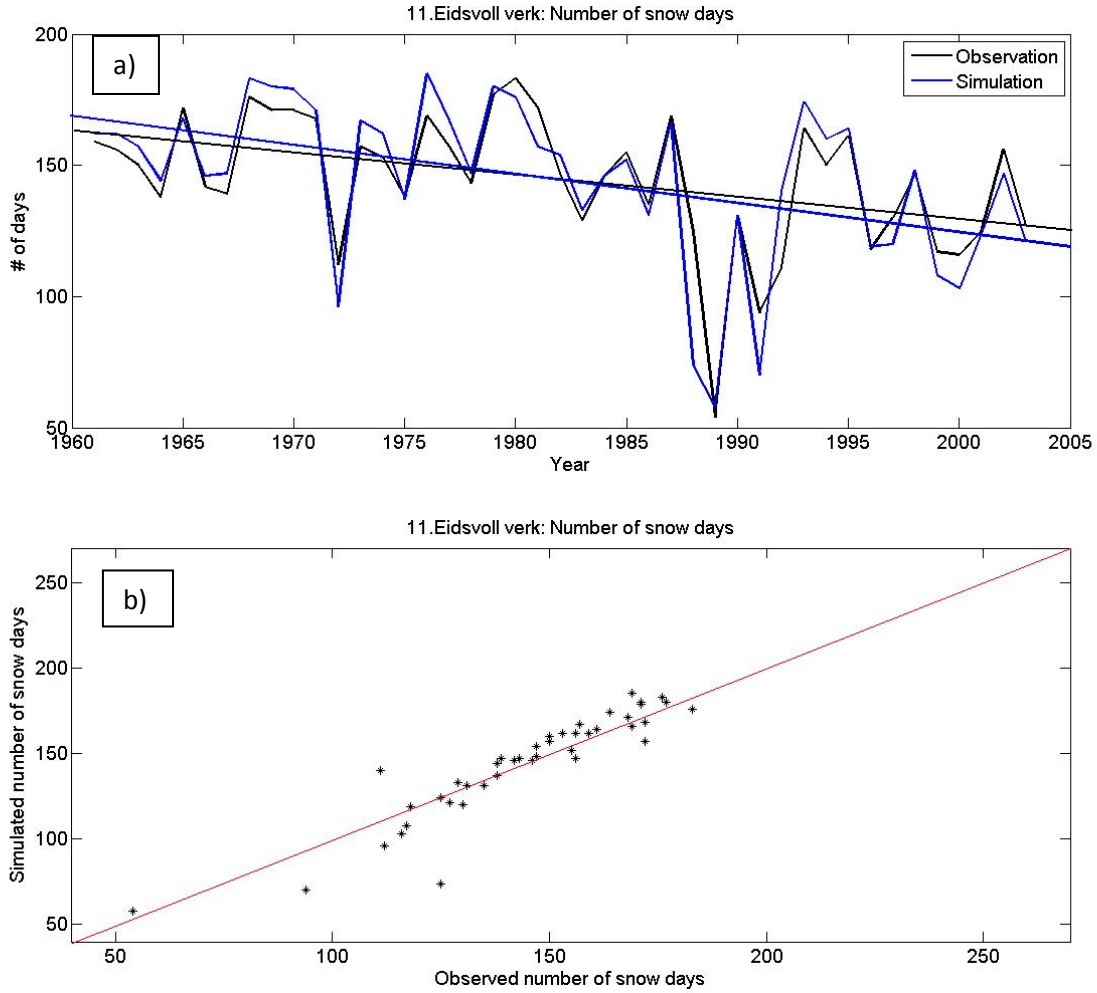

Figure 3.85: Observed and simulated number of snow days per winter season at station 11 Eidsvoll-verk: a) Time series b) Scatter plot.

Table 3.6: Mean observed and simulated dates for start and end of snow season and number of snow days. RMSE = Root mean squared error, R^2 = coefficient of determination.

Station		**Mean ± standard deviation**		**RMSE**	**R^2**
		obs	*sim*		
1.Jotkajavre	Start	12-Oct ± 12	15-Oct ± 14	7.48	0.76
	End	6-Jun ± 9	1-Jun ± 10	7.98	0.60
	# of days	241 ± 12	232 ± 15	12.27	0.68
2.Cuovddatmohki	Start	17-Oct ± 10	20-Oct ± 13	12.74	0.25
	End	22-May ± 6	18-May ± 8	8.50	0.45
	# of days	220 ± 16	214 ± 18	13.58	0.56
3.Karasjok	Start	19-Oct ± 10	24-Oct ± 14	12.11	0.39
	End	11-May ± 9	10-May ± 11	7.17	0.56
	# of days	203 ± 14	200 ± 18	9.18	0.78
4.Sihcajavri	Start	17-Oct ±12	17-Oct ± 13	6.97	0.71
	End	28-May ± 11	22-May ± 10	10.95	0.40
	# of days	223 ± 17	219 ± 16	11.86	0.58
5.Røros	Start	2-Nov ± 14	31-Oct ± 14	8.50	0.67
	End	9-May ± 9	16-May ± 9	9.72	0.51
	# of days	190 ± 13	201 ± 14	12.96	0.77
6.Aursund	Start	27-Oct ± 12	31-Oct ± 16	11.18	0.57
	End	23-May ± 8	19-May ± 10	9.83	0.26
	# of days	209 ± 12	204 ± 15	10.57	0.63
7.Os i Østerdal	Start	25-Oct ± 11	31-Oct ± 16	12.91	0.45
	End	25-May ± 8	10-May ± 9	18.19	0.07
	# of days	213 ± 16	193 ± 17	24.77	0.30
8.Vauldalen	Start	26-Oct ±12	19-Oct ± 12	12.99	0.33
	End	28-May ± 10	31-May ± 9	8.43	0.46
	# of days	217 ± 12	229 ± 13	14.42	0.61
9.Gardermoen	Start	16-Nov ± 17	18-Nov ± 18	15.36	0.40
	End	19-Apr ± 12	20-Apr ± 16	11.50	0.50
	# of days	145 ± 30	151 ± 31	14.94	0.81
10.Ukkestad	Start	24-Nov ± 21	20-Nov ± 22	14.89	0.60
	End	21-Apr ± 13	15-Apr ± 21	17.02	0.42
	# of days	138 ± 32	143 ± 33	13.88	0.84
11.Eidsvoll-verk	Start	20-Nov ± 18	20-Nov ± 19	7.86	0.83
	End	18-Apr ± 11	17-Apr ± 21	14.88	0.52
	# of days	144 ± 25	145 ± 31	12.14	0.85

Table 3.7: Cluster means of the results in Table 3.6 for our three regions.

Region		**Mean ± standard deviation**		**RMSE**	**R^2**
		obs	*sim*		
1.Finnmarksvidda	Start	16-Oct ± 11	19-Oct ± 14	9.82	0.53
	End	25-May ± 10	21-May ± 10	8.65	0.50
	# of days	222 ± 15	217 ± 17	11.72	0.65
2.Røros	Start	28-Oct ± 15	28-Oct ± 15	11.39	0.50
	End	21-May ± 9	19-May ± 9	11.54	0.33
	# of days	207 ± 13	207 ± 15	15.68	0.58
3. Romerike	Start	20-Nov ± 19	19-Nov ± 19	12.70	0.61
	End	10-Apr ± 12	17-Apr ± 19	14.47	0.48
	# of days	142 ± 29	147 ± 31	13.65	0.83

4. Summary and Conclusions

In this study a number of statistical tools are used to investigate the variability in snow depth at eleven selected stations clustered in three different locations in Norway. In addition, the Norwegian snow map service introduced in 2004 is evaluated through comparing simulated snow variables to observations at the same stations. In the first part a time series analysis is performed using spectral analysis and evaluation of trends in snow depth. We also look for trend in the start and end of the snow season, and the number of snow days per winter season. Not surprisingly, we find an overall decreasing trend in daily snow depth at all stations except at station 3 Karasjok, and the decrease in snow depth at Station 6 Aursund is minimal. The two stations with observations back to 1901 demonstrate a ~50 year cycle in snow depth. Station 7 Os i Østerdal illustrates a negative trend the first 60 years, approximately, and a positive trend after that. Snow depth at station 3 Karasjok decreases until 1945, and increased in the last half of the century. The spectral analysis reveals 2-3 year cycles at all stations, probably attributable to the North Atlantic Oscillation and the Scandinavia Index influencing precipitation over Norway. A later start of snow season was seen at all stations in Region 1 and 2, while the stations in Region 3 reveal a slightly earlier start of snow season. There is an earlier end of snow season and a decrease in number of snow days at all eleven stations. Region 3 shows the strongest decrease in the number of snow days and daily snow depth, which is in line with previous findings of

Vikhamar-Schuler et al. (2006) addressed in section 1.1 and stating that strongest decrease in length of snow season will occur in low altitudes and areas close to the sea. As a supplementary method of detecting trends in snow season, we applied a nonlinear fitting model to the daily snow depth data at each station. The results are not very similar to results from the manual analysis, given that the fitting is not perfect and the performance of the nonlinear model fluctuates from year to year and station to station. In Region 3, especially, quite a number of years had to be tossed due to fitting criteria not being met (see Table 3.2). We do however obtain some information on the date of maximum snow depth, which seems to exhibit a negative trend at some stations, revealing an earlier date compared to the beginning of the study period.

An EOF analysis is carried out to determine dominant spatial patterns of winter snow depth in Norway, and a simple correlation analysis was used in identifying leading modes of variability. EOF1, accounting for 41.4 % of snow depth variability, shows decadal variability and mostly affects Southern Norway in a positive fashion. Defining the EOFs showed not to be uncomplicated, as there are correlations to several of the teleconnection patterns included in the study. Furthermore, existing teleconnection patterns are defined to explain precipitation and temperature, whereas snow depth is directly affected by both previous mentioned variables, and these might work against each other. Spatial correlations between EOF1 and global SSTs, however, reveal interesting results. There are strong negative correlations right outside the coast of Southern Norway, indicating that EOF1 is related to a local phenomenon caused by sea surface temperature anomalies. Further investigation

suggests that enhanced onshore flow and precipitation being forced inland by prevailing synoptic winds perpendicular to the southern coast might be the answer. Hence, anomalously cold water and strong large scale wind perpendicular to the coast line results in more snow along the southern coast of Norway. Now, the greater mechanism creating the cold water is unknown. We believe it must be related to internal processes in the ocean, possibly the Gulf Stream, but this is a subject for future research. EOF1 is also negatively correlated to East Atlantic/Western Russia pattern (EA/WR) and the Arctic Oscillation (AO). EOF2 (accounting for 18.6% of snow depth variability) varies inter-annually, and exhibits a positive trend which is most likely linked to climate change. EOF2 seems to be strongly related to the East Atlantic pattern (EA) and the Scandinavian pattern (SCAND), and weakly related to the North Atlantic Oscillation (NAO), which is in line with previous findings of Scherrer and Appenzeller (2006). Further study is needed to evaluate the detailed contributions of the different teleconnection patterns on snow depth in Norway. In addition, we suggest defining teleconnection indices specifically for snow depth, and performing a combined precipitation and temperature EOF analysis.

In the light of climate change, numerous studies show that a global warming of both air and ocean temperatures is occurring and will continue to occur in the future. Precipitation amounts and patterns will also change, but there are greater uncertainties associated with future projections of precipitation. Since snow accumulation is directly influenced by both temperature and precipitation, we cannot say for certain how snow conditions will alter in the future. However, we have found in this study that eight of eleven stations experience a

decrease in snow accumulation and length of snow season today compared to mid-century conditions. This is likely to be connected to the increased temperatures observed in Norway in the last few decades, and is expected to continue in the future.

In the second part of our thesis we find that the precipitation / degree-day snow model exhibits a negative bias in simulating snow depth. This is most likely due to the VIC hydrologic model demonstrating excessive compaction of snow. The performance of the model in simulating onset and withdrawal of the snow season and the total number of snow days is variable between the different stations studied. In our first region in Northern Norway the snow model simulates a shorter snow season than what is observed at all four stations. Worst results are found at our second region in Central Norway. There is no consistency in the results from the four stations, and the difference in the number of snow days is as high as 20 days at one of the stations. The model performs best in our third region in South Eastern Norway, where the correlation between the three observed and simulated snow season indices are all significant at the 0.05 alpha level. There are several possible reasons to why the model performs better in some locations. One might be the fact that station elevations used in the model is very different from real station elevations in Region 2, and we already know that the elevation gradient for precipitation is too large in the model. In addition, Region 1 and Region 2 shows higher variance in station elevation than Region 1, and the distance between stations is greater. We also believe that Region 2 is more sensitive to random variability due to its placement in the transition area between positive and negative loadings of the two leading modes of snow depth variability. The EOF analysis confirmed

that different climatic regimes dominate different parts of the country, resulting in climate and weather modeling being a great challenge. Differences in atmospheric variability and dynamics suggest that a separate snow model for each climate regime would be ideal. A future analysis of snow depth variability is recommended for additional stations in order to evaluate if our conclusions can be extended to other parts of the country. A fourth region along the western coast is of particular interest, since we are likely to find different snow conditions. We would also recommend a cluster analysis using averages from stations sharing the same characteristics.

5. References

Alfnes, E. ,2008: Snow depth algorithms – compaction of snow, NVE internal report.

Bernstein, L. and Coauthors, 2007: IPCC Climate Change 2007 Synthesis Report.

Bjornsson, H. and S. A. Venegas, 1997: A manual for EOF and SVD analysis of climatic data, *CCGCR Report No.* **97-1**, 52pp.

Cherkauer, K. A., and D. P. Lettenmaier, 1999: Hydrologic effects of frozen soils in the upper Mississippi River basin, *J. Geophys. Res*., **104(D16)**, 19,599-19,610.

Climate Prediction Center, "Northern Hemisphere Teleconnection Patterns," National Oceanic and Atmospheric Administration, http://www.cpc.ncep.noaa.gov/data/teledoc/telecontents.shtml, as 21 October 2008.

Cook, J., Woods Hole Oceanographic Institute, Ocean and Climate Change Institute, from Science Daily, http://www.sciencedaily.com/releases/2006/02/060228180303.htm, as 21 October 2008.

Diaz, M., 2008: Personal communication, October.

Drange, H. and Coauthors, 2007: NorClim, Revised version of proposal ES418361 to Theme 2 of the NORKLIMA-programme of the Research Council of Norway.

Earth System Research Laboratory, "NAO data," National Oceanic and Atmospheric Administration, http://www.cdc.noaa.gov/Correlation/nao.data, as 21 October 2008.

Eklima.no, http://eklima.no, as 21 October 2008.

Engeset, R., O. E. Tveito, E. Alfnes, Z. Mengistu, H.-C. Udnæs, K. Isaksen, and E. J. Førland, 2004: Snow map system for Norway, *Proceedings XXIII Nordic Hydrological Conference 2004*, 8-12 August 2004, Tallinn, Estonia.

Engeset, R., O.E. Tveito, H.-C. Udnæs, E. Alfnes, Z. Mengistu, K. Isaksen, and E. J. Førland, 2004: Snow map validation for Norway, *Proceedings XXIII Nordic Hydrological Conference 2004*, 8-12 August 2004, Tallinn, Estonia.

Førland, E. J., 1979: Nedbørens høydeavhengighet (Precipitation and topography, in Norwegian with English summary), *Klima*, **1**, 3–24.

Førland, E. J., 1984: Lokalklima på Vestlandskysten (Local climate in Western Norway, in Norwegian with English summary), *Klima*, **6**, 24–36.

Førland, E. J., 2008: Personal communication, January, July, October

Gámiz-Fortis, S.R., D. Pozo-Vázquez, M. J. Esteban-Parra, and Y. Castro-Díez, 2002: Spectral characteristics and predictability of the NAO assessed through Singular Spectral Analysis, *Journal of Geophysical Research*, **VOL107**, NO. D23.

Garcia, N.O., L. Gimeno, L. De La Torre, R. Nieto, and E. A. Añel, 2005: North Atlantic Oscillation (NAO) and precipitation in Galicia (Spain), *Atmósfera*, 23-32.

Ghil M., R. M. Allen, M. D. Dettinger, K. Ide, D. Kondrashov, M. E. Mann, A. Robertson, A. Saunders, Y. Tian, F. Varadi, and P. Yiou, 2002: Advanced spectral methods for climatic time series, *Rev. Geophys.*, **40(1)**, pp. 3.1-3.41, 10.1029/2000RG000092.

GraphPad Prism version 5.01 for Windows, GraphPad Software, San Diego California USA, www.graphpad.com, as 21 October 2008.

Hurrell, J. W., 1995: Decadal trends in the North Atlantic oscillation: regional temperatures and precipitation. *Science*, **269**, 676–679.

Hurrell JW., 1996: Influence of variations in extratropical wintertime teleconnections on Northern Hemisphere temperature, *Geophysical Res. Lett.*, **23,** 665–668.

Hurrell, J.W. and H. Van Loon, 1997: Decadal variations in climate associated with the North Atlantic Oscillation, *Climatic Change*, **36**: 301-326.

Jansson, A., O.E. Tveito, P. Pirinen, M. Scharling, 2007: NORDGRID
-a preliminary investigation on the potential for creation of a joint Nordic gridded climate dataset, met.no, *climate report no.03/2007*.

Jordan, R., 1991: A one-dimensional temperature model for a snow cover, Technical documentation for SNTHERM.89, *Special technical report 91-16*, *US Army CRREL*, 49 pp.

Journel, A.G. and C.J. Huijbregts, 1978: Mining Geostatistics. *Academic Press London*.

Kielland, G., 2008: Personal communication, September.

Kondrashov, D. and M. Ghil, 2006: Spatio-temporal filling of missing data points in geophysical data sets, *Nonlinear Processes in Geophysics*, **13**, 151–159.

Kushnir Y., 1999: Europe's winter prospects, *Nature* **398**: 289–291.

Liang, X., D. P. Lettenmaier, E. F. Wood, and S. J. Burges, 1994: A simple hydrologically based model of land surface water and energy fluxes for GSMs. *J. Geophys*. Res., **99(D7)**, 14,415-14,428.

Merkel, U., and M. Latif (2002): A high resolution AGCM study of the El Niño impact on the North Atlantic/European sector, *Geophys. Res. Lett.*, **29(9)**, 1291, doi:10.1029/2001GL013726.

Met.no, the Norwegian Meteorological Institute, http://met.no, as 21 October 2008.

Mitchell T., 2004: "Arctic Oscillation (AO) time series, 1899 - June 2002," Joint Institute for the Study of Atmosphere and Ocean, University of Washington, http://jisao.washington.edu/ao/#data, as 21 October 2008.

Monahan, J., 2008: Personal communication, September.

Mysterud, A., N. G. Yoccoz, N. C. Stenseth, and R. Langvatn,2000: Relationships between sex ratio, climate and density in red deer: the importance of spatial scale, *Journal of Animal Ecology*, **69**, 959-974.

NOAA Earth System Research Laboratory, 2008: PSD Gridded Climate Datasets, http://www.esrl.noaa.gov/psd/data/, as 21 October 2008.

North, G.R., T. L. Bell, and R. F. Cahalan, 1982: Sampling errors in estimation of empirical orthogonal functions, *A.Meteorol.Soc.*, **110**, 699-706.

Percival, D. B. and A. T. Walden, 1993: Spectral Analysis for Physical Applications, *Cambridge Univ. Press*, 583 pp.

Popova, V., 2007: Winter snow depth variability over northern Eurasia in relation to recent atmospheric circulation changes, *International Journal of Climatology*, **27**, 1721-1733.

Rodriguez-Puebla, C. and S. Nieto, 2008: Trend of the North Atlantic Oscillation (NAO) under climate change, *Geophysical Research Abstracts*, **10**.

Scherrer, S.C. and C. Appenzeller, 2006: Major patterns of Swiss Alpine snow pack variability: Links to local climate and large-scale flow. *Climate Research*, **32**, 187-199.

Seager, R., Y. Kushnir, M. Visbeck, N. Naik, J. Miller, G. Krahmann, and H. Cullen, 2000: Causes of Atlantic Ocean Climate Variability between 1958 and 1998, *Journal of Climate*, **13**, 2845-2862.

Senorge.no, http://senorge.no, as 21 October 2008.

Simpson, J. E., 1994: Sea Breeze and Local Winds, *Cambridge University Press*, 234 pp.

Skaugen, T., 2008: Personal communication, July.

Thomson, D. J., 1982: Spectrum estimation and harmonic analysis, *Proc. IEEE*, **70**, 1055– 1096.

Toniazzo, T., and A. A. Scaife (2006): The influence of ENSO on winter North Atlantic climate, *Geophys. Res. Lett.*, **33**, L24704, doi:10.1029/2006GL027881.

Tveito, O. E., I. Bjørdal, A. O. Skjelvåg, and B. Aune, 2005: A GIG-based agro-ecological decision system based on gridded climatology, *Meteorological Applications*, **12**, 57-68.

Tveito, O.E. and E. J. Førland, 1999: Mapping temperatures in Norway applying terrain information, geostatistics and GIS, *Norsk geogr. Tidsskr*. **53**, pp 202-212.

Tveito, O.E., E. J. Førland, R. Heino, I. Hanssen-Bauer, H. Alexandersson, B. Dahlström, A. Drebs, C. Kern-Hansen, T. Jónsson, E. Vaarby-Laursen, and Y. Westman, 2000: Nordic Temperature Maps, *met.no Klima report 9/00*, 55 pp.

Tveito, O. E. and W. Schöner, 2002: Applications of spatial interpolation of climatological and meteorological elements by the use of geographical information systems (GIS), *met.no Klima report 28/02*.

Tveito, O.E., H.-C.Udnæs, Z. Mengistu, R. Engeset, and E. J. Førland, 2002: New snow maps for Norway, *Proceedings XXII Nordic Hydrological Conference 2002*, 4-7 August 2002, Røros, Norway.

Uvo, C.B., 2003: Analysis and regionalization of Northern European winter precipitation based on its relationship with the North Atlantic Oscillation, *International Journal of Climatology,* **23**: 1185–1194.

Vikhamar-Schuler, D., S. Beldring, E. J. Førland, L. A. Roald, and T. E. Skaugen, 2006: Snow cover and snow water equivalent in Norway: -current conditions (1961-1990) and scenarios for the future (2071-2100), *met.no climate report no.01/2006*.

Vikhamar-Schuler, D. and E. J. Førland, 2006: Comparison of snow water equivalent estimated by the HIRHAM and the HBV (GWB) models: - current conditions (1961-1990) and scenarios for the future (2071-2100), *met.no climate report no.06/2006*.

Vikhamar-Schuler, D., E. J. Førland, and I. Hanssen-Bauer, 2008: Analyses of Norwegian snow observations during the period 1895-2007, *met.no report* (in prep.).

Vlachos, M., C. Meek, Z. Vagena, D. Gunopulos, 2004: Identification of Similarities, Periodicities & Bursts for Online Queries. In Proc. of International Conference on Management of Data (SOGMOD), Paris, France.

Wilks, D.S., 2006: Statistical methods and in atmospheric sciences, second edition, *International Geophysics Series*, **91**, 463.

Wu, Z., E. K. Schneider, and B. P. Kirtman, 2004: Cause of Low Frequency North Atlantic SST Variability in a Coupled GCM. *Geophys. Res. Lett.*, **31,** L09210, doi:10.1029/2004GL019548.